UNIVERSITY OF CALIFORNIA
RIVERSIDE

Fear Discrimination Learning Modulates Neuronal Ensembles in the Prefrontal Cortex

A Dissertation submitted in partial satisfaction
of the requirements for the degree of

Doctor of Philosophy

in

Biomedical Sciences

by

Alex Andrei Corches

December 2018

Dissertation Committee:
Dr. Edward Korzus, Chairperson
Dr. Iryna Ethell
Dr. Jun-Hyeong Cho

The Dissertation of Alex Andrei Corches is approved:

Committee Chairperson

University of California, Riverside

Acknowledgements

Some text in this dissertation is reprinted from material published in the following journals: *Learning & Memory* in 2014 and *Neurobiology of Learning and Memory* in 2015. This dissertation also contains a reprint of a recently accepted manuscript to the journal, *Behavioural Brain Research*. Edward Korzus, the co-author listed in these publications directed and supervised the research that forms the basis of this dissertation. Additional co-authors that provided technical assistance for this research include Alex Hiroto, Tyler W. Bailey, John H. Speigel III, Justin Pastore, and Mark Mayford

This work was made possible with help from the following research assistants: Niusha Bavadian, Ashley Burroughs, Patrick Crete, Jivan Hovsepyan, Gurpreet Kaur, Christopher Li, Sandra Loza, Lindsay Melendez, Richard Nguyen, Taylor Pope, Kritee Sekhon, Alex Tran, Ryan Wales, and Anqi Yang

Financial support from UCR Graduate Division, UCR Department of Psychology, UCR Division of Biomedical Sciences, and UCR School of Medicine

Advisory support from Edward Korzus, Iryna Ethell, Jun-Hyeong Cho, Emma Wilson, Peter Hickmott, and Weiwei Zhang

Special thanks to my colleagues, family, friends, and fiancé

Dedication

This thesis is dedicated to my parents, Mariana and Gavril Corches and to my grandmother, Simtioana Lomonar.

ABSTRACT OF THE DISSERTATION

Fear Discrimination Learning Modulates Neuronal Ensembles in the Prefrontal Cortex

by

Alex Andrei Corches

Doctor of Philosophy, Graduate Program in Biomedical Sciences
University of California, Riverside, December 2018
Dr. Edward Korzus, Chairperson

Survival relies on the ability to discriminate between danger and safety. Fear discrimination is crucial for appropriate adaptive responses while fear generalization is important for recalling and avoiding dangerous situations. Previous research suggests that fear discrimination learning is mediated by the prefrontal cortex (PFC). It has been demonstrated that disruption in either cAMP element response binding protein (CREB), its co-activator, CREB binding protein (CBP), or N-methyl D-apsarate (NMDA) receptor function specifically within the PFC causes deficits in fear discrimination. Mice exhibiting disruption of these signalling pathways show normal fear responses to aversive stimuli but inappropriate fear responses to similar, yet distinct, non-aversive stimuli. Recent evidence suggests that the prelimbic (PL) and infralimbic (IL) subregions of the PFC provide excitatory and inhibitory effects on the fear circuit, respectively, but the subregion-specific mechanisms driving fear discrimination are unknown. To get insight into the circuit mechanisms underlying fear discrimination, we investigated prefrontal

neuronal ensembles representing distinct experiences associated with learning to disambiguate between dangerous and similar, yet distinct, harmless stimuli. We show distinct quantitative activation differences in response to conditioned and generalized fear responses, as well as modulation of neuronal ensembles associated with successful acquisition of contextual fear. Prefrontal neuronal ensembles of fear memories trace functional context-danger and context-safety associations. The PL subdivision of the PFC monitors context-danger associations to conditioned fear, whereas fear discrimination learning engages memory ensembles associated with the inhibition of generalized fear in both PL and IL subdivisions of the PFC. Our data suggests that fear discrimination learning is associated with the modulation of prefrontal memory representations in a subregion- and experience-specific manner while learning appropriate responses to conditioned and generalized fear experiences is driven by updating and rebalancing these prefrontal memory ensembles. These findings provide novel insight into prefrontal mechanisms that underlie fear generalization, a common symptom in patients with posttraumatic stress disorder, phobia and generalized anxiety disorder.

Table of Contents

List of Figures

Chapter 1: Introduction and review of literature

1.1 Fear memory specificity

Memories allow animals to adapt appropriately in dynamic environments. Memories are always partially generalized which enables animals to respond properly to novel stimuli based on previous experience. Fearful memories are particularly important for survival because they allow animals to predict danger in novel situations. However, overgeneralization of fear memories can cause irrational fear and anxiety as seen in phobias and posttraumatic stress disorder (PTSD) [1]. Recent evidence from both animal and human studies suggest that impairment of prefrontal cortex (PFC) functionality is a hallmark of PTSD and may lead to impaired fear memory specificity and fear discrimination learning [2-5]. Studying the mechanism by which the PFC modulates fear memory specificity and generalization is important for characterizing and treating fear and anxiety-related disorders such as PTSD, phobias, and generalized anxiety disorder.

Fear conditioning is the paradigm of choice when investigating fear memory specificity. Fear conditioning is a form of Pavlonian classical conditioning, an associative learning process where a neutral stimulus called the conditioned stimulus (CS) is paired with an unconditioned stimulus (US) to drive a conditioned response (CR) [6]. In fear conditioning, a neutral stimulus, such as a tone (CS), is repeatedly paired with an aversive footshock (US). Through repeated CS-US pairings, associative learning occurs and eventually the CS alone will lead to fear expression (CR). There are two main forms of fear conditioning: contextual and cued. In contextual fear conditioning, the context is the CS while in cued fear conditioning, a cue, such as a tone, is the CS. Most theories of

associate learning emphasize the role of the prediction error (PE), the difference between received and expected events. The Rescorla-Wagner model, asserts that PE determines the effectiveness of the reinforcement or US, in that more surprising reinforcers are more effective than those expected [7]. On the other hand, the Pearce-Hall model argues that PE determines the associability of the conditioned stimuli [8].

Fear conditioning studies revealed that contextual fear acquisition is encoded via a direct pathway between the hippocampus, a region involved in spatial and temporal processing, and the amygdala, a crucial region for fear processing [9, 10]. On the other hand, auditory fear conditioning acquisition is encoded via synaptic plasticity in the auditory projections onto the amygdala directly from the auditory cortex [11-13]. Studies investigating fear modulation after successful fear acquisition have revealed that contextual fear modulation is distributed among the amydala-hippocampus-medial PFC (mPFC) circuitry [14]. Subsequent sections within this chapter will focus on neuronal circuits and mechanisms within the PFC that underlie fear acquisition, fear modulation, and fear extinction.

1.2 Neuronal circuits underlying fear modulation

Contextual fear memory involves amygdala-hippocampus-mPFC circuitry. During contextual fear conditioning, the hippocampus conveys information about the context to the amygdala and mPFC [15]. This contextual information is associated with footshock through synaptic plasticity in the hippocampal-amygdalar pathway and consolidated via the hippocampal-prefrontal pathway [9, 16-19]. This is consistent with the widely recognized multiple memory systems theory postulates that different types of memory are consolidated via hardwired pathways [20]. Another important property of fear conditioning termed fear extinction involves repeatedly presenting the CS without the US leading to reduction of fear to the CS. Early lesion studies investigating the role of the mPFC in fear conditioning found that prefrontal lesions before conditioning did not have an effect on fear acquisition or fear expression of either contextual or cued fear [21]. However, these animals took longer to extinguish their conditioned fear suggesting that the mPFC plays a role in extinction learning.

Recent studies investigating the circuitry within the mPFC show that fear expression is differentially regulated by the prelimbic (PL) and infralimbic (IL) subregions of the mPFC. Inactivation of the PL reduced conditioned fear expression while microstimulation increased fear expression suggesting the PL region is crucial for appropriate fear expression [22, 23]. One study found that PL inactivation in rats trained on a contextual discrimination task impaired both encoding and expression of appropriate attentional responses to the CS [24]. Moreover, PL inactivation disrupted recent and remote contextual fear memories after a brief memory retrieval task indicating that the

PL may be involved in reconsolidation of contextual memories [25]. These data suggests that the PL may help integrate contextual information used to modulate responses to predictive cues in ambiguous settings. On the other hand, IL inactivation increases conditioned fear whereas IL activation before extinction training reduces fear expression and enhances subsequent extinction recall suggesting the IL region is critical for fear suppression and fear extinction [22, 26]. Additionally, when conditioned tones are paired with an electrical stimulation in the IL of rats, freezing decreases which suggests that IL activation is sufficient to mimic extinction [27, 28]. Others have shown that IL activation rescues extinction in extinction-deficient mice [29]. More recently, it was found that activation of deep layer PL neurons projecting to deep layer IL neurons enhances fear extinction learning suggesting that an intrinsic connectivity within the mPFC is important for fear modulation [30]. In summary, both PL and IL signaling is important for the acquisition, expression, and extinction of conditioned fear.

There is evidence to suggest that the division of function between the IL and PL subregions within the mPFC is due to differential connectivity to the amygdala. Studies in rats have shown that the IL projects to inhibitory intercalated amygdala neurons providing feed-forward inhibition that suppresses central amygdala activity leading to fear suppression while the PL innervates the basolateral amygdala (BLA) and leads to fear expression [31-35]. However, recent data challenges this notion [36-38]. Diffusion tensor imaging and tract-tracing techniques in mice further demonstrate virtually indistinguishable amygdalar projections from PL and IL [39]. Moreover, PL and IL have

direct projections to the periaqueductal gray, a region crucial for freezing behavior suggesting the mPFC may bypass the amygdala to directly influence freezing [40-42].

The mPFC is crucial for other forms of contextual fear modulation such as fear discrimination [4, 5, 43], fear extinction [5, 22, 44] and can even compensate for contextual learning after hippocampal loss [19]. Research investigating the role of the mPFC in fear memory specificity have found that hypofunctionality in this region leads to maladaptive fear responses in ambiguous situations. In a separate set of studies, it was found that hypofunction of both CREB and CBP signaling specifically within the mPFC lead to impaired contextual and auditory fear discrimination [4, 5]. Interestingly, the deficit in fear discrimination learning was due to improper fear responses to similar, yet distinct, non-aversive stimuli while maintaining appropriate fear responses to aversive stimuli. In a study in which rats were trained on a contextual fear discrimination task, PL inactivation impaired both the encoding and expression of appropriate CS responses which suggests that the PL may integrate contextual information for both learning and responding to conditioned stimuli [45]. Recently, it was shown optogenetically stimulating BLA inputs to PL, during a task where competing aversive and non-aversive cues were simultaneously presented, increased freezing while chemogenetic and optogenetically inhibiting these inputs decreased freezing [46]. Studies investigating the role of the IL have found that both IL lesions and IL inactivation caused an impairment in contextual fear discrimination learning [19, 47]. These studies demonstrate that both PL and IL signaling within the mPFC is critical for governing appropriate behavioral responses to conflicting danger and safety cues in the environment. The Hull-Spence

continuity theory of discrimination learning postulates that conditioned excitation (the result of reinforcement) and inhibition (the result of non-reinforcement) have generalization gradients and that discrimination learning is the summation of excitation and inhibition [48-50].

Fear discrimination is the process of inhibiting generalized fear to a non-aversive and non-reinforced stimuli, while fear extinction is the process of diminishing fear to aversive and reinforced stimuli. Research over the last few decades has revealed that fear modulation associated with fear extinction learning involves the formation of new memory trace that suppresses fear expression [51, 52]. It is traditionally believed that the IL circuitry alone mediates the extinction learning underlying fear inhibition. Milad and Quirk demonstrated that the CS-evoked responses in the IL coincide with learned fear suppression [27] which was later reproduced in several studies [22, 53]. The current model of fear extinction learning predicts that the CS would induce IL activation during successful recall of fear extinction learning which suppresses fear by tapping into the fear circuit via the monosynaptic IL→GABAergic intercalated amygdala neurons (ITC) [34, 37] or di-synaptic IL→BLA→ITC pathway [32, 33, 38]. However, not all data suggests a division of labor within the mPFC during fear extinction. For example, both IL and PL show elevated firing rates during extinction recall [54] and both PL→BLA and IL→BLA pathways show synaptic plasticity during extinction recall [36]. In summary, the acquistion, recall, and extinction of fear memories requires carefully coordinated neuronal activity in the amygdala, hippocampus, and mPFC to properly gate contextual contingencies during regulation of adaptive fear responses.

1.3 Immediate early gene studies

Immediate early gene (IEG) activation is an useful tool for tracking functional circuit level activity with temporal and cellular resolution. Expression of IEGs such as Arc, cFos, and Zif268 are often used as markers of neuronal activity to track subregion-specific changes in activation during contextual fear learning. One particular IEG, Arc, has garnered attention in the learning and memory field. It has been found that Arc expression increases after context-specific spatial learning and Arc regulates α-amino-3-hydroxy-5-methyl-4-isoxazolepropionic acid (AMPA) receptor trafficking, a key component of synaptic plasticity required for learning and memory [55, 56]. Specific Arc expression knockdown in the hippocampus drastically impairs contextual fear conditioning [57]. Moreover, Arc is required for hippocampal LTP and consolidation of contextual and fear memories in both the hippocampus and amygdala [58, 59].

In general, IEG studies have supported the opposing roles of the PL and IL. One study showed increased cFos expression in PL upon fear renewal whereas presentation of the extinguished CS in the extinction context induced greater cFos expression in IL [60]. In line with this findings, others founds that levels of Zif268 increased in PL upon contextual fear retrieval while levels of Arc mRNA increased in IL upon extinction retrieval [25, 61]. Moreover, extinction-deficient mice have reduced cFos and Zif268 levels in IL implying that reduced IL activity may lead to impaired fear extinction [62]. Together these data suggest that PL and IL IEG expression is context-specific with PL activation during a high fear state and IL activation during a low fear states.

However, immediate early gene studies investigating the specific role of these subregions in fear learning have revealed some overlapping functionality. For example, both PL and IL exhibited greater cFos expression after fear conditioning suggesting that PFC activity is important for new learning [63, 64]. Injecting an antisense oligonucleotides against cFos simultaneously into both PL and IL 12 h before conditioning attenuated fear responses during an extinction session [63]. Interestingly, this effect was seen with simultaneous manipulations of PL and IL suggesting there is functional overlap between the regions. In support of this idea, a previous study showed PL and IL had similar cFos and Zif268 expression upon recent and remote contextual fear retrieval [65]. These data that PL and IL activity can fluctuate similarly during the acquisition and extinction of conditioned fear.

In conclusion, the PFC plays a critical role in fear and anxiety disorders. Animals studies demonstrate that mPFC function is important for fear acquisition, fear extinction and fear discrimination learning [4, 5, 22]. Similarly, human studies have shown that PTSD symptoms such as fear generalization may be due to impaired PFC functionality [2, 66]. Together these data suggest IEG studies are effective for circuit-level analyses which reveal that proper PFC function is crucial for appropriate adaptive responses to fearful stimuli.

1.4 Genetic tagging systems

Activity-based IEGs are useful in identifying and then genetically modifying neurons naturally activated by contextual experiences. Recent studies using this approach have used opto- and chemogenetic regulators of neuronal activity so that neurons naturally recruited during learning can be artificially reactivated to directly test their role in environmental encoding. These advances represent a powerful tool for testing the principles by which the brain encodes external information and how these circuits are modified with learning.

One advantage of IEGs such as Arc, cFos, and Zif268 is that they provide a transcriptional marker for environmentally activated neuronal ensembles. This was first shown in transgenic mouse in which a promoter element from the cFos gene was used to drive the expression of a lacZ protein marker [67]. Following seizure, the lacZ marker was strongly induced throughout the brain. In addition, the suprachiamastic nucleus, a region involved in circadian rhythm regulation, strongly expressed the lacZ marker after exposure to a light pulse during the animal's dark cycle. These early data suggested that IEG-driven genetic tagging systems may be valuable tools to study the circuitry encoding contextual information. More recently, a number of transgenic mouse lines have been developed which drive green fluorescent protein (GFP) in an activity-dependent manner [68, 69]. Using fluorescent markers compatible with live tissue imaging allows for recording neurons in brain slices or anaesthetized animals specifically from activated cFos positive cells. More importantly, fluorescent tagging can be used to determine contextual or memory representations which are cells spontaneously activated by an

environment. One study used a transgenic mouse in which GFP was driven by the Zif268 promoter and they found slowly developing and highly sparse contextual representations that were stable for up to 2 months after fear conditioning [70]. Similar results were obtained using a cFos GFP reporter system to examine the formation of spatial representations in the retrosplenial cortex, indicating that various regions within the cortex encode contextual information [71].

To investigate the function of these activated neuronal ensembles, researchers have developed IEG-based transgenic mouse lines that allow the expression of effector molecules in neurons that are activated at a specific time point. By using the cFos promoter alongside the tetracycline system for control of gene expression, the Reijmers group produced a bi-transgneic mouse in which neurons naturally activated during a given tagging window could be genetically modified to express essentially any gene [69]. This bi-transgenic approach requires that two transgenes be introduced into the same animal. The first transgene consists of the cFos promotor driving the expression of tetracycline transactivator (tTA), which is transcription factor that can be regulated with the antibiotic doxycycline (Dox) [72]. The second transgene carries a tetracycline-responsive element promoter (TRE) to drive the expression of any gene of interest. When Dox is present in the diet of the animals, the cFos promoter will drive expression of tTA in activated neurons, however, transcription of the second TRE-linked gene is blocked. When Dox is removed, a tagging time window opens during which neurons that are sufficiently active to induce cFos-tTA will express the TRE-linked transgene via tTA-driven transcription at the TRE promoter. To validate their model, investigators used

these mice to determine which neuronal ensembles in the amygdala are activated with contextual fear learning and fear retrieval. Using a long-lasting lacZ marker protein in neurons activated during learning and comparing the degree to which neurons are reactivated during fear retrieval, they found that amygdala neurons activated during learning are initially responsive primarily to the shock (US) and that after training these neurons were activated by the context (CS) alone [69]. Moreover, the degree of amydalar reactivation correlated with the fear memory expression. These data suggest a model where pairing of CS and US during fear conditioning produces plasticity within the circuit that allows the CS to recruit US neurons. These results are consistent with previous literature on the amygdala circuit during fear conditioning and therefore provides validation for these genetic models.

Next, researchers developed a more direct test of the functional relevance of these distributed neuronal ensembles by using a cFos based genetic tagging system in conjunction with channelrhodopsin (ChR2) [73] to locally stimulate the hippocampus [74]. In this experiment, a cFos-tTA transgenic mouse line was used to express a virally delivered TRE-ChR2 transgene specifically in the dentate gyrus of the hippocampus. Animals were then contextually fear conditioned to allow the expression of ChR2 in the learning-induced population of neurons. Then the animals were moved to a neutral context that did not induce fear and light-induced firing of ChR2-labeled dentate gyrus neurons was able to produce a fear response. In a separate study using the same technique [75], dentate gyrus neurons activated by exploring a specific context (ctxA), without foot shock, were labeled with ChR2. Artificial stimulation of these neurons with light was

then paired with a foot shock in a different context (ctxB) and when animals were placed back into ctxA, where they never received a shock, they showed a fear response. These data suggest that artificial stimulation of a distributed cFos-positive neuronal ensemble within the hippocampus labeled during exploration of ctxA is sufficient to produce a neuronal representation of that complex environment. The hippocampal formation has been the focus of study in regards to spatial and contextual learning, however, similar results have been reported in the neocortical region called the retrosplenial cortex, an output area of the hippocampus with projections to a wide variety of other cortical areas [76]. Investigators found that stimulation of naturally activated ChR2-labeled neurons in the retrosplenial cortex at the time of contextual fear conditioning was sufficient to produce a fear response [77]. These data suggest that at the time of learning, a neuronal ensemble representing the context forms in the neocortex as well as the hippocampus. Next, to investigate the contribution of each two neuronal representation of context, researchers pharmacologically inactivated the hippocampus and although this produced an impairment in natural context recall, this effect could be rescued by direct stimulation of neuronal ensembles in the retrosplenial cortex. This suggests that the contextual representation in the retrosplenial cortex is downstream of the hippocampus and may function independent of the hippocampal memory representation.

In conclusion, during contextual fear conditioning, artificial reactivation of learning-induced neuronal ensembles in either the hippocampus or the neocortex can substitute for the context itself and cause irrational fear in novel and neutral environments. Taken together these data reveal that activation of a sparsely distributed

sensory-induced neuronal population is sufficient to reproduce a complex sensory experience. These advances in activity-based genetic systems represent a powerful tool for testing the circuit-level mechanisms by which the brain encodes contextual information and the modification of these circuits upon learning.

1.5 Neuronal circuits underlying fear related disorders

Similar to the animal studies described above, human neuroimaging studies have revealed that the amygdala, hippocampus, and PFC are dysfunctional in the common fear disorder, posttraumatic stress disorder (PTSD). PTSD is a disabling psychiatric disorder that has a lifetime prevalence of 6.8% in adult Americans [78]. PTSD is characterized by recurrent recall of traumatic events such as domestic violence, car crashes, or military experience typically months or years after the traumatic event has occurred [79-81]. A traumatic event is typically relived through recollections, flashbacks or nightmares that can lead to anxiety and helplessness. Typically, PTSD patients display fear over-generalization and deficiency in extinction of fear memory which may lead to irrational fear and anxiety [2]. Human studies are in conjunction with animal studies which suggest dysfunction in the amygdala-hippocampus-PFC circuit leads to impaired fear memory specificity and fear extinction.

Previous research has demonstrated that the etiology of PTSD is associated with hyperarousal of the amygdala [2, 66]. Indeed, several neuroimaging studies have shown increased amygdalar activity in PTSD during the presentation of traumatic narratives [82], combat sounds [83, 84], combat photographs [83, 85] and during acquisition of fear conditioning [66]. However, investigators have shown that amygdala hyperactivity is not equally present among all PTSD patients. In one study, PET scans showed that upon exposure to emotional and aversive stimuli, there was no increased amygdala activity among PTSD patients compared to the control group [86]. It has been postulated that experience itself may affect differences in the functionality of neuronal circuits for

emotional processing in PTSD, social anxiety, and specific phobia. One meta-analysis study showed increased amygdalar activity in both PTSD and control groups during presentation of negative emotional stimuli yet this activation was smaller in the social anxiety and specific phobia cases [87]. Moreover, the level of amydala activity was shown to positively correlate with severity of symptoms [82, 87]. These results indicate that hyperarousal of the amygdala during experience with negative, emotional stimuli is a common hallmark of fear related disorders. Other researchers have found a relationship between smaller amygdala volume, increased levels of fear conditioning and excessive stress response in mice [88, 89]. Human research also suggests there is a relationship between smaller amydalar volume, stronger fear conditioning, and stress response in PTSD patients [90]. A meta-analysis composed of 11 studies pointed out a decreased volume within the left amygdala of PTSD patients as opposed to control groups [91]. In an effort to relate PTSD symptom severity and amygdala volume, a recent study used high resolution MRI scanning to show that subject with more severe PTSD symptoms showed an indentation in the right amygdala [92]. However, not all studies have shown changes in amygdala volume associated with PTSD. Other studies including two meta-analyses failed to identify differences in amygdalar volume in PTSD patients versus healthy controls [93-96]. In conclusion, the etymology of fear related disorders such as PTSD is associated with smaller amygdala volume and increased amygdalar activity to traumatic stimuli however these clinical correlates are not universal and may depend on symptom severity.

The hippocampal formation plays a key role in the control of stress responses, declarative memory, and fear conditioning thus making it one of the most investigated structures in regards to PTSD [2, 97]. Trauma and stress have been shown to induce synaptic degeneration and neuronal atrophy in the hippocampus [98, 99] while many studies have shown decreased hippocampus volume [90, 100-102]. In fact, in one of the largest PTSD meta-analyses which included data from over 1800 subjects and 16 cohorts, suggests there is a connection between PTSD and lowered hippocampal volume [103]. However, these results are not consistent across all studies [104-106]. In terms of activation, several studies have shown that PTSD patients have deficits in hippocampal activity when solving tasks related to verbal declarative memory [107, 108]. One study investigating blood flow changes showed decreased regional blood flow in the hippocampus during recollection of non-emotional material [109]. These data together suggest that decreased hippocampal volume and activity are associated with the etymology of PTSD. However, based on this research it is not possible to confidently claim whether decreased hippocampus volume is considered a cause or a result of PTSD. One study revealed that smaller hippocampus volume may constitute be a risk factor for developing PTSD after a traumatic event [110]. It may be possible that a diminished hippocampus presents both an increased risk for developing PTSD and a consequence of trauma.

Neuroimaging studies have found that two regions within the PFC, the anterior cingulate cortex (ACC) and ventromedial prefrontal cortex (vmPFC), are implicated in PTSD. In a PET study, PTSD patients failed to activate the ACC during exposure to

traumatic versus neutral scripts when compared to sexual abuse survivors not diagnosed with PTSD [83]. More recently, it was found that survivors of a mining accident with acute PTSD had decreased ACC activation in response to traumatic versus neutral pictures when compared to mining accident survivors without PTSD [111]. Within the vmPFC, two separate studies found less activation in medial frontal gyrus in response to traumatic stimuli in PTSD patients relative to those without [82, 112]. In conjunction with these results, others found decreased ACC and medial frontal gyrus activation in a traumatic imagery condition among those with PTSD compared to traumatized individuals without PTSD [113]. Moreover, several MRI studies have reported decreased frontal cortex volume in PTSD [93, 114, 115]. Taken together these research studies suggest that decreased prefrontal activity and volume is associated with PTSD. Functional neuroimaging studies have found that the vmPFC is also involved during the recall of fear extinction in humans. In one study, activation of the amygdala and vmPFC was observed as participants acquired conditioned fear and extinguished their conditioned fear in the same session and recalled this extinction learning the following day. During the recall of the extinction, activation of the vmPFC predicted extinction success and correlated with amygdala activity [116] which is consistent with animal studies showing that the infralimbic cortex inhibits the amygdala during extinction recall [27]. In a morphometric MRI study, investigators found that cortical thickness was directly correlated with the magnitude of extinction recall [117]. Next, they further extended these results to investigate extinction recall the day following extinction training using fMRI. PTSD patients had reduced activity in the vmPFC and hippocampus, yet increased ACC

activity during extinction recall [2]. Moreover, there was a positive correlation between the degree of extinction recall and activity in both the vmPFC and the hippocampus across all subjects. A subsequent study showed that during extinction recall, participants with PTSD had both reduced vmPFC activity and increased ACC activity during exposure to the extinction context [118]. These findings indicate that hyperactivation of the ACC and hypoactivation of the vmPFC may lead to impairment in fear extinction and an inability to use contextual cues to predict safety leading to overgeneralized fear, a clinical hallmark of PTSD.

Ultimately, the etiology of fear related disorders such as PTSD involves structural and functional dysfunction of the following regions: amygdala, hippocampus and PFC. Neuroimaging research have revealed that increased activation of the amygdala accompanied by diminished activity of the PFC is associated with the etiology of PTSD. Additionally, evidence suggests that hippocampal volume, integrity and functionality may be also impaired in PTSD. The current model suggests that decreased PFC and hippocampal functionality leads to reduced inhibitory control of the amygdala that then drives increased amydalar activity leading to irrational fear and anxiety [2].

Chapter 2.1: Prefrontal consolidation supports the attainment of fear memory accuracy

A version of this chapter is published in:
Vieira PA, Lovelace JW, **Corches A**, Rashid AJ, Josselyn SA, Korzus E: Prefrontal consolidation supports the attainment of fear memory accuracy. *Learn Mem* 2014, 21(8):394-405

Abstract

The neural mechanisms underlying the attainment of fear memory accuracy for appropriate discriminative responses to aversive and non-aversive stimuli are unclear. Considerable evidence indicates that coactivator of transcription and histone acetyltransferase cAMP response element binding protein (CREB) binding protein (CBP) is critically required for normal neural function. CBP hypofunction leads to severe psychopathological symptoms in human and cognitive abnormalities in genetic mutant mice with severity dependent on the neural locus and developmental time of the gene inactivation. Here, we showed that an acute hypofunction of CBP in the medial prefrontal cortex (mPFC) results in a disruption of fear memory accuracy in mice. In addition, interruption of CREB function in the mPFC also leads to a deficit in auditory discrimination of fearful stimuli. While mice with deficient CBP/CREB signaling in the mPFC maintain normal responses to aversive stimuli, they exhibit abnormal responses to similar but non-relevant stimuli when compared to control animals. These data indicate that improvement of fear memory accuracy involves mPFC-dependent suppression of fear responses to non-relevant stimuli. Evidence from a context discriminatory task and a newly developed task that depends on the ability to distinguish discrete auditory cues indicated that CBP-dependent neural signaling within the mPFC circuitry is an important

component of the mechanism for disambiguating the meaning of fear signals with two opposing values: aversive and non-aversive.

Introduction

The ability to discriminate between similar, yet different, stimuli is critical for cognitive functioning [119] and is referred to as memory specificity or memory accuracy. Failure to discriminate between aversive and non-aversive stimuli during recall may indicate decreased memory resolution (i.e. reduced access to memory details) or generalized fear or both, and may lead to inappropriate stimulus generalization. Generalization is not always inappropriate and this type of reduced fear memory accuracy is observed when one responds the same to two stimuli that are not identical. After initial generalization, fear memory accuracy can be increased through additional experiences with reinforced aversive stimulus and non-reinforced non-aversive stimulus. Conversely, overgeneralized fear is a typical symptom of anxiety disorders including phobias and posttraumatic stress disorder (PTSD), which are triggered by cues resembling traumatic experience in a secure environment [1]. Studies of neural substrates and mechanisms underlying memory resolution are focused on the hippocampal circuit [120, 121]. Recent studies also implicate prefrontal circuitry in the contextual fear memory specificity and generalization [3, 122] or discrimination of more discrete multiple odor stimuli [123].

Regulatory mechanisms direct cAMP response element binding protein (CREB)-dependent transcription subsequent to learning-induced molecular changes in which neurons play a pivotal role in the conversion of short-term to long-term memory across species [124-129]. Phosphorylation of CREB at serine 133 is required for the recruitment of the chromatin remodeling factor with intrinsic acetyltransferase activity CREB binding protein (CBP), both events critical for CREB-dependent transcription [130, 131]. CBP

integrates multiple signaling pathways via direct interactions with independently regulated multiple transcriptional factors and components of transcriptional machinery. In addition, CBP comprises enzymatic activity referred to as HAT (histone acetyltransferase), which enables acetylation of conserved lysine amino acids on proteins by catalyzing the transfer of an acetyl group of acetyl CoA to form ε-*N*-acetyl-lysine [132, 133]. Initially, histones were considered as primary natural substrates for CBP enzymatic activity. However histones are not the only targets for CBP's HAT activity and a number of non-histone potential targets for CBP's HAT activity have been found, including proteins regulating chromatin remodeling and gene expression such as p53 [134], CREB [135] and many others [136-140]. The impact of histone and non-histone protein acetylation by CBP is not fully understood. Despite uncertainty in respect to how CBP controls neuronal function via its interaction with multiple regulatory proteins and acetyltransferase activity, considerable evidence indicates that CBP is a critical component of the neural signaling underlying cognitive functioning [141-149]. However, it is difficult to separate developmental defects, compensatory developmental effects and acute function in the adult brain of a gene with pronounced developmental functions. To avoid developmental confounds, four independent manipulations to downregulate CBP acetyltransferase activity specifically in the adult living brain have been reported to date. Acute CBP hypofunction targeted specifically in adult mice by means of Tet-regulatable expression of CBPΔHAT targeted to excitatory forebrain neurons [142] or hippocampal focal knockout of CBP [145] or intra lateral amygdala infusion of c646, a selective pharmacological inhibitor of p300/CBP activity, shortly following fear conditioning

resulted in selective impairment of long-term potentiation [145, 148] and long-term memory [142, 145, 148]. In addition, ablation of CBP in the adult brain resulted in impaired environmental enrichment-induced neurogenesis [150], which suggest additional role of CBP in adult neurogenesis-dependent enhancement of adaptability toward novel experiences [121, 151]. These data strongly implicate CBP acetyltransferase activity in neural epigenetic signaling underlying long-term memory consolidation.

Although there has been extensive research into the function of the PFC during information acquisition and retrieval, a fundamental question that has escaped resolution is whether CBP-dependent signaling within the prefrontal cortex supports mechanisms in which fear memories are encoded and retrieved without confusion. Using mutant mice expressing dominant negative CBP with eliminated acetyltransferase activity, we have tested the impact of CBP-dependent mechanisms in the mPFC on fear memory accuracy. Evidence from context and auditory discriminatory tasks indicated that the mPFC circuitry is critical for the acquisition of fear memory accuracy necessary for the recognition of subtle differences between aversive and non-aversive stimuli. These data indicate that CBP-dependent signaling in the mPFC is critical for the suppression of fear responses to non-relevant stimuli, which is a necessary process towards improvement of fear memory accuracy.

Materials and Methods

Subjects

C57BL/6J mice were used for all experiments. Prior to any procedure, the mice are weaned at postnatal day 21, housed 4 animals to a cage with same sex littermates, maintained on a 12 hr light/dark cycle, and had *ad libitum* access to food and water. Autoclaved bedding was changed every week. All procedures were approved by the UC Riverside Institutional Animal Care and Use Committee in accordance with the NIH guidelines for the care and use of laboratory mice.

Surgery

The injection protocol has been previously described by Cetin et al. [152]. In this study, 2-4-month-old mice were individually housed and weighed to determine the appropriate drug ratios to use. Atropine was injected to help with breathing (.02 mg/kg body weight). The mice were then placed into an isoflurane chamber to induce anesthesia, mounted in a heated stereotaxic apparatus and supplied with a constant flow of isoflurane/oxygen mix. The scalp was shaved and sanitized with 70% ethanol. The ear bars, bite bar, and nose clamp were adjusted to firmly hold the head in place. A midline incision was made on the scalp, and surgical hooks were placed to keep the skull exposed. Sterile PBS was added as needed to prevent the skull from drying. The head was leveled by comparing bregma and lambda coordinates until they were equivalent. Injection sites were calculated based on bregma coordinates, and a dental drill was used to thin the skull over the injection site. A 27G needle was then used to remove the thinned bone. A 5-µl calibrated glass micropipette (8 mm taper, 8 µm internal tip

diameter) was fitted with a plastic tube connected to a 10-ml syringe and lowered onto a square of Parafilm containing a 4-µl drop of virus. The syringe was aspirated to fill the micropipette with solution before moving it to the injection site. The micropipette was slowly lowered to the proper stereotaxic coordinates and pressure was applied to the syringe to inject 1 µl of solution at a rate of 50 nl/min. After the total volume was injected, the micropipette was withdrawn slowly to avoid backflow, and the injection site was cleaned with sterile cotton swabs. The skin was sutured, and antibiotic was applied to the scalp. Lidocaine was subcutaneously injected near the site followed by an intraperitoneal injection of sterile PBS (30 ml/kg body weight) to prevent dehydration. The mouse was kept warm by placing its cage on a heated plate and injected with buprenorphine (.05 mg/kg) for pain relief. On post-surgical days 1 and 2, the mouse received subcutaneous injections of meloxicam (1 mg/kg) to relieve pain. Animals were monitored for any signs of distress or inflammation for 3 days after surgery. Behavioral experiments were initiated 3 days after surgery. The infralimbic and prelimbic cortices were targeted at the following stereotaxic coordinates: Bregma; AP 1.8, ML±0.4, DV 1.4.

Viruses

Surgical procedures were standardized to minimize the variability of HSV virus injections, using the same stereotaxic coordinates for the mPFC and the same amount of HSV injected into the mPFC for all mice. CBPΔHAT or mCREB and/or EGFP were cloned into the HSV amplicon and packaged using a replication-defective helper virus as previously described [153, 154]. The viruses (HSV/CMV-CBPΔHAT-IRES2-EGFP, HSV/CMV-EGFP and HSV/mCREB-EGFP) were prepared by Dr. Rachael Neve (MIT,

Viral Core Facility). The average titer of the recombinant virus stocks was typically 4.0 x 10^7 infectious units/ml. HSV viruses are effectively expressed in neurons in the PFC. The CBPΔHAT mutant, a dominant-negative inhibitor of CBP-dependent histone acetylation, harbors a substitution mutation of two conserved residues (Tyr^{1540}/Phe^{1541} to Ala^{1540}/Ala^{1541}) in the acetyl CoA binding domain [133]. It has been also demonstrated that CBPΔHAT lacks histone acetyltransferase activity [142] and blocks c-fos expression in neurons [142]. The dominant negative CREB mutant (mCREB) carries substitution mutation Ser^{133} to Ala^{133}. Previous studies indicate that mCREB decreased CREB function and block neuronal CREB dependent gene expression [130, 131, 155, 156].

Behavioral Assays

Fear conditioning was performed as previously described [142]. Fear conditioning training was performed in the fear conditioning box from Coulburn Instruments Inc. After being handled, individual mice were exposed to context A. Context A was the unmodified fear conditioning box, which was placed inside of a sound attenuated chamber with the house light and house fan turned on. Performance was scored by measuring freezing behavior, the complete absence of movement [157]. Freezing was scored and analyzed automatically by a Video-based system (Freeze Frame software ActiMetrics Inc.). Video was recorded at 30 frames per s. The Freeze Frame software calculated a difference between consecutive frames by comparing gray scale value for each pixel in frame. Freezing was defined based on experimenter observations and set as sub-threshold activity for longer then 1 s. Freezing was expressed as a % Freezing, which was calculated as a percent of freezing time per total time spent in the testing chamber.

The chamber was cleaned in between trials with Quatracide, 70% ethanol, and distilled water.

For contextual fear conditioning, mice were trained in a standard fear conditioning chamber (Coulburn Instruments Inc.). The individual mice were exposed to context A for 180 s and received a 0.75 mA, 2 s foot shock (context A – foot shock pairing). The animals were then left for another 180 s inside the chamber. For the memory retention test, the mice are placed back into the training chamber for 180 s. Freezing was scored and analyzed automatically as described above.

For cued fear conditioning, mice were trained in a standard fear conditioning chamber (Coulburn Instruments Inc.). After a three-minute baseline period, one, two, or three-20 second tones (2800 Hz, 75dB) were played and a shock (0.75 mA, 2 sec) was delivered during the final 2 sec of the tone. Twenty-four hours, mice were placed in a novel enclosure and after a three-minute baseline exposure, a series of three tones identical to that given in the training session was played. Freezing was scored and analyzed automatically as described above.

The context discrimination assay was preformed similarly as previously described [43]. After being handled, individual mice were exposed to context A one day before training. The protocol included 14 days of training, which was divided into three phases: initial training phase, generalization test and discrimination phase (Fig. 2.1). During the initial training phase (day 1), mice were placed in the context A for 180 s followed by a single foot shock and left for another 60 s inside the chamber. Context A (CS+) was the unmodified fear conditioning box (Coulburn Instruments Inc.), which was placed inside

of a sound attenuated chamber with the house light and house fan on. The chamber was cleaned with Quatricide, 70% ethanol, and distilled water. For generalization test and during discrimination phase, the individual mice were exposed to Context A for 180 s and received a 0.75 mA, 2 s foot shock, and left for another 60 s inside the chamber. Four hours later, the mice were exposed to the similar Context B (CS-) for 242 s and received no footshock. Context A and B were similar but not the same. Context B was the modified fear conditioning chamber, with angular wall inserts, house fan off, and scented with Simple Green. Thus animals were exposed to CS^+ 13 times before the final test. The order of exposure to different contexts was counter balanced. Additionally, the context cues themselves were counter balanced within each group in order to isolate the effect of the CS+.

The auditory discrimination task is divided into three phases: initial training phase, generalization test, and discrimination phase (Fig. 2.2). The conditioned stimuli (CS) for auditory fear conditioning were 20-s trains of frequency modulated (FM)-sweeps for a 400-ms duration, logarithmically modulated between 2 and 13 kHz (upsweep) or 13 and 2 kHz (downsweep) delivered at 1 Hz at 75 dB. After habituation, the CS+ was paired with a foot shock (2 s, 0.75 mA). The onset of the US coincided with the onset of the last sweep for the CS. For fear conditioning acquisition (days 1-3; initial training phase), the animals were presented with a single US-CS pairing per day. The FM-sweep Fear Retrieval (day 4) and Generalization (day 4-5) were tested (freezing to 3x CS^- for 30 s followed by 3x 30 s CS^+ without US; 3 min baseline and 3 min ITI) in context C, which significantly differed from the training chamber (context A). The discrimination phase of

FM sweep direction discrimination training was performed over three sessions a day for 6 days (days 7-12): Session 1 was the performance test, Session 2 was the presentation to 1x UC-CS+ pairing after 3 min baseline, and Session 3 was the presentation to the US-CS- pairing after a 3 min baseline. The CS+ and CS- were counterbalance such that half of the CS+ group was upsweep and the other half CS+ was downsweep.

Histology

Mice were anesthetized using nembutal (200mg/kg, i.p. injection) and transcardially perfused first with PBS and then 4% PFA. The extracted brain was soaked in 4% PFA overnight and then transferred to PBS until histological sectioning. In this study, 100-μm-thick sections of the mPFC were obtained using a Compresstome VF-300 (Precisionary Instr., Greenville, NC) and placed in a 24-well plate for free-floating immunohistochemistry (IHC) according to a previously described protocol [142]. The sections are washed 3 times for 10 min in a wash buffer (PBS, 0.3% Triton x-100, 0.02% NaN_2) followed by a 1-hr incubation in blocking buffer (5% normal goat serum in washing buffer), followed by a 10-min incubation in the wash buffer. The sections were incubated overnight at 4C° with primary antibodies: anti-NeuN (Millipore 1:2000), chicken anti-GFP (Molecular Probes, 1:1000); anti-acetyl-Histone H3 (Millipore, 1:2000) or anti-acetyl-Histone H4 (Millipore, 1:2000). After three washes with the wash buffer, the sections were incubated with secondary antibodies (Alexa647-goat anti-mouse IgG; Alexa488 goat anti-chicken IgG; Alexa647-goat anti-rabbit IgG; Molecular Probes, 1:1000), in blocking buffer for 4 hr at room temperature. The sections were washed again three times with the wash buffer before mounting for viewing. Negative control slices

were performed for each row of the well plate, undergoing the same IHC procedure in addition to receiving primary antibodies. After immunostaining, the tissue was mounted directly onto glass slides, covered, and sealed with nail polish before imaging.

Imaging

The slides were placed on the stage of an Olympus FV1000 laser scanning confocal microscope controlled using the FluoView software. GFP, and Alexa-647 were imaged using 473-nm, and 647-nm lasers, respectively. The background fluorescence was measured and subtracted for each image. The fluorescence intensity was compared to the negative control slices, which did not receive any primary antibodies. Immunostained tissue was analyzed using a semi-automatic Olympus FV1000 laser scanning confocal microscope controlled by the FluoView software. Multiple brain sections were imaged using identical microscope settings. Eighty-micrometer z-stacks were obtained from the PL region in the mPFC, and ROI analysis was used for quantification. The background fluorescence was measured for each imaged and then subtracted. The intensity quantification was performed using the FluoView Olympus software and NIH Image J.

Histone acetylation assay

Individual mice were trained on a fear conditioning paradigm in which they were presented with a 20 sec auditory stimulus followed immediately by a 2 sec foot shock (0.75 mA intensity). The auditory stimulus is the same used for behavioral training in which logarithmically modulated upward (2 kHz-13 kHz) frequency-modulated sweeps are presented in 400ms bouts at a 1 Hz frequency for a total duration of 20 sec. 3 min after the foot shock, mice were placed in their home cage for 25 min undisturbed.

Immunohistology and imaging were performed as described above. The region of interest (ROI) was a 5 μm circle placed on cells expressing GFP within cortical layer 2/3 in mPFC and fluorescence corresponding to acetylated histone H3 or H4 was measured from randomly selected 50-60 cell per hemisphere. The fluorescence intensity quantification was performed on original images by the use of Olympus Fluoview software.

Data analysis

The experimenters were blind to the group conditions. Data are expressed as the means ± SEM. N indicates number of animals unless stated otherwise. Statistical analysis was performed using Excel (Microsoft Inc.) or SPSS (IBM Inc.). The Student's *t*-test or ANOVA was used for statistical comparisons. Pearson's correlation (*r*) was used as an *effect size*. In cases where the repeated measures ANOVA (RM-ANOVA) was utilized and assumptions of sphericity were violated (via Mauchly's Test), the analysis was performed using the Greenhouse-Geisser correction. Where applicable, *post hoc* analysis with Bonferroni correction was performed for multiple comparisons, which allows for substantially conservative control of the error rate. A p-value of <0.05 was considered statistically significant. The asterisks indicate statistical significance: *, $p < 0.05$, **, $p < 0.01$, ***, $p < 0.001$ and n.s. indicates not significant.

Results

Impairment of contextual fear memory specificity in CBPΔHAT^{PFC} mice

The CBPΔHAT mutant, a dominant-negative inhibitor of CBP-dependent lysine acetylation, harbors a substitution mutation of two conserved residues (Tyr^{1540}/Phe^{1541} to Ala^{1540}/Ala^{1541}) in the acetyl CoA binding domain [133, 142]. This mutant has no intrinsic acetyltransferase activity due to its inability to interact with a donor of acetyl group, acetyl-CoA, but retains all protein-protein interaction domains [133]. When expressed acutely in adult excitatory neurons, CBPΔHAT functions as a specific blocker of long-term memory consolidation without affecting information acquisition or short-term memory [142]. To test the impact of CBP-dependent signaling in the medial prefrontal cortex (mPFC) on fear memory specificity, we generated mice expressing CBPΔHAT and eGFP in the mPFC using virus-mediated gene transfer (referred to as CBPΔHAT^{PFC} mice) (Fig. 2.1A). For control mice, we injected virus-expressing eGFP only in the mPFC. Cytohistological analysis of brain tissue isolated from CBPΔHAT^{PFC} and control animals revealed that the majority of cells expressing mutant protein in the mPFC were neurons (Ctrl: 93.85 ± 0.006%, n = 3; CBPΔHAT^{PFC}: 92.06 ± 0.012 %, n = 3; $t_{(2)}$ = -0.03, p = 0.511, r = 0.013, data not shown). Conditioned CBPΔHAT^{PFC} mice display decreased levels of acetylated histone, H3, (t-test: t(10) = 2.38 , p = 0.0382, r = 0.6013; Ctrl: 1 ± 0.06, n = 5, CBPΔHAT^{PFC}: 0.74 ± 0.06, n = 7) and acetylated histone, H4, (Ac-H4; right panel; t-test: t(10) = 2.9718 , p = 0.0140, r = 0.6848; Ctrl: 1 ± 0.04, n = 6, CBPΔHAT^{PFC}: 0.67 ± 0.10, n = 6) in cells expressing GFP when compared to conditioned control animals (Fig. 2.1B). These data are consistent with previous studies

reporting decreased levels of acetylated histones in CBP mutant mice [141, 143-147].

We examined CBPΔHAT^{PFC} mice using the fear conditioning paradigm (Fig. 2.1C). CBPΔHAT^{PFC} mice performed similar to controls in the contextual version of the fear conditioning task after a 24 h delay (Fig. 2.1C; Ctrl: 25.78 %, n = 10; CBPΔHAT^{PFC}: 22.14 %, n = 10; $t_{(18)} = 1.28$, $p = 0.108$). To determine whether the mPFC supports fear memory accuracy, we examined CBPΔHAT^{PFC} mice using the context fear discrimination task (Fig. 2.1D) [43]. First, we tested CBPΔHAT^{PFC} and control mice on a generalization task, in which we examined the freezing responses to the novel, Context B, after training on the fear conditioning task to Context A. Context B was similar yet not identical to the training Context A. We found no difference in freezing responses to context A or B in CBPΔHAT^{PFC} and control mice (Fig. 2.1E. Context A vs. B t-test: Ctrl, n = 9, p = 0.805; CBPΔHAT^{PFC}, n = 11, p = 0.851). Thus, CBPΔHAT^{PFC} mice did not demonstrate any obvious abnormalities in fear memory generality during the initial presentation of novel Context B. Next, CBPΔHAT^{PFC} mice and control littermates were trained to distinguish between the conditioned Context A, which was paired with a footshock (CS^+) and an unconditioned Context B, which was not paired with any reinforcement (CS^-) over the multiple training sessions (Fig. 2.1D). This task requires temporal integration because animals learn subtle differences between Context A and B over multiple days with a single exposure to each context once per day. Initially, the control and CBPΔHAT^{PFC} mice generalized their conditioned responses and exhibited similar freezing levels to both the CS^+ and CS^- contexts (block trials 1-4). However, the control animals began to freeze significantly less in response to Context B compared to

Context A after 4 block trials of training, demonstrating the ability to consistently distinguish between similar yet distinct contexts (block trials 5-6) (Fig. 2.1F; RM-ANOVA of trial block and context: Context: $F_{(1,8)} = 9.423$, $p = 0.015$; Trial block, $F_{[158]} = 3.24$, $p = 0.015$; Trial block x Context: $F_{[158]} = 6.58$, $p = 0.0001$; $n = 9$). *Post hoc* analysis using Bonferroni correction for multiple comparisons indicated that differences were present during trial blocks 5 ($p = 0.003$) and 6 ($p = 0.005$). In contrast to the control animals, CBPΔHAT^{PFC} mice failed to distinguish between Context A and B and continued to generalize their conditioned responses throughout all 12 days of training (Fig. 2.1G, RM-ANOVA of trial block and context: Context: $F_{(1,10)} = 5.42$, $p = 0.04$; Trial block: $F_{(2,15)} = 11.09$, $p = 0.002$; Trial Block x Context: $F_{(3,27)} = 1.62$, $p = 0.21$; $n = 11$). These data demonstrated that CBPΔHAT expressed in the mPFC resulted in imbalanced neural processes underlying fear memory specificity and generalization. Analysis of the context discrimination ratio confirmed that at the end of the training, the control animals performed better on the context discrimination task compared to the CBPΔHAT^{PFC} mice. Figure 2.1H shows no difference in performance between control and CBPΔHAT^{PFC} animals on trial block 1 (t-test: $t_{(18)} = 0.02$, $p = 0.99$, $r = 0.005$), but a marked difference on trial block 6 (t-test: $t_{(18)} = 2.60$, $p = 0.018$, $r = 0.52$). These findings demonstrate that CBPΔHAT^{PFC} mice have a strong deficit in context discrimination.

Hypothetically, learning of appropriate responses to fearful and similar but non-relevant stimuli may involve changes in response to aversive or non-aversive stimuli or both across the entire training. Therefore, we analyzed fear responses to Context A (CS+) and, separately, to Context B (CS-) in CBPΔHAT^{PFC} and control mice. There was no

difference in responses to the conditioned stimuli, CS+, between CBPΔHAT^{PFC} and control mice across the entire context discrimination training (Fig. 2.1F-G; RM-ANOVA of trial blocks 1-5 and group: Trial Block X Group: $F_{(2.7,\ 47.9)} = 1.782$, $p = 0.169$). However, CBPΔHAT^{PFC} and control mice responded differently to non-relevant stimuli CS- across training on the contextual discrimination task (Fig. 2.1F-G; RM-ANOVA of trial blocks 1-5 and group: Trial Block x Group: $F_{(2.9,\ 51.6)} = 4.919$, $p = 0.005$). Change in freezing to CS- across the training (freezing delta) was significantly higher in CBPΔHAT^{PFC} when compared to control mice (Fig. 2.1I; t-test: $t_{(18)} = -2.235$, $p = 0.038$). However, calculations of freezing delta consider only performance on trial blocks 1 and 6. In order to include performance of tested animals on each day across the entire training on the context discrimination task (Fig. 2.1F-G; Trial Blocks 1-6), we compared average slopes (α) of fitted learning curves (Fig. 2.1J). The learning of appropriate responses to CS+ shows a positive slope in both control (α= 4.76±1.07; where α= slope) and CBPΔHAT^{PFC} (α= 6.35±1.61) mice while there is no difference between groups (t-test; $t_{(18)} = -0.778$, $p = 0.446$). The learning of appropriate response to CS- shows a negative slope in the control group (α= -0.88±1.34), which significantly improved fear memory accuracy at the end of training (Fig. 2.1F). In contrast, the CBPΔHAT^{PFC} group, which failed to improve fear memory accuracy across training (Fig. 2.1G), showed a positive slope for CS- (α= 4.26±1.4), a marked difference from control responses to the CS- (CS-/Ctrl: α= -0.88±1.34; CS-/CBPΔHAT^{PFC}: α= 4.26±1.4); CS- slope/Ctrl vs CBPΔHAT^{PFC} t-test; $t_{(18)} = -2.614$, $p = 0.018$). In summary, analysis of response patterns to Context A (CS+) and Context B (CS-) in control animals revealed that the improvement of

contextual fear memory accuracy was due to increased freezing behavior to the CS+ and a decrease in freezing to CS-. CBP hypofunction in the mPFC altered the ability to learn discriminatory responses to CS+ versus CS- by disrupting the learning pattern curve for CS- only. These data suggest that the mPFC supports the improvement of contextual fear memory accuracy by controlling the acquisition of appropriate responses to non-relevant stimuli.

Figure 2.1

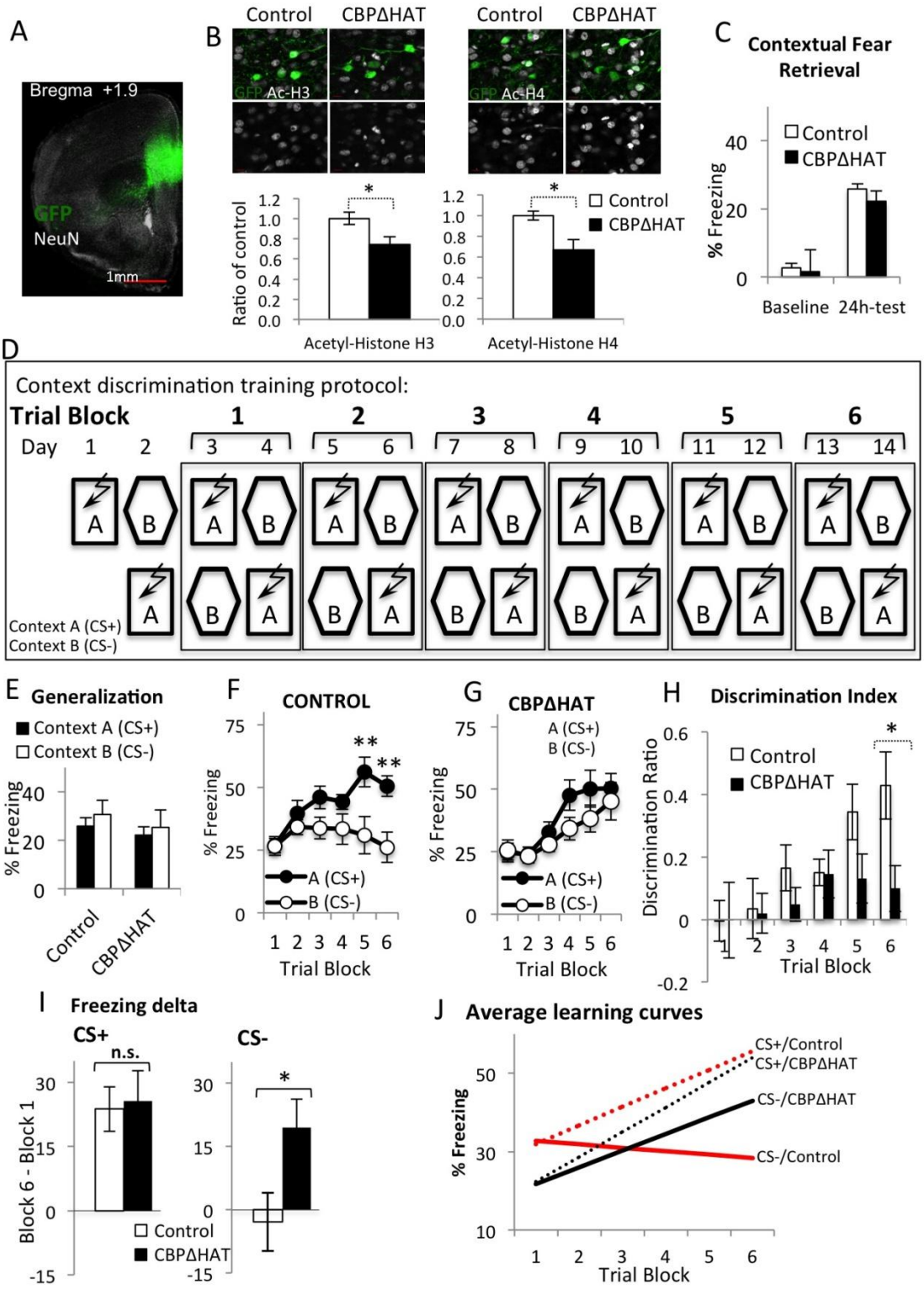
A
Bregma +1.9
GFP
NeuN
1mm
B
Control
CBPΔHAT
Control
CBPΔHAT
GFP Ac-H3
GFP Ac-H4
Ratio of control
Acetyl-Histone H3
Acetyl-Histone H4
Control
CBPΔHAT
C
Contextual Fear Retrieval
% Freezing
Control
CBPΔHAT
Baseline
24h-test
D
Context discrimination training protocol:
Trial Block
1
2
3
4
5
6
Day
Context A (CS+)
Context B (CS-)
E
Generalization
Context A (CS+)
Context B (CS-)
% Freezing
Control
CBPΔHAT
F
CONTROL
% Freezing
A (CS+)
B (CS-)
Trial Block
G
CBPΔHAT
A (CS+)
B (CS-)
% Freezing
Trial Block
H
Discrimination Index
Discrimination Ratio
Control
CBPΔHAT
Trial Block
I
Freezing delta
CS+
CS-
n.s.
Block 6 - Block 1
Control
CBPΔHAT
J
Average learning curves
% Freezing
CS+/Control
CS+/CBPΔHAT
CS-/CBPΔHAT
CS-/Control
Trial Block

(Previous Page) Figure 2.1: Contextual fear memory specificity is deficient in CBPΔHAT^{PFC} mice. (**A**) Viral-mediated delivery to the mPFC. Long-term expression HSV-1 viruses carrying CBPΔHAT (HSV/CBPΔHAT-IRES2-EGFP) or eGFP as the control (HSV/EGFP) were injected into the mPFC. To determine the pattern of GFP-tagged virus expression, the imaged tissue was compared to the Paxinos and Franklin mouse atlas [159] and areas of maximal GFP expression were labeled as injection sites. A representative image of mPFC viral infection showed the precision of our viral-targeting procedures. The pattern of EGFP expression was similar 4 or 20 days after HSV virus injection into the mPFC. Green, GFP; white, NeuN neuronal marker. (**B**) CBPΔHAT blocks acetylation of histone H3 and H4 in the mPFC**.** To determine the effects of viral infection with CBPΔHAT on neuronal signaling, the levels of acetylated histones H3 and H4 were assessed in the brains of infected animals and compared to controls in a standard IHC analysis 25 min after auditory fear conditioning (see Methods). Cells expressing viral CBPΔHAT showed significantly lower levels of acetylated histone H3 and H4 when compared to control animals expressing GFP only. Representative images show GFP (in green) and acetylated histone H3 (Ac-H3, left panel; t-test: $t(10) = 2.38$, $p = 0.0382$, effect size $r = 0.6013$) or acetylated histone H4 (Ac-H4; left panel; t-test: $t(10) = 2.9718$, $p = 0.0140$, effect size $r = 0.6848$) CBPΔHAT^{PFC} mice. 3 animals were used per group. GFP, green; Ac-H3, white; Ac-H4, white; red bar, 10 μm (**C**) Pavlovian contextual fear conditioning was normal in CBPΔHAT^{PFC} mice. CBPΔHAT^{PFC} and control (Ctrl) mice showed normal acquisition and retention of contextual fear conditioning. Contextual fear was tested in Context A at 24 h after a single Context A-foot shock pairing. (**D**) Experimental design for the context discrimination test. Context A and B were similar but not identical. The protocol included 14 days of training. The mice were placed in Context A (CS+) for 180 s followed by a foot shock (arrow), and Context B (CS-) lacked any reinforcement. (**E)** Generalization test shows similar freezing behavior to Context A and a similar but not identical Context B after conditioning. Freezing to Context A after Context A-foot shock pairing was not different in both groups. Freezing in both tested groups were comparable in response to both contexts, indicating that Context A was sufficiently similar to Context B that generalization occurred early in training. (**F**) After the initial generalization of fear conditioned responses, control mice exhibited robust fear memory specificity. (**G**) CBPΔHAT^{PFC} mice exhibited a deficit in context discrimination. (**H)** The context discrimination ratio (DI) was calculated using the freezing responses to CS+ and CS- according to the formula DI = ((Context A - Context B) / (Context A + Context B)). Analyses revealed differences in the performance during trial block 6 between CBPΔHAT^{PFC} and control mice, but not during trial blocks 1 – 5. CBPΔHAT^{PFC} mice, n=11. Control, n=9. (**I**) Change in freezing across training (freezing delta), calculated as the (freezing on Trial Block 6 – freezing on Trial Block 1). There was no difference in responses to conditioned stimuli CS+ between CBPΔHAT^{PFC} and control mice. Change in freezing to CS- across the training was significantly higher in CBPΔHAT^{PFC} when compared to control mice. (**J**) Average learning curves for learning of appropriate responses to CS+ and CS- were calculated based on the performance of control and CBPΔHAT^{PFC} group across the entire training (Fig. 2.1F-G; Block Trials 1 through 6)

followed by fitting the regression line and t-test analysis on the mean of those slopes. The analysis of patterns of responses to CS+ and CS- in control animals tested on the context fear discriminatory task revealed that the improvement of fear memory accuracy was due to incline in freezing to CS+ and a slight decline in freezing to CS- (CS+/Ctrl:α= 4.76±1.07; CS-/Ctrl: α= -0.88±1.34). The learning of appropriate responses to CS+ shows a positive slope (α) in both control and CBPΔHAT^{PFC} mice and there is no difference between groups (CS+/Ctrl:α= 4.76±1.07; CS+/CBPΔHAT^{PFC}:α= 6.35±1.61; CS+ slope/Ctrl vs CBPΔHAT^{PFC} t-test; $t_{(18)}$ = -0.778, p = 0.446). The CBPΔHAT^{PFC} group, which failed to improve fear memory accuracy, showed a positive slope for CS-, a marked difference from control responses to the CS- (CS-/Ctrl: α= -0.88±1.34; CS-/CBPΔHAT^{PFC}: α= 4.26±1.4); CS- slope/Ctrl vs CBPΔHAT^{PFC} t-test; $t_{(18)}$ = -2.614, p = 0.018). The asterisks indicate statistical significance: *, $p < 0.05$, **, $p < 0.01$ and n.s. indicates not significant.

Impairment of auditory memory specificity in CBPΔHAT^{PFC} mice

To evaluate if the deficiency in discrimination was sensory input-specific, we examined CBPΔHAT^{PFC} mice using a novel auditory discrimination task, which tests the ability of subjects to recognize the direction of frequency modulated (FM)-sweeps (Fig. 2.2). This assay includes 3 days of acquisition (single CS^+ footshock pairing) followed by a 24 hr test on Day 4 and a generalization test on Day 4-5. Discrimination training takes place on Days 7-12 in which animals run through 3 sessions: first, they are tested for freezing to CS^+ and CS^- (in Context C); second, they are exposed to CS^+ (or CS^-); third, they are exposed to CS^- (or CS^+).

In parallel experiments, we also microinjected an HSV virus encoding a mutant form of CREB [156] into the mPFC and tested these mice (mCREB^{PFC}) in the auditory discrimination task. CREB is implicated in memory consolidation across variety of species [124-129] and functions immediately upstream of CBP. mCREB (CREB^{S133A} mutation) cannot be phosphorylated at the key serine 133 residue and, therefore, cannot recruit CBP and activate transcription [130, 131]. Thus, we have tested a possible involvement of this well-known mediator of memory consolidation in auditory fear discrimination in parallel experiments to those performed in CBPΔHAT^{PFC} mice.

We first examined FM-sweep fear conditioning acquisition in CBPΔHAT^{PFC} and mCREB^{PFC} mice. All three groups: CBPΔHAT^{PFC}, mCREB^{PFC} and control mice similarly acquired this form of Pavlovian conditioning (Fig. 2.3A; RM-ANOVA of Day and Group: $F_{(4,82)} = 0.975$, $p = 0.426$) and showed the same performance on the 24-hr memory test (Fig. 2.3B; two way ANOVA of Group and Baseline/24 h-Test; Group:

$F_{(2,82)}$ = 0.777, p = 0.463; Baseline/24 h-Test: $F_{(1,82)}$ = 688.3, p = $1.2x10^{-41}$; Group x Baseline/24 h-Test: $F_{(2,82)}$ = 0.205, p = 0.815). These data demonstrate that information acquisition and long-term memory tested after a 24-hr delay on FM-sweep fear conditioning was normal in CBPΔHAT^{PFC} and mCREB^{PFC} mice. We also tested CBPΔHAT^{PFC}, mCREB^{PFC} and control mice on generalization tasks, in which we examined their freezing responses to a novel downward FM sweep (CS-) after training on an upward FM-sweep (CS+) fear conditioning task. The generalization test revealed that there was no difference in the freezing responses to the CS- or CS+ between CBPΔHAT^{PFC} , mCREB^{PFC} and control mice (Fig. 2.3C; ANOVA of FM-sweep direction and group during day 4 and 5: Group: $F_{(2,82)}$ = 0.37, p = 0.692; ANOVA of FM-sweep direction: $F_{(1,82)}$ = 3.458, p = 0.067; Group x FM-Sweep Direction: $F_{(2,82)}$ = 0.090, p = 0.914). These data indicate that strong generalization was observed during days 4 and 5 in all three tested groups.

Next, the animals underwent auditory discrimination training (Fig. 2.3D-F). Initially, the control, CBPΔHAT^{PFC} and mCREB^{PFC} mice generalized their conditioned responses and exhibited similar levels of freezing responses to both CS^+ and CS^- (days 1-2). However, after 2 days of training, the control animals exhibited a higher number of freezing responses to CS^+ and significantly fewer freezing responses to CS^- compared to CS^+, demonstrating the ability to consistently distinguish between similar yet different auditory patterns (days 9-12) (Fig. 2.3D; RM-ANOVA of Day and FM-sweep direction: Day x FM-sweep direction: $F_{(2.2,33.5)}$ = 10.776, p = 0.0002, n = 16). *Post hoc* analysis using Bonferroni correction (alpha = 0.0083) for multiple comparisons indicated that

differences were present during days 9 (CS^+ vs CS^- t-test: $t_{(30)} = 3.632$, $p = 0.001$, $r = 0.55$), 10 ($t_{(30)} = 5.227$, $p = 0.00001$, $r = 0.69$), 11 ($t_{(30)} = 7.540$, $p = 2.1 \times 10^{-08}$, $r = 0.81$) and 12 ($t_{(30)} = 9.253$, $p = 2.7 \times 10^{-10}$, $r = 0.86$) only.

$CBP\Delta HAT^{PFC}$ mice demonstrated a weak ability to discriminate between CS^+ and CS^-, and only successfully discriminated during the last two days of training (Fig. 2.3E, RM-ANOVA of Day and FM-sweep direction: Day x FM-sweep direction: $F_{(5,70)} = 5.071$, $p = 0.001$, $n = 15$). *Post hoc* analysis using Bonferroni correction for multiple comparisons indicated that differences were present during days 11 (CS^+ vs CS^- t-test: $t_{(28)} = 3.149$, $p = 0.004$, $r = 0.51$) and 12 ($t_{(28)} = 3.325$, $p = 0.002$, $r = 0.53$) only. In contrast to the control animals, $CBP\Delta HAT^{PFC}$ mice continued to generalize their conditioned responses after 2 days of training and failed to distinguish between Context A and B during days 9 and 10 (Day 9: $p = 0.286$; Day 10: $p = 0.291$).

Clearly, $CBP\Delta HAT^{PFC}$ mice demonstrated a strong deficit in auditory memory specificity when compared to controls (Fig. 2.3D-E, RM-ANOVA of Group and FM-sweep direction and Day 7-12: Group x FM-sweep direction x Day: $F_{(2.8,81.4)} = 3.033$, $p = 0.037$; Group x FM-sweep direction: $F_{(1,29)} = 7.86$, $p = 0.009$; $CBP\Delta HAT^{PFC}$, n=15; Ctrl, n = 16). Furthermore, analysis of discrimination ratios shows a difference in performance between control and $CBP\Delta HAT^{PFC}$ animals on days 10-12 (Fig. 2.3G. Discrimination Index $CBP\Delta HAT^{PFC}$ vs. Ctrl t-test: Day 10: $t_{(29)} = 2.813$, $p = 0.0087$, $r = 0.46$; Day 11: $t_{(29)} = 3.546$, $p = 0.001$, $r = 0.55$, Day 12: $t_{(29)} = 3.643$, $p = 0.001$, $r = 0.56$; $CBP\Delta HAT^{PFC}$, n=15; Ctrl, n = 16) but not during the initial phase of training. Clearly, control mice show better performance than $CBP\Delta HAT^{PFC}$ mice on auditory discrimination (Fig. 2.3D-E, G).

Taken together, these data demonstrate that CBPΔHAT expressed in the mPFC resulted in abnormal auditory fear memory specificity.

Similarly to CBPΔHAT^{PFC} animals, mCREB^{PFC} mice demonstrated a strong deficit in memory specificity during the discrimination phase when compared to controls on the auditory discrimination task (Fig. 2.3F; RM-ANOVA, Group x FM-sweep direction x Day: $F_{(2.8,79.6)} = 4.644$, $p = 0.006$; mCREB^{PFC}, n=14; Ctrl, n = 16). These data demonstrated that mCREB^{PFC} expressed in the mPFC prevented auditory memory accuracy improvement across the training (Fig. 2.3D). Analysis of the auditory discrimination ratio confirmed that at the end of the training, the control animals performed better on the auditory discrimination task compared to the mCREB^{PFC} mice (Fig. 2.3H, RM-ANOVA of Day and Group: Day x Group: $F_{(2.5,69.0)} = 5.149$, $p = 0.005$; mCREB^{PFC}, n=14; Ctrl, n = 16). Furthermore, analysis of discrimination ratios showed a strong difference in performance between control and mCREB^{PFC} animals on days 10-12 (t-test; day 10: $t_{(28)} = 2.232$, $p = 0.034$, $r = 0.39$; day 11: $t_{(28)} = 4.130$, $p = 0.0003$, $r = 0.62$; day 12: $t_{(28)} = 4.313$, $p = 0.0002$, $r = 0.63$; mCREB^{PFC}, n=14; Ctrl, n = 16).

Next, we performed an analysis of fear responses to upsweep (CS+) and, separately, to downsweep (CS-) in control, CBPΔHAT^{PFC} and mCREB^{PFC} mice tested on FM-sweep direction fear discriminatory task (Fig. 2.3). There was no difference in responses to conditioned stimuli CS+ between CBPΔHAT^{PFC} and control mice across the entire FM-sweep direction discrimination training (Fig. 2.3D-E; CS+/CBPΔHAT^{PFC} vs Ctrl; RM-ANOVA of days 7-12 and group: Day X Group, $F_{(2.8,\ 81.6)} = 0.756$, $p = 0.514$). Similarly, there was no difference in responses to conditioned stimuli CS+ between

mCREB^{PFC} and control mice across entire FM-sweep direction discrimination training (Fig. 2.3D, F; CS+/mCREB^{PFC} vs Ctrl; RM-ANOVA of days 7-12 and group: Day X Group: $F_{(2.8, 79.5)} = 1.808$, $p = 0.155$). An analysis of learning curves (Fig. 2.3J) showed a positive slope to CS+ in control ($\alpha = 2.366 \pm 0.82$) and CBPΔHAT^{PFC} ($\alpha = 2.384 \pm 0.894$) mice or no change in freezing responses to CS+ in mCREB^{PFC} mice ($\alpha = -0.278 \pm 1.15$) across the entire FM-sweep direction fear discriminatory task. In fact, there was no difference in the learning slopes of appropriate responses to CS+ between CBPΔHAT^{PFC} and control groups (Fig. 2.3J; CS+ slope/Ctrl vs CBPΔHAT^{PFC} t-test; $t_{(29)} = -0.015$, $p = 0.988$) or mCREB^{PFC} and control mice (Fig. 2.3J; CS+ slope/Ctrl vs mCREB^{PFC} t-test; $t_{(28)} = 1.906$, $p = 0.067$). However, CBPΔHAT^{PFC} and mCREB^{PFC} mice responded differently to non-relevant stimuli CS- across training on the auditory discriminatory task when compared to normal mice (Fig. 2.3D-E; CS-/CBPΔHAT^{PFC} vs Ctrl; RM-ANOVA of days 1-5 and group: Day X Group, $F_{(3.8, 111,4)} = 6.151$, $p = 0.0002$; Fig. 2.3D,F; CS-/mCREB^{PFC} vs Ctrl; RM-ANOVA of days 1-5 and group: Day X Group: $F_{(3.7, 103.8)} = 5.685$, $p = 0.0005$). When compared to control mice, change in freezing (freezing delta) to CS- across the training was also significantly different in CBPΔHAT^{PFC} (Fig. 2.3I; t-test: $t_{(29)} = -2.798$, $p = 0.009$) and in mCREB^{PFC} mice (Fig. 2.3I; t-test: $t_{(28)} = -2.466$, $p = 0.02$). The marked improvement of discrimination observed on the FM-sweep direction fear discriminatory task in control mice (Fig. 2.3D, G, J) coincides with the significant negative slope of the learning curve for CS- (Fig. 2.3J; $\alpha = -6.176 \pm 1.22$). The CBPΔHAT^{PFC} group, which failed to improve fear memory accuracy across training (Fig. 2.3E, G), shows only a slight negative slope for CS- across the training (Fig. 2.3J; α= -

1.22±0.78) and a marked difference when compared to the CS- slope observed in control animals (Fig. 2.3J; CS- slope/Ctrl vs $CBP\Delta HAT^{PFC}$ t-test; $t_{(29)} = -3.368$, $p = 0.002$). The $mCREB^{PFC}$ group, which did not improve performance on the auditory discrimination task as well (Fig. 2.3F, H), exhibited similar patterns of learning to the $CBP\Delta HAT^{PFC}$ mice. While responses to CS+ do not vary from those observed for control mice (Fig. 2.3I, J), the CS- learning curve is significantly different in $mCREB^{PFC}$ mice compared to control mice (Fig. 2.3J; CS-/Ctrl: $\alpha = -6.176 \pm 1.22$; CS-/$mCREB^{PFC}$: $\alpha = -0.746 \pm 1.03$; CS- slope/Ctrl vs $mCREB^{PFC}$ t-test: $t_{(28)} = -3.347$, $p = 0.002$).

In summary, analysis of patterns of responses to CS+ and CS- in control animals tested on the FM-sweep direction fear discriminatory task revealed that the improvement of auditory fear memory accuracy was due to only slight incline in freezing to CS+ and rapid decline in freezing to CS-. CBP hypofunction or CREB hypofunction in the mPFC altered the ability to learn auditory discriminatory responses to CS+ versus CS- by disrupting the pattern of learning for CS- only, while responses to CS+ remained similar to control mice. Consistent with conclusions regarding contextual fear memory specificity, these data demonstrate that the mPFC supports the improvement of auditory fear memory accuracy by controlling acquisition of appropriate responses to non-relevant stimuli.

Figure 2.2

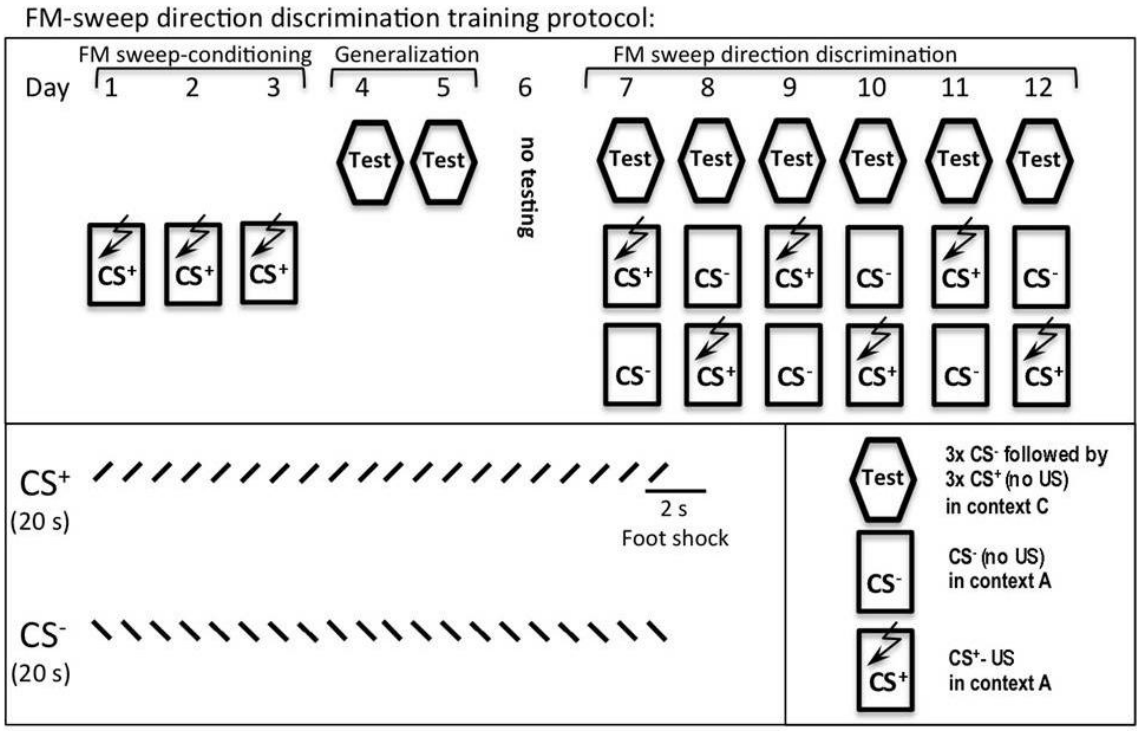

Figure 2.2: Experimental design for the auditory discrimination test. The auditory discrimination task tests the ability of subjects to recognize a direction of FM-sweeps (trains of upward and downward FM-sweeps). The conditioned stimuli (CS) for auditory fear conditioning were 20 sec trains of FM-sweeps for a 400 msec duration, logarithmically modulated between 2 and 13 kHz (upsweep) or 13 and 2 kHz (downsweep) delivered at 1 Hz at 75 dB. As described in methods, these assay includes 3 phases: FM-sweep conditioning (day 1-3), generalization (day 4-5) and FM-sweep direction discrimination training (day 6-12).

Figure 2.3

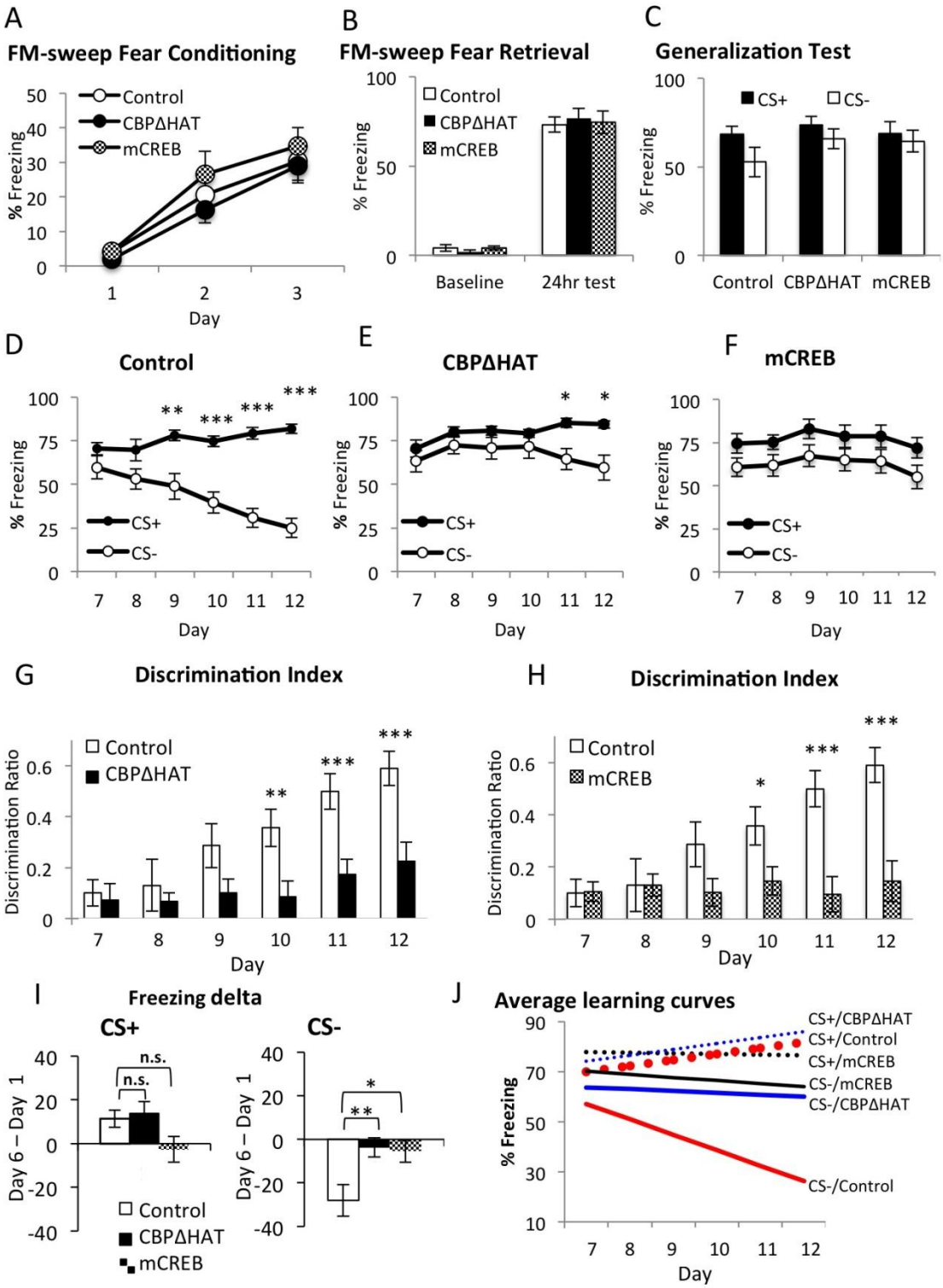
A
FM-sweep Fear Conditioning
Control
CBPΔHAT
mCREB
% Freezing
Day
B
FM-sweep Fear Retrieval
Control
CBPΔHAT
mCREB
% Freezing
Baseline
24hr test
C
Generalization Test
CS+
CS-
% Freezing
Control
CBPΔHAT
mCREB
D
Control
E
CBPΔHAT
F
mCREB
% Freezing
CS+
CS-
Day
G
Discrimination Index
Control
CBPΔHAT
Discrimination Ratio
Day
H
Discrimination Index
Control
mCREB
Discrimination Ratio
Day
I
Freezing delta
CS+
CS-
n.s.
Day 6 – Day 1
Control
CBPΔHAT
mCREB
J
Average learning curves
CS+/CBPΔHAT
CS+/Control
CS+/mCREB
CS-/mCREB
CS-/CBPΔHAT
CS-/Control
% Freezing
Day

(Previous page) Figure 2.3: FM-sweep direction fear memory specificity is deficient in CBPΔHAT^{PFC} mice. (**A-B**)**.** Pavlovian FM-sweep fear conditioning was normal in CBPΔHAT^{PFC} and mCREB^{PFC} mice. CBPΔHAT^{PFC} and mCREB^{PFC} mice showed similar acquisition (**A**) and retention (**B**) of FM-sweep fear conditioning to control (Ctrl) mice. FM-sweep fear was tested in Context C at 24 h after three upsweep-foot shock pairings. (**C**) All three groups (CBPΔHAT^{PFC}, mCREB^{PFC} and Ctrl) show no difference in the freezing responses to CS^+ and CS^- ($p>0.05$) during day 4 and 5 of training, indicating that initially, the CBPΔHAT^{PFC} and mCREB^{PFC} mice generalized responses and did not discriminate between upsweep and downsweep. (**D**) After the initial generalization of fear conditioned responses, control mice exhibited robust fear memory specificity. (**E**) CBPΔHAT^{PFC} mice did not discriminate between upsweep and downsweep and exhibited a deficit in auditory fear memory specificity. CBPΔHAT^{PFC} mice demonstrated a strong deficit in auditory memory specificity when compared to controls (RM-ANOVA, Treatment x context x trial blocks 1-6: $F_{(2.806,\ 81.366)}=3.033$, $p=0.037$). (**F**) Similarly to CBPΔHAT^{PFC}, mCREB^{PFC} mice did not discriminate between upsweep and downsweep and exhibited a deficit in auditory fear memory specificity. (**G**) The FM-sweep direction discrimination ratios (DI) were calculated using the freezing responses to CS+ and CS- according to the formula DI = ((Upsweep - Downsweep) / (Upsweep + Downsweep)). Analyses revealed differences between CBPΔHAT^{PFC} and control mice in the performance during Days 11 - 12 between CBPΔHAT^{PFC} and control mice. CBPΔHAT^{PFC}, n=15; Ctrl, n = 16. (**H**) Analyses revealed differences between mCREB^{PFC} and control mice in the performance during days 11 - 12. mCREB^{PFC}, n=14; Ctrl, n = 16). (**I**) Change in freezing across training (freezing delta), calculated as the (freezing on day 12 – freezing on day 7). There was no difference in responses to conditioned stimuli CS+ between CBPΔHAT^{PFC}, mCREB^{PFC} and control mice. Change in freezing to CS- across the training was significantly higher in CBPΔHAT^{PFC} and mCREB^{PFC} when compared to control mice. (**J**) Average learning curves for learning of appropriate responses to CS+ and CS- were calculated based on the performance of control and CBPΔHAT^{PFC} group across the entire training (Fig. 2.3D-F; days 7 to 14) followed by fitting the regression line and t-test analysis on the mean of those slopes (α). The analysis of patterns of responses to CS+ and CS- in control animals tested on the FM-sweep direction fear discriminatory task revealed that the improvement of auditory fear memory accuracy was due to slight incline in freezing to CS+ and rapid decline in freezing to CS- (CS+/Ctrl: $\alpha= 2.366\pm0.82$; CS-/Ctrl: $\alpha= -6.176\pm1.22$). There was no difference in the learning slopes of appropriate responses to CS+ between CBPΔHAT^{PFC} and control groups (CS+/Ctrl: $\alpha= 2.366\pm0.82$; CS+/CBPΔHAT^{PFC}: $\alpha=2.384\pm0.894$; CS+ slope/Ctrl vs CBPΔHAT^{PFC} t-test: $t_{(29)} = -0.015$, $p = 0.988$) or mCREB^{PFC} and control mice (CS+/Ctrl: $\alpha= 2.366\pm0.82$; CS+/mCREB^{PFC}: $\alpha=-0.278\pm1.15$; CS+ slope/Ctrl vs mCREB^{PFC} t-test: $t_{(28)} = 1.906$, $p = 0.067$). The CBPΔHAT^{PFC} group, which failed to improve fear memory accuracy, showed a positive slope for CS-, a marked difference from control responses to the CS- (CS-/Ctrl: $\alpha= -6.176\pm1.22$; CS-/CBPΔHAT^{PFC}: $\alpha= -1.22\pm0.78$; CS- slope/Ctrl vs CBPΔHAT^{PFC} t-test; $t_{(29)} = -3.368$, $p = 0.002$). Similar to the CBPΔHAT^{PFC} group, the mCREB^{PFC} group did not improve performance on the auditory discrimination task and showed a positive slope for CS-, a marked difference

from control responses to the CS- (CS-/Ctrl: α= -6.176±1.22; CS-/mCREB^{PFC}: α= -0.746±1.03; CS- slope/Ctrl vs mCREB^{PFC} t-test: $t_{(28)} = -3.347$, $p = 0.002$). The asterisks indicate statistical significance: *, $p < 0.05$, **, $p < 0.01$, ***, $p < 0.001$ and n.s. indicates not significant.

Discussion

The present findings are the first evidence of the critical role that the mPFC plays in the attainment of fear memory accuracy for appropriate discriminative responses to aversive and non-aversive stimuli. They add substantially to the understanding of the circuitry and molecular mechanisms underlying fear memory specificity and generalization. We demonstrated that CBP-dependent signaling in the mPFC is required for fear memory accuracy. In addition, fear memory accuracy was also abnormal in mutant mice with disrupted CREB function, which is one of the most widely studied mediators of cellular memory consolidation in Drosophila, Aplysia, and mice [124-129]. The requirement of CBP acetyltransferase activity for memory consolidation has been demonstrated before including acetylatation/deacetylation-targeted pharmacological rescue of memory consolidation in CBPΔHAT mutant mice [141, 142] or late-phase LTP in CBP deficient mutant mice [141], and also in Aplysia [160].

It is important to note that Pavlovian auditory and contextual fear conditioning were intact in CBPΔHAT^{PFC} and mCREB^{PFC} mice. Memory generalization measured immediately after initial fear conditioning was also unchanged in CBPΔHAT^{PFC} and mCREB^{PFC} mice. In addition, there was no difference between tested groups in responses to CS+ across the entire contextual or auditory discriminatory tasks. The abnormal performance of mutant mice in contextual and auditory discriminatory tasks was specific to deficits in responsiveness to CS- only and during later phases of the tasks. These data suggest that the prefrontal circuit is critically involved in learning appropriate responses to non-relevant stimuli that are similar yet not identical to aversive stimuli. These data are

consistent with the previously described function of the PFC in fear memory extinction. Increasing evidence from human [161, 162] and animal [163-171] studies implicate the PFC in extinction of conditioned fear [172, 173] and conditioned taste aversion [174].

There is converging evidence that links fear memory specificity and generality with information processing in the hippocampus-thalamus-PFC-amygdala circuit [3, 119, 120, 122, 175-179]. Involvement of the PFC in context or odor discrimination during information acquisition has been previously studied [3, 122, 123]; however, the contribution of the PFC in the discrimination of auditory patterns, such as FM-sweep direction, has not been previously explored. FM-sweep direction discrimination is important in speech recognition [180] but its underlying neural mechanism is unknown. Auditory fear conditioning has been extensively studied and depends on synaptic plasticity within the amygdala [181, 182] but neural substrates for auditory fear discrimination is less well studied in mice. Recently, it was suggested that stimulus convergence in the auditory cortex is necessary for the associative fear learning of frequency-modulated sweeps [183]. A reduced reliance on FM-sweep direction stimuli in $CBP\Delta HAT^{PFC}$ and $mCREB^{PFC}$ mice indicates that the mPFC supports directly auditory fear memory specificity.

There is a general difference in the patterns of freezing responses to CS+/CS- between auditory and context discrimination in control animals. While the direction of the learning curves remains the same, their steepness varies. In the context discrimination assay (Fig. 2.1), the learning of the appropriate response to CS+ showed a significantly positive slope (Fig. 2.1J; CS+/Control, $\alpha = 4.76 \pm 1.07$; where α= slope),

while the learning of the appropriate response to CS- showed a slight negative slope (Fig. 2.1J; CS-/Control, α= -0.88±1.34). The marked improvement of discrimination observed on the FM-sweep direction fear discriminatory task in control mice (Fig. 2.3D) coincides with the slight positive slope of the learning curve for CS+ (Fig. 2.3J; CS+/Control, α= 2.366±0.82) and the significant negative slope of the learning curve for CS- (Fig. 2.3J; CS-/Control, α= -6.176±1.22). Two possible factors may have an effect on the steepness of learning curves for responses to CS+/CS- in these discriminatory tasks. First, it is possible that there is a "floor" effect on CS- curve in the contextual discriminatory task and a "ceiling" effect on CS+ curve in the auditory discriminatory task that may account for these differences. The initial level of freezing is substantially lower in the contextual discriminatory task (Fig 2.1F-G; ~25% of initial freezing) when compared to the auditory discrimination task (Fig. 2.2D-F; above 75% of initial freezing). Second, it may be more difficult to extinguish responses to non-relevant stimuli (Context B) because of the high complexity of a multimodal contextual stimuli. Conversely, the rapid decline of responses to downsweep (CS-) may result from the lower complexity (single modality) of the auditory stimuli and, subsequently, leads to more effective discrimination training.

Recently, it has been proposed that disruption of the PFC circuit during information acquisition may result in over-generality. Inactivation of prefrontal inputs to the nucleus reuniens resulted in an increased fear generalization to novel contextual stimuli [122]. Our manipulation of the mPFC differed in that we targeted CBP-dependent nuclear processes, which may not produce immediate global effects on firing properties of the mPFC neurons during information acquisition, but rather have effects on the

properties of the neural circuits relevant to long-term memory consolidation. However, it is unclear whether the abnormality in fear memory accuracy found in CBPΔHAT^{PFC} mice resulted from fear driven over-generalization or a deficit to access memory details (i.e. memory resolution).

The difficulties with studying CBP function in cognition is confounded by the high complexity of the CBP protein, which can integrate or antagonize multiple signaling pathways and by its distinctive roles in developing and mature circuits. Haploid insufficiency mutations in CBP [131] or its homolog p300 [184] results in Rubinstein-Taybe syndrome (RTS) [185, 186], which is developmental disorder characterized by severe mental retardation. CBP and p300 both share a very similar molecular structure [187] including intrinsic acetyltransferase activity [188] and are capable to mediate similar cellular functions including CREB-dependent transcriptional activation. The functional differences between these two redundant genes are due to their highly overlapping but different patterns of expression and not yet understood functional specificity. Prenatal lethality in CBP knockout mice demonstrates an essential role of this gene in embryogenesis [189]. CBP hemizygote or CBP mutations targeted to excitatory forebrain neurons using CamKIIα promoter driven expression such as conditional knockout or transgenic mice expressing dominant negative variants display specific deficits in long-term memory but not in short-term memory suggesting that CBP function may support long-term memory encoding. However these results are not consistent across all CBP mutant strains. In one study, CamKIIα-dependent conditional knockout of CBP targeted to excitatory neurons during postnatal brain development

resulted in deficient short-term memory [144]. Although, CamKIIα gene product levels are low during early phases of brain development, a large increase in the expression is usually observed between postnatal days 10 to 30 [190, 191] coinciding with postnatal brain development. Since the developmental time of CBP conditional deletion was not reported in this study, one cannot eliminate developmental confounds underlying the behavioral phenotype. Thus, it is difficult to dissociate between developmental defects, developmental compensatory effects and acute deficits in mutant mice with CBP hypofunction during critical periods of postnatal brain development. However, when manipulation of CBP activity is performed in the adult brain, data consistently implicate CBP acetyltransferase function in neural epigenetic signaling underlying long-term synaptic plasticity and long-term memory consolidation [142, 145, 148]. In addition, testing of CamKIIα positive cells-restricted and adult mice induced CBP knockout mice indicated that environment-induced adult neurogenesis is extrinsically regulated by CBP function in mature hippocampal granule cells [150]. Considering that adult neurogenesis in the hippocampus constitutes an adaptive mechanism to optimally encode contextual information important for memory resolution [121, 151] and CBP mutant demonstrates deficiency in spatial discrimination [150] it is likely that CBP is also involved is adult neurogenesis-dependent long term encoding of contextual information. However, in $CBP\Delta HAT^{PFC}$ or $mCREB^{PFC}$ mice hypofunction was targeted to the mPFC and it is unlikely that this manipulation would have an effect on adult neurogenesis in the hippocampus.

How can CBP enzymatic activity regulate neural function? The regulation of gene expression requires not only an activation of transcription factors but also the recruitment of multifunctional co-activators that are independently regulated and directly involved in the chromatin remodeling underlying epigenetic regulatory mechanisms [192]. For example, recent work demonstrated the importance of chromatin remodeling factors like the SWI/SNF complex in neuronal function underlying memory [193]. While CBP's function as a platform to recruit other required coactivators appears to be indispensable for CREB-dependent transcription, the recruitment for lysine acetyltransferase activity is transcription unit specific and may depend on the structure of chromatin at a specific locus and/or a specific cell type [133, 194]. Changes in histone acetylation are predictive for gene expression [195, 196]. The concordance between the histone acetylation and transcription levels increases over time and the positive correlation between both has been confirmed in genome-wide studies[197-199]. It is important to emphasize that these are correlations only and that causal relationships between histone modification and gene expression in the brain in vivo will require additional investigation. In addition, a number of non-histone proteins have been identified as substrates for CBP [136-140] including CREB [135]. Regardless of the uncertainty of the CBP's acetyltransferase critical target(s), genetic and pharmacological studies have indicated that hypofunction of CBP's acetyltransferase activity interferes with mechanisms that support memory consolidation and reconsolidation in brain neural networks [142, 148]. Current data indicate that the acquisition fear memory accuracy involves CBP-dependent mechanism within mPFC circuitry.

Locomotor activity, anxiety-related responses, and fear conditioning were normal in CBPΔHAT^{PFC} mice, yet these mutant mice showed a strong deficit in fear memory accuracy in both contextual and auditory discrimination assays. Both context and auditory fear discrimination tasks required temporal integration because the animals learned subtle differences between relevant and non-relevant stimuli over many days with a single exposure to both CS+ and CS- per day. Inhibition of a component of neural signaling immediately upstream of CBP by a direct blockade of CREB ability to recruit CBP to the target promoter in the mPFC produced identical effects as CBPΔHAT on the capability of mice to learn the distinction between auditory stimuli. Thus, impairment of either component of CREB/CBP-dependent signaling (CREB phosphorylation or CBP's acetyltransferase activity) within the mPFC circuitry resulted in a deficit in auditory fear memory specificity indicating that the mPFC circuitry supports the disambiguation of auditory fear signals.

How CBP and CREB control memory accuracy in the mPFC is unclear. Both CBP and especially CREB have been implicated in long-term plasticity and memory consolidation in Aplysia, Drosophila and mice. Thus it is possible that long term coding within mPFC network involving LTP-mediated modification of prefrontal circuits is critical during contextual and auditory fear discrimination. This type of plasticity in the mPFC might be required to extinguish CS- responses, which would be consistent with the recognized role of the mPFC in fear memory extinction. In addition, CREB has been strongly implicated in adaptive alteration of neuronal excitability and memory allocation [200] and it is possible that CBP may mediate CREB-dependent changes in neuronal

excitability.

There is converging evidence that links contextual fear memory specificity and generality with information processing in the hippocampus-thalamus-PFC-amygdala circuit [3, 119, 120, 122, 175-179]. Our findings are consistent with the conclusions reported by DeVito et al., who suggested that the mPFC circuit was critical for the acquisition of overlapping odor discrimination problems [123]. Thus, the present findings of the critical role of the mPFC in auditory and context discrimination provides further evidence for the high integration-dependent disambiguation function of the mPFC because similar contexts (or up/down FM-sweeps) were both presented during multiple day training consisting of discontiguous episodes before the animals acquired the ability to properly respond to these signals. These data indicate that certain types of prefrontal dysfunction are likely to contribute to overgeneralized fear, a clinical condition present in anxiety related disorders such as PTSD.

Chapter 2.2: Prefrontal NMDA receptors control fear discrimination and fear extinction

A version of this chapter is published in:
Vieira PA, **Corches A**, Lovelace JW, Westbrook KB, Mendoza M, Korzus E: Prefrontal NMDA receptors expressed in excitatory neurons control fear discrimination and fear extinction. *Neurobiol Learn Mem* 2015, 119:52-62.

Abstract

N-methyl-D-aspartate receptors (NMDARs) are critically involved in various learning mechanisms including modulation of fear memory, brain development and brain disorders. While NMDARs mediate opposite effects on medial prefrontal cortex (mPFC) interneurons and excitatory neurons, NMDAR antagonists trigger profound cortical activation. The objectives of the present study were to determine the involvement of NMDARs expressed specifically in excitatory neurons in mPFC-dependent adaptive behaviors such as fear discrimination and fear extinction. To achieve this, we tested mice with locally deleted *Grin 1* gene encoding the obligatory NR1 subunit of the NMDAR from prefrontal CamKIIα positive neurons for their ability to distinguish frequency modulated (FM) tones in fear discrimination test. We demonstrated that NMDAR-dependent signaling in the mPFC is critical for effective fear discrimination following initial generalization of conditioned fear. While mice with deficient NMDARs in prefrontal excitatory neurons maintain normal responses to a dangerous fear-conditioned stimulus, they exhibit abnormal generalization decrement. These studies provide evidence that NMDAR-dependent neural signaling in the mPFC is a component of neural mechanism for disambiguating the meaning of fear signals and supports discriminative fear learning by retaining proper gating information, *viz.* both dangerous and harmless

cues. We also found that selective deletion of NMDAR from excitatory neurons in the mPFC leads to a deficit in fear extinction of auditory conditioned stimulus. These studies suggest that prefrontal NMDARs expressed in excitatory neurons are involved in adaptive behavior.

Introduction

Normal brain functioning relies critically on the ability to keep fear memories distinct and resistant to confusion. Fear behavior is controlled by adaptive processes including discrimination, generalization and extinction, which are likely regulated by separate neural mechanisms. While fear memory accuracy is critical for survival and balanced fear generalization allows avoidance of dangerous situations, circuit and molecular level mechanisms for fear discrimination remain unclear. Multiple memory systems theory postulates that different types of memory are consolidated via hardwired pathways [201]. In tone fear conditioning, tone [conditional stimulus (CS)]-foot shock [unconditional stimulus (US)] associations are directly encoded through synaptic plasticity in the amygdala, which receives direct auditory inputs [202]. During contextual fear conditioning, the contextual stimulus (CS) is encoded by the dorsal hippocampus whose outputs are subsequently associated with the US through synaptic plasticity in the amygdala [9, 16], and later consolidated by the hippocampal-prefrontal circuitry [17-19, 65, 203]. In fact, the medial prefrontal cortex (mPFC) can compensate for absence of dorsal hippocampus in contextual fear learning [19]. In addition, fear behavior is differentially regulated by infralimbic (IL) and prelimbic (PL) subregions of the mPFC [22, 53, 172, 173] via fear excitation and inhibition, respectively [22, 204], which may be due to differential connectivity with the amygdala [205, 206]. For example, differential conditioning increases unit and field responses within the amygdala to the conditioned stimulus, paired with US (CS+), whereas responses to the second stimulus that was never paired with US (CS−) decreased [207].

Studies show that mPFC lesions enhance generalization. In absence of IL mPFC, rats become more fearful of a novel environment after fear conditioning [19]. In addition, lesions of mPFC disrupts discrimination of more discrete multiple odor stimuli [123]. Furthermore, inactivation of pathways (in either direction) between mPFC and nucleus reuniens of thalamus [3] enhances fear memory generalization [3, 122]. We have recently demonstrated that prefrontal hypofunction of transcription regulators implicated in the mechanism underlying long-term memory consolidation results in abnormal generalization decrement during contextual and auditory fear discrimination learning in mice [4]. These data indicate that the prefrontal circuit might be involved in fear discrimination between the conditioned stimulus CS+ (reinforced with a foot shock) and CS- [174].

There is a strong evidence for prefrontal N-methyl-D-aspartate receptors (NMDARs) in mechanism underlying extinction of conditioned fear [208, 209]. While fear extinction is widely considered as a new learning event rather then forgetting [210], it is postulated that fear extinction involves inhibition of an existing response [211]. In agreement with the data showing that lesions in the mPFC produce deficit in extinction of conditioned fear [21, 166, 212-214], consolidation of fear extinction memory recruits mechanisms controlled by NMDARs, mitogen-activated protein kinase and protein synthesis [173, 215]. Involvement of NMDAR in mPFC-dependent learning mechanism is supported by the studies showing that NMDAR receptors are effective mediators of synaptic plasticity in prefrontal excitatory neurons [216]. However, NMDARs in the mPFC mediate opposite effects on interneurons and excitatory neurons [217, 218].

Pharmacological blockers of NMDAR trigger profound cortical activation in behaving rodents [218] and human volunteers [219-222] suggesting that the effect of NMDAR antagonists in pharmacological studies is predominately targeted to inhibitory neurons producing disinhibition of excitatory network. The objective of the present study was to determine involvement of NMDARs expressed specifically in CamKIIα positive excitatory neurons in mPFC-dependent adaptive behaviors such as fear discrimination and fear extinction.

Based on the studies discussed above, discrimination between dangerous, fear-conditioned CS+ and nonreinfoced CS- auditory cues likely involves mPFC functional interactions. Still unknown are the neural mechanisms underlying the attainment of fear memory accuracy for appropriate discriminative responses to CS+ and CS- stimuli. To explore the potential impact of prefrontal NMDARs on fear discrimination, we generated mutant mice with locally deleted obligatory subunit of the NMDAR in prefrontal excitatory CamKIIα positive neurons and examined their capability to distinguish between dangerous, fear-conditioned stimulus and nonreinforced stimulus in fear discrimination procedure. For behavioral evaluations, we used an auditory fear discrimination task that depends on the ability to distinguish discrete auditory cues constructed of frequency modulated (FM) upward or downward tone sweeps. This auditory fear discrimination task indicated that NMDAR-dependent neural signaling within mPFC circuitry is an important component of the mechanism for disambiguating the meaning of fear signals. We have also demonstrated that NMDAR inactivation in the prefrontal excitatory neurons impairs fear extinction.

Materials and Methods

Subjects

The UC Riverside Institutional Animal Care and Use Committee approved all procedures in accordance with the NIH guidelines for the care and use of laboratory animals. We used C57BL/6J mice for all experiments. Mice were weaned at postnatal day 21, housed 4 animals to a cage with same sex littermates with ad libitum access to food and water and maintained on a 12 hr light/dark cycle. Old bedding was exchanged for fresh autoclaved bedding every week.

Surgery

We used the same rescue surgery protocol as described previously [4] Briefly, 2-3-month-old mice were separated into individual cages prior to surgery. Anesthesia was induced by placing individual mice in chamber filled with isoflurane. After induction, anesthesia was maintained by mounting the mouse in a heated stereotaxic apparatus and supplying a constant flow of isoflurane/oxygen mix. After adjusting the ear bars, bite bar, and nose clamp, the scalp was shaved, sanitized, and incised along the midline. A dental drill was used to thin the skull over the injection sites. The thinned bone was then removed with a needle tip. A 5-µl calibrated glass micropipette (8 mm taper, 8 µm internal tip diameter) was fitted with a plastic tube connected to a 10-ml syringe and lowered onto a square of Parafilm containing a 4-µl drop of virus. After filling the micropipette, it was lowered to the proper stereotaxic coordinates and pressure was applied to the syringe to inject 0.7 µl of solution at a rate of 50 nl/min. After completing the bilateral injection and removing the micropipette, the skin was sutured and antibiotic

was applied to the scalp. The mouse was kept warm by placing its cage on a heated plate and injected with buprenorphine (0.05 mg/kg) for pain relief. The water bottle in the cage was mixed with meloxicam (1 mg/kg) to relieve pain during subsequent recovery days. Animals were monitored for any signs of distress or inflammation for 3 days after surgery. Behavioral experiments were initiated 3 days after surgery. The mPFC was targeted at the following stereotaxic coordinates: Bregma; AP 1.8, ML±0.4, DV 1.4.

Viruses

Surgical procedures were standardized to minimize the variability of HSV virus injections, using the same stereotaxic coordinates for the mPFC and the same amount of HSV injected into the mPFC for all mice. CRE and/or mCherry under control of CamKIIα Promoter were cloned into the HSV amplicon and packaged using a replication-defective helper virus as previously described [153, 154]. The viruses were prepared by Dr. Rachael Neve (MIT, Viral Core Facility). The average titer of the recombinant virus stocks was typically 4.0 x 107 infectious units/ml. HSV viruses are effectively expressed in neurons in the PFC.

Behavioral Assays

Fear conditioning was performed in a fear conditioning box (Coulburn Instruments Inc.) located in a sound attenuated chamber and analyzed automatically by a Video-based system (Freeze Frame software ActiMetrics Inc.). Freezing was expressed as "% Freezing", which was calculated as a percent of freezing time per total time spent in the testing chamber or time window during which the CS was presented. The chamber was cleaned in between trials with Quatracide, 70% ethanol, and distilled water.

The FM-sweep direction auditory fear discrimination task was performed according to a previously described protocol [4]. This task is divided into three phases: FM-sweep conditioning, generalization test and discrimination phase (Fig. 2.2). The conditioned stimuli (CS) were 20 s trains of frequency modulated (FM)-sweeps for a 400 ms duration, logarithmically modulated between 2 and 13 kHz (upsweep) or 13 and 2 kHz (downsweep) delivered at 1 Hz at 75 dB. While the CS+ (conditioned upsweep or conditioned downsweep) was paired with a foot shock (2 s, 0.75 mA), the CS- (upsweep or downsweep) was never reinforced with foot shock. The onset of the US coincided with the onset of the last sweep for the CS. The assignment of the FM stimuli to CS+ or CS- was counterbalanced between subjects. For fear conditioning acquisition (days 1-3; initial training phase), the animals were presented with a single CS-US pairing per day. The FM-sweep Fear Retrieval (day 4) and Generalization (day 4-5) were tested during so called "Test" in context C. "Test" involved measurements of freezing to 3x CS- for 30 s and 3x 30 s CS+ without US presented after 3 min baseline and with 3 min inter trial intervals (ITI). During "Test", both CS+ and CS- were not reinforced with US and CS+/CS- stimuli were presented in alternated, counterbalanced order. Context C was significantly differed from the training chamber (context A), in which animals displayed low context baseline [223]. The discrimination phase of FM sweep direction discrimination training was performed over three sessions a day for 6 days (days 7-12): Session 1 was the performance test ("Test"), Session 2 was the presentation to CS+ paired with US (or CS-) after 3 min in Context A, and Session 3 was the presentation to the CS- (or CS+ paired with US) after 3 min in Context A. CS+ and CS- order was

counterbalanced.

The fear exintction task is divided into two phases: FM-sweep conditioning and fear extinction phase. The conditioned stimuli (CS+) were 20-s trains of frequency modulated (FM)-sweeps for a 400-ms duration, logarithmically modulated between 2 and 13 kHz (upsweep) or 13 and 2 kHz (downsweep) delivered at 1 Hz at 75 dB. While the CS+ was paired with a foot shock (2 s, 0.75 mA), the CS- (upsweep or downsweep) was never reinforced. The assignment of the stimuli to CS+ or CS- was counterbalanced between subjects. For fear conditioning acquisition, the animals were presented with a three CS-US pairings with 3 min ITI. Fear extinction involves following 7 days of trainings (Fig 2.6A, days 2-8) in Context C. Each day, 3x 30 s CS- and 3x 30 s CS+ are presented after 3 min baseline and with 3 min ITI. Both CS+ and CS- were not reinforced during extinction and stimuli are presented in alternated, counterbalanced order.

Histology

Histology was performed as described before [43]. Briefly, anesthetized (Nembutal 200mg/kg, i.p. injection) mice were transcardially perfused first with PBS and then 4% PFA. Brains were extracted, soaked in 4% PFA overnight, soaked in 20% sucrose until they sank, and then flash frozen using embedding media, dry ice, and ethanol before being stored in a -80^{o}C freezer. The frozen brain was then mounted on cryostat for 50-μm-thick sectioning of the mPFC. Free-floating immunohistochemistry (IHC) was performed on sections according to a previously described protocol [142]. The sections are washed 3 times for 10 min in a wash buffer (PBS, 0.3% Triton x-100, 0.02% NaN2) followed by a 1-hr incubation in blocking buffer (5% normal goat serum in

washing buffer), followed by a 10-min incubation in the wash buffer. The sections were incubated overnight at 4C° with primary antibodies (mouse anti-NeuN monoclonal antibody (Millipore, 1:2000) and rat anti-mCherry (Molecular Probes, 1:10,000) or mouse anti-CaMKII antibody (Fisher, clone: 6G9: 1:1,000) and rat anti-mCherry.

After three washes with the wash buffer, the sections were incubated with appropriate secondary antibodies (Alexa488 goat anti-mouse IgG or Biotin-anti-rat IgG or Alexa647 goat anti-mouse IgG; Molecular Probes, 1:1,000), in blocking buffer overnight at 4C°. The sections were washed again three times with the wash buffer, incubated with Streptavidin-Alexa 568 (Molecular Probes, 1:1,000) in blocking buffer for 4 hr at room temperature, and washed before mounting for viewing. Negative control slices were collected at the same time, undergoing the same IHC procedure in addition to receiving primary antibodies. After immunostaining, the tissue was mounted with mounting medium (ProLong Antifade, LifeTechnologies) before imaging. The negative control slice was from animals infected with HSV/CamKIIα Promoter-mCherry Control virus targeted to mPFC.

Fluorescent In situ hybridization (FISH) of NR1 mRNA,

Coronal sections (25 μm in thickness) were cut on a ryostat. Hybridization was performed at 56^{o}C for 18 hours in a hybridization buffer (KPL, Inc). The NR1 probe template derived from the 723-bp DNA fragment of rat NR1 cDNA (pCI-SEP-NRI, Adgene) containing *NR1* sequences spanning exon 13 to exon 17 (corresponding to nucleotides 1983 to 2735 based on NCBI Sequence L08228.1). NR1 complementary RNA (cRNA) was labeled with fluorescein (Roche) and used as the probe for detecting

NR1 mRNA in the mouse brain. After hybridization, the sections were washed and incubated with HRP conjugated anti-fluorescent antibody (Perkin Elmer) overnight at 4^{o}C. NR1 signal was detected with the Perkin Elmer kit using fluorescein-tyramide (TSA Plus, Perkin Elmer). Following FISH, mCherry signal was detected with rat anti-Cherry antibodies/Biotin-anti-rat IgG/ Streptavidin-Alexa 568 immunodetection system as described above. The negative control slice was from animals infected with HSV/CamKIIα Promoter-mCherry Control virus targeted to mPFC.

Imaging

Images were taken using an Olympus FV1000 laser scanning confocal microscope controlled using the FluoView software. Fluorescence was measured from mPFC slices using objective 40x/0.80 LUMPlanFL40x objective. Alexa488, Alexa568 and Alexa-647 were imaged using a 473-nm, 559-nm and 647-nm laser, respectively. Gain and offset of each channel were balanced manually using Fluoview saturation tools for maximal contrast. All settings were tested on multiple slices before data collection and brain slices were imaged using identical microscope settings once established. The fluorescence intensity was compared to the negative control slices, which did not receive any primary antibodies. Forty-micrometer z-stacks were obtained from the entire mPFC for assessing the site of injection. For other measurements, a single optical section was acquired and analyzed. The fluorescence intensity quantification was performed on original images by the use of Olympus Fluoview software without any non-linear image adjustments. The region of interest (ROI) was a cell-size circle placed on cells expressing mCherry within cortical layer 2/3 in mPFC and fluorescence corresponding to Grin1

(FISH) or CamKII was measured from randomly selected 20–30 cells per hemisphere. The fluorescence intensity quantification was performed on original images by the use of Olympus Fluoview software without *post-hoc* manipulations.

Data analysis

The experimenters were blind to the group conditions. N indicates sample size and error bars use the standard error of the mean. Statistical analysis was performed using Excel (Microsoft Inc.) or SPSS (IBM Inc.). The Student's t-test or ANOVA was used for statistical comparisons. Pearson's correlation (*r*) was used as an effect size. In cases where the repeated measures ANOVA (RM-ANOVA) was utilized and assumptions of sphericity were violated (via Mauchly's Test), the analysis was performed using the Greenhouse-Geisser correction. Bonferroni corrected post hoc analysis was performed for multiple comparisons, which allows for substantially conservative control of the error rate. Significance values were set at $p<0.05$. The asterisks indicate statistical significance: *, $p < 0.05$, **, $p < 0.01$, ***, $p < 0.001$ and n.s. indicates not significant.

Results

Generation of mPFC-NR1 KO mice

In this study, we focused on the NMDAR, which is a known regulator of synaptic activity. This receptor has been implicated in various forms of synaptic plasticity underlying memory [224, 225]. Loss of NMDAR function is achieved by the conditional deletion of the *GRIN1* gene, which encodes an obligatory NR1 subunit for functional NMDAR [225]. In these experiments, we injected Herpes Simplex Virus (HSV) expressing monomeric fluorescent protein mCherry [5] or mCherry and Cre recombinase under the control of CamKIIα promoter [5] (Fig. 2.4A) into the mPFC of floxed-NR1 mice to generate Control or mPFC-NR1 KO mice, respectively (Fig. 2.4A, B). Cre recombinase is the second gene in our CamKIIα-mCherry/Cre bicistronic vector and linked to mCherry with the internal ribosome entry site (IRES) of encepahlomyocarditis virus (EMCV). We have previously reported that more than 98% HSV infected cell are neurons [4]. Immunostaining with antibodies directed against CamKIIα and mCherry revealed that the virus expression was targeted to CamKIIα positive cells (Fig. 2.4C). To evaluate NR1 gene deletion in mPFC-NR1 KO, we employed fluorescence in situ hybridization (FISH) to examine expression of NR1 mRNA levels in infected neurons (mCherry expressing cells) (Fig. 2.4D). mPFC-NR1 KO mice show decreased levels of expression of NR1 mRNA in cells infected with CamKIIα-mCherry/Cre virus within the mPFC (Fig. 2.4D). We found a significant decrease of NR1 mRNA signal in neurons expressing mCherry protein in the mPFC-NR1 KO when compared to control (Fig. 2.4D; Ctrl vs. mPFC-NR1 KO: t-test; $t_{(11)} = 3.4048$, $p = 0.0059$, $r = 0.71632$).

Figure 2.4

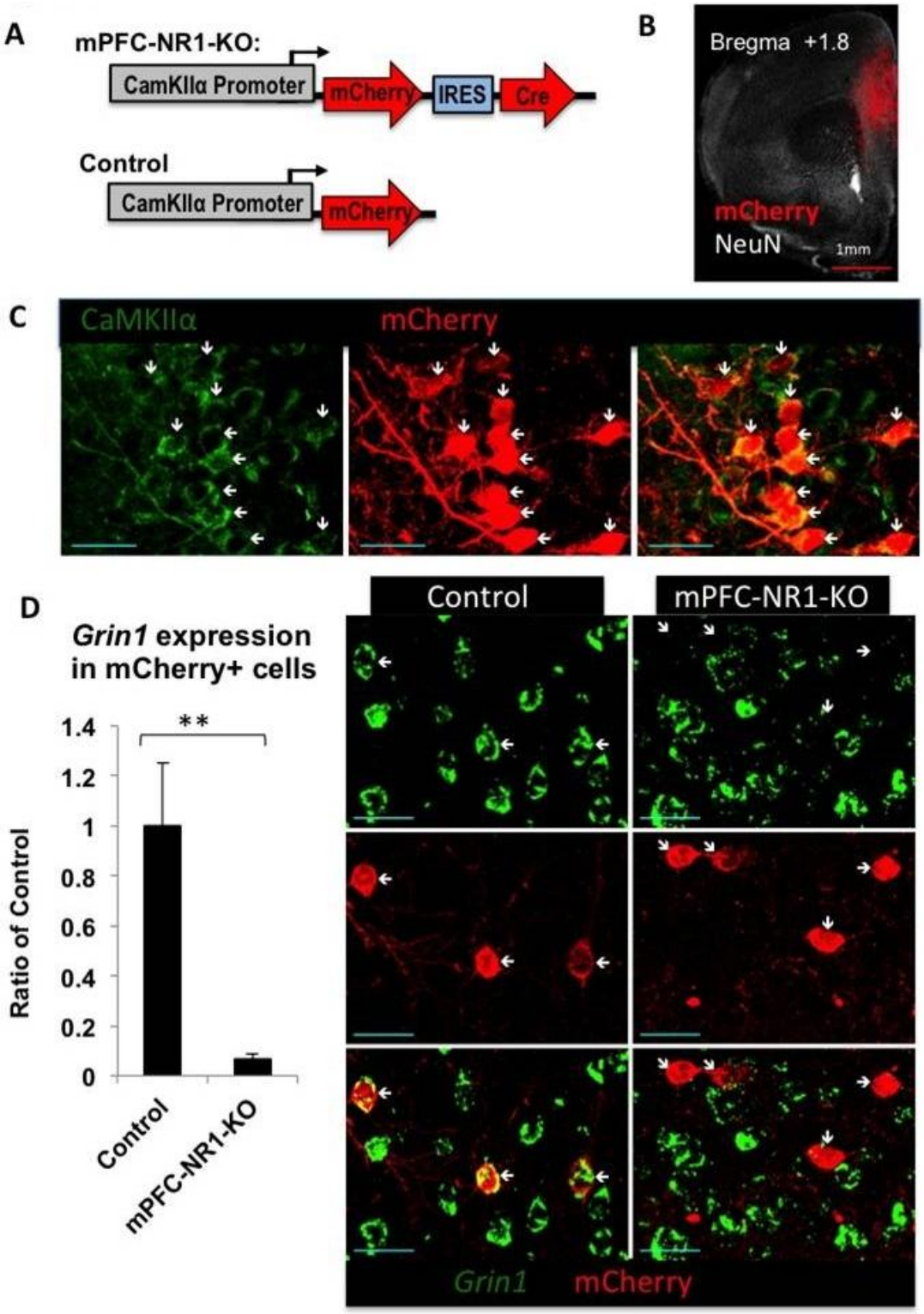
A
mPFC-NR1-KO:
CamKIIα Promoter
mCherry
IRES
Cre
Control
CamKIIα Promoter
mCherry
B
Bregma +1.8
mCherry
NeuN
1mm
C
CaMKIIα
mCherry
D
Grin1 expression in mCherry+ cells
**
Ratio of Control
1.4
1.2
1
0.8
0.6
0.4
0.2
0
Control
mPFC-NR1-KO
Control
mPFC-NR1-KO
Grin1
mCherry

(Previous page) Figure 2.4: Generation of mPFC-NR1 KO mice. (**A**) Viral construct for generating mPFC-NR1 KO and control mice: HSV/CaMKIIα-mCherry-IRES-Cre and HSV/CaMKIIα-mCherry, respectively. (**B**) Representative image indicating mPFC infection of the virus. Long-term expression HSV-1 viruses carrying CRE (HSV/CaMKIIα-mCherry-IRES-Cre) or mCherry as the control (HSV/CaMKIIα-mCherry) were injected into the mPFC. To determine the pattern of mCherry-tagged virus expression, the imaged tissue was compared to the Paxinos and Franklin mouse atlas [159] and areas of maximal mCherry expression were labeled as injection sites. Red, mCherry; white, NeuN neuronal marker. (**C**) Multiplex immunohistochemistry with anti-mCherry and anti-CamKIIα antibodies revealed that mCherry expression from HSV/CaMKIIα-mCherry-IRES-Cre virus was targeted to CamKIIα positive cells in mPFC-NR1 KO mice. Red, mCherry; green, CaMKIIα. White arrows indicate position of mCherry positive neurons expressing CamKII. Blue scale bar indicates 30 μm. (**D**) NR1 expression was markedly decreased in mPFC-NR1 KO mice. Fluorescent in situ hybridization (FISH) was used to measure the levels of NR1 mRNA in combination with immunohistochemistry of mCherry in the mPFC of mPFC-NR1 KO and control mice. Cells co-expressing mCherry in the mPFC showed significantly lower levels of Grin1 expression when compared to control animals expressing mCherry only. Red, mCherry; green, *GRIN1*. White arrows indicate the position of mCherry positive neurons. Blue scale bar indicates 30 μm. The asterisks indicate statistical significance: **, $p < 0.01$.

Impairment of fear discrimination in mPFC-NR1 KO mice

We tested mPFC-NR1 KO mice using an auditory discrimination task, which tests the ability of mice to recognize the direction (upward or downward) of frequency modulated (FM)-sweeps (Fig. 2.2). This fear discrimination task requires learning of a dangerous stimulus (CS+) via classical fear conditioning (pairing with foot shock, US) and then a harmless stimulus (CS-) is associated with the absence of US. This assay begins with 3 days of acquisition (a single CS-US pairing per day) followed by a 24 hr fear retrieval test on day 4 and a generalization test on days 4-5. The mice then run through discrimination training on days 7-12 in which they experience 3 sessions: first, they are tested for freezing to CS+ and CS- in Context C (without any reinforcement); second, they are exposed to CS+ paired with US (or CS-); third, they are exposed to CS- (or CS+ paired with US). CS- is never reinforced through the entire procedure. During generalization and discrimination, performance was tested in Context C, which is substantially different from conditioning chamber (Context A).

We examined FM-sweep fear conditioning acquisition in mPFC-NR1 KO mice and control mice, and both groups successfully acquired this form of classical conditioning (Fig. 2.5A; RM-ANOVA of Day and Group: $F_{(2,38)} = 0.800$, $p = 0.457$). Both groups also showed similar retrieval on a 24-hr memory test (Fig. 2.6B; two way ANOVA of Group and Baseline/24 h-Test; Group: $F_{(1,38)} = 0.941$, $p = 0.338$; Baseline/24 h-Test: $F_{(1,38)} = 422.288$, $p = 3.509^{-22}$; Group x Baseline/24 h-Test: $F_{(1,38)} = 0.553$, $p = 0.462$). We next tested the amount of generalized fear expressed by mPFC-NR1 KO and control mice, in which we examined their freezing responses to a novel FM sweep (CS-),

revealing no difference in the freezing responses to the CS- or CS+ between mPFC-NR1 KO and control mice (Fig. 2.5C; ANOVA of FM-sweep direction and group during day 4 and 5: Group: $F_{(1,38)} = 0.363$, $p = 0.550$; ANOVA of FM-sweep direction: $F_{(1,38)} = 0.385$, $p = 0.539$; Group x FM-Sweep Direction: $F_{(1,38)} = 0.002$, $p = 0.966$). Taken together, these data indicate that both groups of mice show normal conditioned fear acquisition, 24hr retrieval, and generalization.

We next ran control and mPFC-NR1 KO mice on auditory discrimination training (Fig. 2.5D-F). Initially, both groups of mice generalized their conditioned responses, exhibiting similar levels of freezing responses to both CS+ and CS- (days 7-8). However, following 2 days of training, control mice demonstrated the ability to consistently distinguish between similar yet different auditory patterns (days 10-12), exhibiting a higher freezing to CS+ and significantly lower freezing to CS- compared to CS+ (Fig. 2.5D; RM-ANOVA of Day and FM-sweep direction: Day x FM-sweep direction: $F_{(5,45)} = 8.728$, $p = 0.000007$, $n = 10$). *Post hoc* analysis using Bonferroni correction (alpha = 0.0083) for multiple comparisons indicated that differences were present during days 10 ($t_{(9)} = 3.487$, $p = 0.007$, $r = 0.76$), 11 ($t_{(9)} = 7.209$, $p = 0.00005$, $r = 0.92$) and 12 ($t_{(9)} = 8.147$, $p = 0.00002$, $r = 0.94$) only.

The mPFC-NR1 KO mice demonstrated deficient discrimination between CS+ and CS-, never showing a significant difference in freezing response between up and down auditory sweeps. (Fig. 2.5E, RM-ANOVA of Day and FM-sweep direction: Day x FM-sweep direction: $F_{(2.7,26.5)} = 2.787$, $p = 0.066$, $n = 11$). *Post hoc* analysis using Bonferroni correction for multiple comparisons indicated that no differences were present

during days 9 (CS+ vs CS- t-test: $t_{(10)} = 2.515$, $p = 0.031$, $r = 0.62$), 10 ($t_{(10)} = 0.655$, $p = 0.528$, $r = 0.20$), 11 ($t_{(10)} = 3.131$, $p = 0.011$, $r = 0.70$) and 12 ($t_{(10)} = 1.728$, $p = 0.115$, $r = 0.48$). In contrast to the control animals, mPFC-NR1 KO mice continued to generalize their conditioned responses throughout the entire auditory discrimination training and failed to distinguish between CS+ and CS-.

There is a clear deficit in mPFC-NR1 KO mice in auditory fear discrimination when compared to controls (Fig. 2.5D-E, RM-ANOVA of Group and FM-sweep direction and Day 7-12: Group x FM-sweep direction x Day: $F_{(5,95)} = 3.619$, $p = 0.005$; Group x FM-sweep direction: $F_{(1,19)} = 5.972$, $p = 0.024$; mPFC-NR1 KO, n=11; Ctrl, n = 10). Analysis of discrimination ratios supports the difference in performance between control and mPFC-NR1 KO animals on days 10-12 (Fig. 2.6F. Discrimination Index mPFC-NR1 KO vs. Ctrl t-test: Day 10: $t_{(19)} = 3.322$, $p = 0.004$, $r = 0.61$; Day 11: $t_{(19)} = 4.719$, $p = 0.0001$, $r = 0.73$, Day 12: $t_{(19)} = 3.850$, $p = 0.001$, $r = 0.66$; MPFC-NR1 KO , n=11; Ctrl, n = 10), but not during the initial 3 days of training ($p>0.05$). Control mice clearly show a better performance than mPFC-NR1 KO mice on auditory discrimination (Fig. 2.5D-F). In summary, these data suggest that knockout of NR1 in the mPFC results in abnormal auditory fear memory specificity. Moreover, the fear baseline measured before tone presentation during testing was not different between groups or across the discriminatory training (Fig. 2.6D-E).

We also analyzed fear responses to upsweep (CS+) and, separately, to downsweep (CS-) in control and mPFC-NR1 KO tested on FM-sweep direction fear discrimination task (Fig. 2.5). There was no difference in responses to conditioned

stimuli CS+ between mPFC-NR1 KO and control mice across the entire FM-sweep direction discrimination training (Fig. 2.5D-E; CS+/mPFC-NR1 KO vs Ctrl; RM-ANOVA of days 7-12 and group: Day X Group, $F_{(3.1,\ 59.1)} = 0.546$, $p = 0.659$). An analysis of learning curves (Fig. 2.6G) showed a positive slope to CS+ in control ($\alpha = 2.05 \pm 1.22$) and mPFC-NR1 KO ($\alpha = 1.91 \pm 1.06$) across the entire FM-sweep direction fear discrimination task. In fact, there was no difference in the learning slopes of appropriate responses to CS+ between mPFC-NR1 KO and control groups (Fig. 2.5G; CS+ slope/Ctrl vs mPFC-NR1 KO t-test; $t_{(19)} = 0.088$, $p = 0.931$, $r = 0.02$). However, mPFC-NR1 KO mice responded differently to non-relevant stimuli CS- across training on the auditory discrimination task when compared to control mice (Fig. 2.5D-E; CS-/mPFC-NR1 KO vs Ctrl; RM-ANOVA of days 1-5 and group: Day X Group, $F_{(3.4,63.7)} = 3.447$, $p = 0.018$). The marked improvement of discrimination observed on the FM-sweep direction fear discrimination task in control mice (Fig. 2.5D, F, G) coincides with the significant negative slope of the learning curve for CS- (Fig. 2.5G; $\alpha = -5.17 \pm 0.79$). The mPFC-NR1 KO group, which failed to improve fear memory accuracy across training (Fig. 2.5E-F), shows a slight positive slope for CS- across the training (Fig. 2.5G; $\alpha = 0.412 \pm 1.20$) and a marked difference when compared to the CS- slope observed in control animals (Fig. 2.5H; CS- slope/Ctrl vs mPFC-NR1 KO t-test; $t_{(19)} = -3.803$, $p = 0.001$, $r = 0.66$).

In summary, analysis of patterns of responses to CS+ and CS- in control animals tested on the FM-sweep direction fear discrimination task revealed that the improvement of auditory fear memory accuracy was due to only slight incline in freezing to CS+ and

rapid decline in freezing to CS-. NMDA receptor hypofunction in the mPFC altered the ability to learn auditory discrimination responses to CS+ versus CS- by disrupting the pattern of learning for CS- only, while responses to CS+ remained similar to control mice. These data demonstrate that the mPFC supports the improvement of auditory fear memory accuracy by controlling acquisition of appropriate responses to non-relevant stimuli.

Figure 2.5

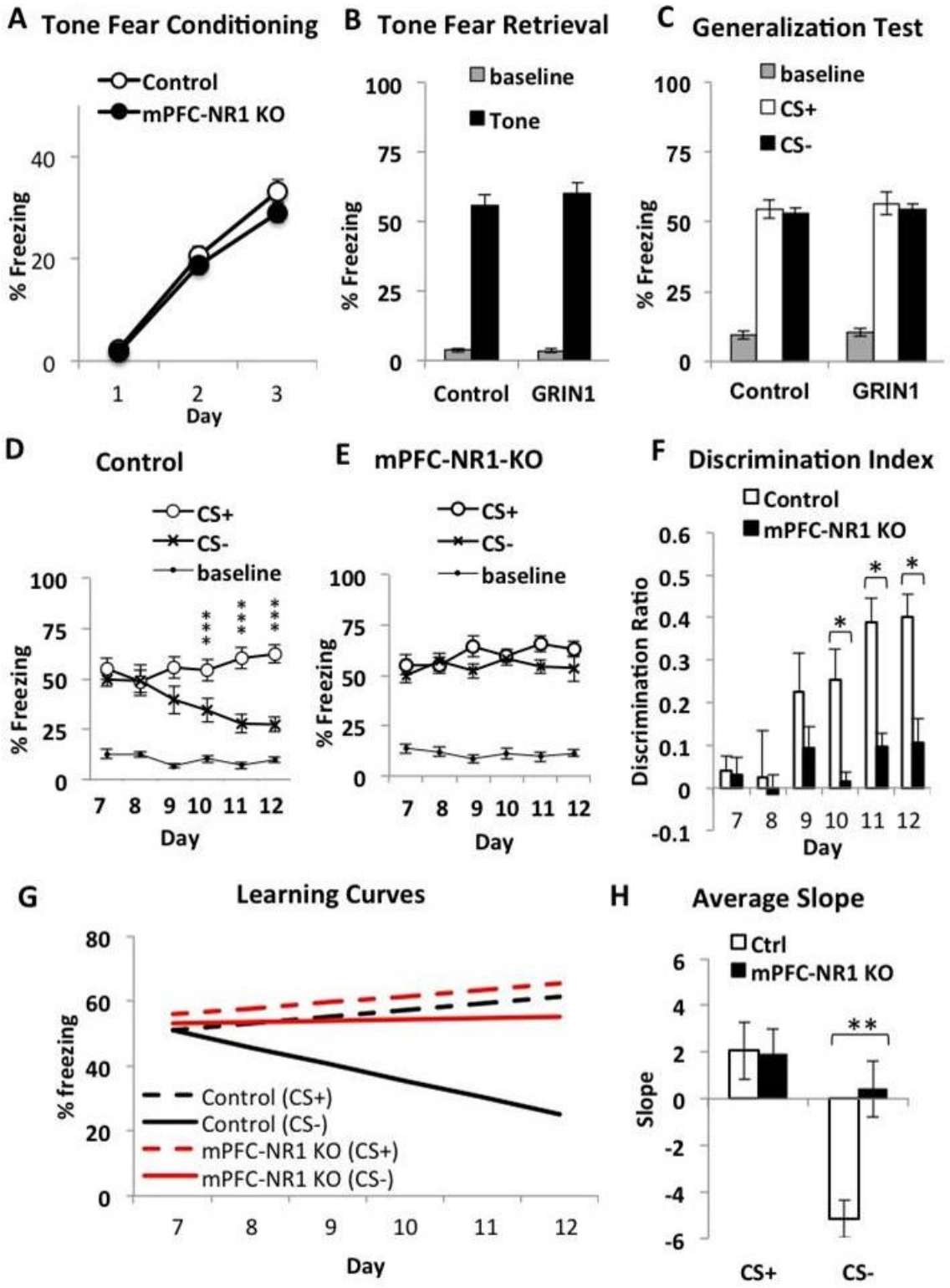
A Tone Fear Conditioning
Control
mPFC-NR1 KO
% Freezing
Day
B Tone Fear Retrieval
baseline
Tone
% Freezing
Control
GRIN1
C Generalization Test
baseline
CS+
CS-
% Freezing
Control
GRIN1
D Control
CS+
CS-
baseline
% Freezing
Day
E mPFC-NR1-KO
CS+
CS-
baseline
% Freezing
Day
F Discrimination Index
Control
mPFC-NR1 KO
Discrimination Ratio
Day
G Learning Curves
% freezing
Control (CS+)
Control (CS-)
mPFC-NR1 KO (CS+)
mPFC-NR1 KO (CS-)
Day
H Average Slope
Ctrl
mPFC-NR1 KO
Slope
CS+
CS-

(Previous Page) Figure 2.5: FM-sweep direction fear memory specificity is deficient in mPFC-NR1 KO mice. (**A-B**). Pavlovian tone fear conditioning was normal in mPFC-NR1 KO, showing normal acquisition (**A**) and retention (**B**) of FM-sweep fear conditioning compared to control (Ctrl) mice. FM-sweep fear was tested in Context C at 24 hr after a three upsweeps-foot shock pairing. Shown here fear baseline is % freezing recorded before fear conditioning (day 1). (**C**) Both groups (mPFC-NR1 KO and Ctrl) show no difference in the freezing responses to CS+ and CS- ($p>0.05$) during day 4 and 5 of training, indicating that initially, the mPFC-NR1 KO and control mice generalized responses and did not discriminate between CS+ and CS-. Shown here fear baseline is the percent of freezing recorded before tone was presented during generalization test. (**D**) After the initial generalization of fear conditioned responses, control mice exhibited robust fear discrimination on days 10-12. (**E**) mPFC-NR1 KO mice demonstrated a deficit in auditory fear discrimination when compared to controls (**D**). Shown here (and F) fear baseline is the percent of freezing recorded before tone was presented during discriminatory phase (days 7-12). (**F**) The FM-sweep direction discrimination ratios (DI) were calculated using the freezing responses to CS+ and CS- according to the formula DI = (([CS+] – [CS-]) / ([CS+] + [CS-])). Analyses revealed differences between mPFC-NR1 KO and control mice in the performance during days 10 – 12. (**G**) Average learning curves for learning of appropriate responses to CS+ and CS- were calculated based on the performance of control and mPFC-NR1 KO group across the entire training (Fig. 2.5D-E; days 7 to 12) followed by fitting the regression line and t-test analysis on the mean of those slopes (α). The analysis response patterns to CS+ and CS- in control animals tested on the FM-sweep direction fear discriminatory task revealed that auditory memory accuracy improvement was due to a slight incline in freezing to CS+ and a rapid decline in freezing to CS- (CS+/Ctrl: $\alpha= 2.05\pm1.22$; CS-/Ctrl: $\alpha= -5.17\pm0.79$). There was no difference in the learning slopes of appropriate responses to CS+ between mPFC-NR1 KO and control groups. The mPFC-NR1 KO group, which failed to improve fear memory accuracy, showed a positive slope for CS-, a marked difference from control responses to the CS-. (**H**) Graph showing average slopes on the same analysis. Data presented in B-F were acquired in Context C during "Test" (Fig. 2.2). The asterisks indicate statistical significance: *, $p < 0.05$, **, $p < 0.01$, ***, $p < 0.001$.

Impairment of auditory fear memory extinction in mPFC-NR1 KO mice

Previous work on fear memory and mPFC NMDA receptor function demonstrated that infusion of CPP, a potent NMDA receptor antagonist [208], or more selective NR2B-specific blocker ifenprodil [215] impaired extinction memory consolidation. However, these pharmacological manipulation prevents testing cell-type specific effects. To evaluate specific role of NMDARs expressed in excitatory neurons we tested mPFC-NR1 KO mice on an auditory extinction task (Fig. 2.6) in which mice are initially trained with 3 pairings of upward FM sweeps (CS+) and foot shocks on day 1, followed by 7 days of extinction in which they are presented with non-reinforced upward (CS+) and downward (CS-) FM auditory sweeps in a novel context while measuring freezing responses. No further pairing of CS+ and foot shocks was done after the initial training on day 1. Control mice extinguish freezing to CS+ and CS- differently across extinction training (Fig. 2.6B, RM-ANOVA of Day and FM-sweep direction: Day x FM-sweep direction = $F_{(6,60)} = 2.565$, $p = 0.028$). *Post hoc* analysis indicated that differences between CS+ and CS- were present during days 4 ($p < 0.05$), and 7 ($p < 0.05$), only. The mPFC-NR1 KO mice show no difference between CS+ and CS- in decline of freezing responses across fear extinction training (Fig. 2.6C RM-ANOVA of Day and FM-sweep direction: Day x FM-sweep direction = $F_{(6,66)} = 2.225$, $p = 0.051$).

Analysis of learning curves (Fig. 2.6D, Control CS+ $\alpha = -9.51 \pm 0.72$, mPFC-NR1 KO CS+ $\alpha = -6.07 \pm 0.64$, Control CS- $\alpha = -9.11 \pm 1.10$, mPFC-NR1 KO CS- $\alpha = -6.34 \pm 0.74$) shows a significant difference in the rate of extinction of CS+ and CS- between control and mPFC-NR1 KO mice when comparing average slopes of both CS+

(Fig 2.6E, CS+ slope/Ctrl vs mPFC-NR1 KO t-test; $t_{(21)} = -3.573$, $p = 0.002$, $r = 0.61$) and CS- (CS- slope/Ctrl vs mPFC-NR1 KO t-test; $t_{(21)} = -2.113$, $p = 0.047$, $r = 0.52$). Taken together, these data indicate that both control and mPFC-NR1 KO groups extinguish CS+ and CS- across extinction training, but that control mice extinguish fear responses to both FM-sweep directions more rapidly than mPFC-NR1 KO mice. While freezing responses to conditioned stimulus CS+ and nonreinforced stimulus CS- declined to the level of fear baseline by day 7 of extinction learning in control group (Fig 2.6B; Day 7, CS+ vs baseline (CTRL) t-test$_{(10)} = 1.7465$, $n = 11$, $p = 0.1113$, $r = 0.3637$; CS- vs Baseline (CTRL) t-test$_{(10)} = 0.0277$, $n = 11$, $p = 0.9785$, $r = 0.01$), mPFC-NR1 KO mice show still significant levels of freezing to CS+ and CS- above the baseline on day 7 of extinction training (Fig. 2.6C; Day 7, CS+ vs baseline (mPFC-NR1 KO) t-test$_{(11)} = 7.5947$, $n = 12$, $p = 0.00001$, $r = 0.85$; CS- vs baseline (mPFC-NR1 KO) t-test$_{(11)} = 3.911$, $n = 12$, $p = 0.000002$, $r = 0.64$) . Coincidently, generalized fear responses to CS-, which was never reinforced, show similar patterns of decline to those observed in case of CS+ in mPFC-NR1 KO and control mice across the training of fear extinction paradigm (Fig. 2.6). In general, the decrease of generalized fear (responses to CS-) correlates well with the decrease of fear responses to CS+ across fear extinction training, although control mice show a slightly steeper decline of CS- when compared to CS+ (Fig. 2.6) while both CS+ and CS- decline slower but at the same rate in mPFC-NR1 KO mice In summary, these data demonstrate that NMDARs expressed in excitatory neurons in the mPFC not only mediate mechanism underlying fear extinction (Fig. 2.6) but are also involved in controlling a decline of generalized responses to CS- (observed in Fig. 2.5).

Figure 2.6

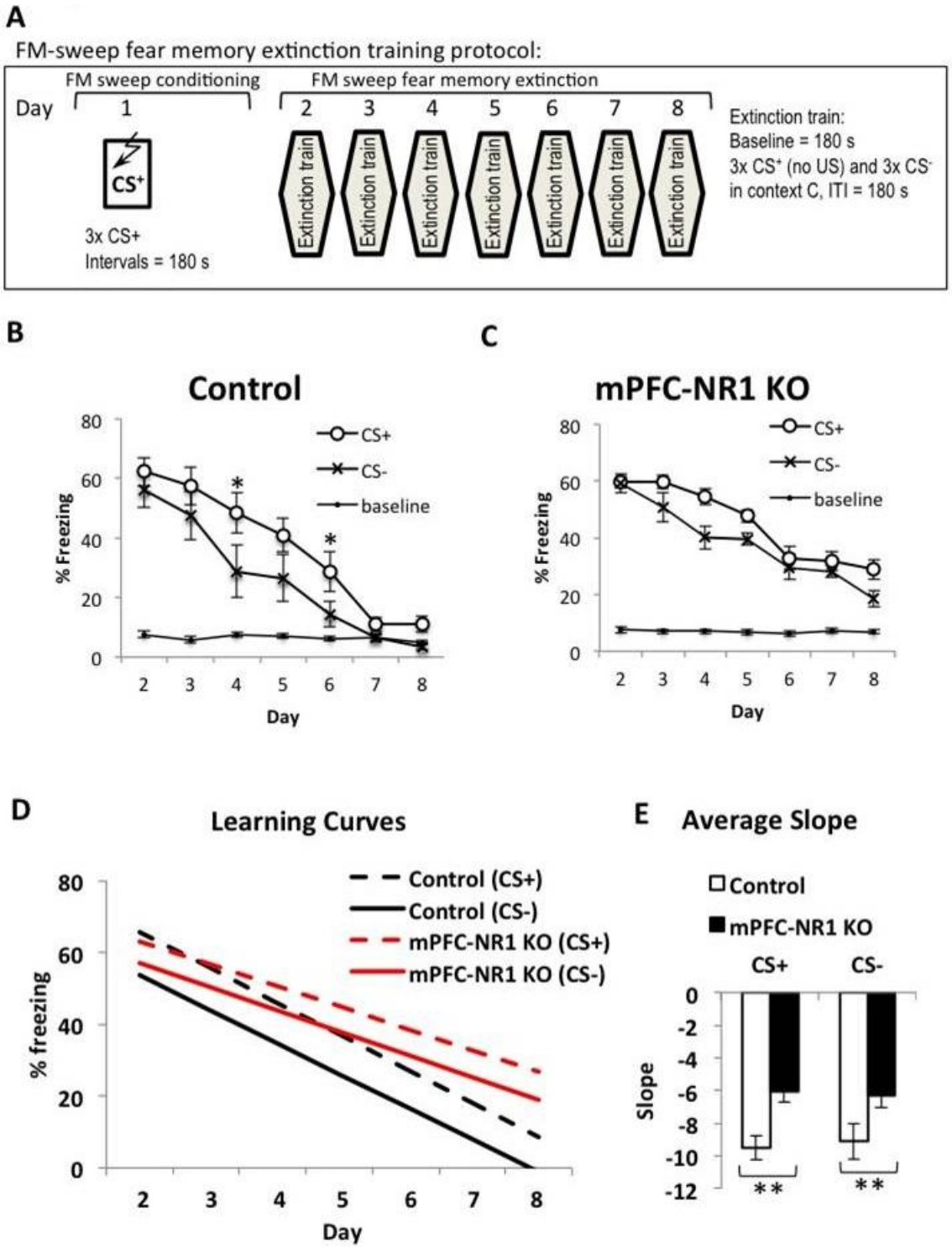
A
FM-sweep fear memory extinction training protocol:
FM sweep conditioning
FM sweep fear memory extinction
Day
1
2
3
4
5
6
7
8
CS+
3x CS+
Intervals = 180 s
Extinction train
Extinction train:
Baseline = 180 s
3x CS+ (no US) and 3x CS-
in context C, ITI = 180 s
B
Control
C
mPFC-NR1 KO
CS+
CS-
baseline
% Freezing
Day
D
Learning Curves
Control (CS+)
Control (CS-)
mPFC-NR1 KO (CS+)
mPFC-NR1 KO (CS-)
% freezing
E
Average Slope
Control
mPFC-NR1 KO
CS+
CS-
Slope
**

(Previous page) Figure 2.6: mPFC-NR1 KO mice show deficient fear memory extinction. (**A**) Experimental design for the extinction protocol. A single day of training in which the animal receives 3 upsweep-foot shock pairings followed by 7 days of extinction in which freezing is measured during the presentation of 3x CS- (downward sweeping FM tones) followed by 3x CS+ (unpaired with foot shock) in a separate context from training [226]. (**B**) Percent of total time spent freezing during the sweep presentation plotted across days. Control animals extinguish freezing to both CS+ and CS- significantly different. Asterisk refers to a difference between CS+ and CS-. (**C**) mPFC-NR1 KO mice extinguish CS+ and CS- the same rate. (**D**) Learning curves comparing slopes of extinction to CS+ and CS- between control (CS+ slope(α)= -9.51±0.72, CS- slope(α)= -9.11±1.10) and mPFC-NR1 KO mice (CS+ slope(α)= -6.07±0.64, CS- slope(α)= -6.34±0.74. (**E**) Average slope comparison of extinction curves to CS+ and CS- between control and mPFC-NR1 KO mice shows a significant difference in rate of extinction to CS+ and CS-. Shown here (B-C) fear baseline is % freezing recorded before tone was presented during extinction (days 2-8). The asterisks indicate statistical significance: *, $p < 0.05$, **, $p < 0.01$.

Discussion

This study shows that after fear generalization occurs, successful fear discrimination involves prefrontal NMDAR-dependent decline of generalized fear responses to harmless nonreinforced stimuli. Conditional deletion of the NMDAR in CamKIIα positive excitatory neurons within the mPFC resulted in abnormal fear discrimination. Patterns of fear responses in control animals suggest that the fear discrimination procedure involves a diminution of freezing responses to harmless nonreinforced stimuli after initial strong generalization. In addition, mPFC-NR1 KO mice show a moderate deficiency in fear extinction, which is consistent with prior studies demonstrating that infusion of NMDAR antagonist CPP or more selective NR2B specific antagonist ifenprodil into the mPFC prevented consolidation of extinction learning [208, 209, 215].

How can NMDARs in the mPFC control fear discrimination? This study shows that fear discrimination involves a prefrontal mechanism that is mediated by NMDARs expressed in excitatory CamKIIα positive neurons. These studies are consistent with our previous report showing that an interruption of cAMP response element binding protein (CREB) function or an inhibition of histone acetyltransferase CREB binding protein (CBP) activity in the mPFC also leads to a strong deficit in fear discrimination [4]. Both CREB and CBP histone acetyltransferase (HAT) activity has been implicated in the putative molecular mechanism underlying memory consolidation and NMDAR-dependent synaptic plasticity. Thus, fear discrimination appears to rely on prefrontal circuitry through a process by which initially generalized fear memories are sharpened by

selective reduction of the response to non-reinforced stimuli. These studies are consistent with other reports. Critical involvement of mPFC in fear generalization has been demonstrated through prefrontal lesion studies [19] and direct inactivation of connectivity between mPFC and nucleus reuniens of thalamus [3], which in both studies enhanced fear responses to a novel environment [3]. In fact, optogenetic activation of action-potential firing of NR neurons stimulated throughout the 6 min training period by either a 4 Hz tonic stimulation or a 30 Hz phasic stimulation administered for 0.5 s every 5 s during fear memory acquisition (but not during fear memory retrieval) reduced or enhanced memory generalization, respectively [3]. Other studies showed that a general inactivation of the mPFC with the GABAA receptor antagonist muscimol did not interfere with differential fear learning but it produced deficit in the differential fear conditioning if muscimol was administered into the mPFC just before retrieval but not during aquisition [227]. These data may indicate that the differential fear learning may occur in absence of the mPFC due to compensatory effects in a similar manner as prefrontal microcircuit can compensate contextual learning after hippocampal loss [19]. However, when required information related to differential fear acquisition is encoded and consolidated in available mPFC network in a NMDAR-dependent manner, then the mPFC becomes indispensable for differential fear retrieval. In summary, these data suggest that fear discrimination recruits a mechanism relying on NMDARs expressed in prefrontal excitatory neurons and controlling a generalization decrement.

The mPFC-NR1 KO mice showed also a moderate deficit in extinction of fear to the conditioned stimuli CS+ (Fig. 2.6), which is consistent with previous reports. It is

generally believed that fear behavior is differentially regulated by the PL and IL divisions of the mPFC [22, 53, 172, 173]. Electrophysiological findings suggest that the IL and PL cortices may have opposite effects on fear expression [23, 228]. It has been suggested that the PL promotes fear expression by activating neurons of the basolateral nucleus of the amygdala (BLA) projecting to the central nucleus of the amygdala (CeM) [229], a critical subregion for fear expression. Conversely, electrical stimulation of IL inhibits the CeM output through the amygdala intercalated neurons (ITC) relay [32], providing an alternative mechanism for extinction [34]. Thus, IL mPFC projections to the amygdala inhibit conditioned fear and it is postulated that the learning of fear extinction in rat involves both increased neuronal activity in the IL mPFC [27] and protein synthesis in the mPFC [169].

NMDARs have been strongly implicated in fear extinction. NMDAR-dependent long-term potentiation is an experimental model of synaptic plasticity and is widely hypothesized to be the neural mechanism by which memory traces are encoded and stored in the brain [230]. Infusion of the NMDAR blocker 2-amino-5-phosphonovalerate (APV) into the amygdala during extinction substantially interferes with extinction of conditioned fear to tone, light, and contextual stimuli [231, 232] while overexpression of NMDAR subunit NR2B in mice improves extinction learning [233]. In addition, pre-training injections of antagonist of NMDARs, 3-(2-carboxypiperazin-4-yl)-propyl-1-phosphonic acid (CPP), directly to the mPFC demonstrated that NMDA receptors are not required fear extinction training while immediate post-training (but not 2 hr after) injections of CCP impaired subsequent retrieval of extinction implicating NMDAR in

long-term memory [208, 209]. In addition, consolidation of fear extinction requires NMDAR-dependent bursting in the mPFC [208] suggesting that fear extinction learning involves extinction memory through NMDAR-mediated plasticity in prefrontal–amygdala circuits. Furthermore, the NR2B subunit of prefrontal NMDARs, which has been implicated in induction of synaptic plasticity [234, 235] appears to be critical for fear extinction consolidation but is dispensable during fear extinction training [215].

While decline of fear response to CS+ due to fear memory extinction (Fig. 2.6) and reduction of responses to CS- due to a generalization decline (Fig. 2.5) show similar behavioral patterns, the circuit-level mechanisms are likely different. Reduction of responses to conditioned stimulus CS+ is linked to well-studied mechanisms underlying fear memory extinction and decline of fear responses to non-reinforced CS- is connected to a generalization decrement. The mPFC-NR1 KO mice show deficits in both of these mechanisms suggesting that they may share similar requirements for prefrontal excitatory neurons expressing NMDARs. However, it is unclear if the same excitatory neurons in the mPFC govern both fear memory extinction and a generalization decrement or separate prefrontal circuits control these two mechanisms. The fact that behavioral effects of NMDARs deletion from prefrontal excitatory neurons is less severe in case of fear memory extinction (Fig. 2.6) when compared to fear discrimination (Fig. 2.5) may indicate that fear extinction learning and a generalization decline are governed through a separate neuronal populations and varying involvement of the PL and/or IL.

Additional supporting evidence for the mPFC as a locus for gating fear discrimination includes animal studies in which a mPFC lesion impairs the ability to

guide behavior, specifically when memory retrieval resolves conflicting dangerous and harmless contextual cues [236-239]. Fear decline is associated with elevated activity in the mPFC as determined by activation of immediate-early genes [60, 64], increased blood oxygenation levels [116], cell firing [208] and magnitude of local field potentials [240]. The mPFC has dense reciprocal anatomical and functional connections with sensory cortices, thalamic sensory relays and memory systems including the hippocampus and basolateral amygdala (BLA), the critical locus for fear processing. In addition, considerable evidence indicates that neurons in the mPFC, BLA and hippocampus are functionally coupled at the theta range (4-12 Hz oscillations) during fear conditioning [241, 242], conditioned extinction [240] and discriminative fear learning [243]. These studies have clinical implications because overgeneralized fear is a typical symptom of anxiety disorders including generalized anxiety disorder [244, 245] and posttraumatic stress disorder (PTSD) [246], which are triggered by cues in a secure environment that resemble those of the traumatic experience. Failure to discriminate between dangerous and harmless stimuli can lead to intrusive recollection of aversive memories. Our studies reveal that NMDARs expressed in prefrontal excitatory neurons control the ability to distinguish between dangerous and harmless stimuli.

Chapter 3: Fear discrimination learning generates prefrontal neuronal ensembles of safety

A version of this chapter is published in:
Corches A, Hiroto A, Bailey TW, Speigel III JH, Pastore J, Mayford M, Korzus E: Differential fear conditioning generates prefrontal neural ensembles of safety signals. *Behavioural Brain Research* 2018, *In press*.

Abstract

Fear discrimination is critical for survival while fear generalization is effective for avoiding dangerous situations. Overgeneralized fear is a typical symptom of anxiety disorders including generalized anxiety disorder and posttraumatic stress disorder (PTSD). Previous research has demonstrated that fear discrimination learning is mediated by prefrontal mechanisms. While the prelimbic (PL) and infralimbic (IL) subdivisions of the medial prefrontal cortex (mPFC) are recognized for their excitatory and inhibitory effects on the fear circuit, respectively, the mechanisms driving fear discrimination are unknown. To obtain insight into the mechanisms underlying context-specific fear discrimination, we investigated prefrontal neuronal ensembles representing distinct experiences associated with learning to disambiguate between dangerous and similar, yet distinct, harmless stimuli. Here, we show distinct quantitative activation differences in response to conditioned and generalized fear experiences, as well as modulation of the neuronal ensembles associated with successful acquisition of context-safety contingencies. These findings suggest that prefrontal neuronal ensembles patterns code functional context-danger and context-safety relationships. The PL subdivision of the mPFC monitors context-danger associations to conditioned fear, whereas differential conditioning generates additional ensembles associated with the inhibition of generalized

fear in both the PL and IL subdivisions of the mPFC. Our data suggests that fear discrimination learning is associated with modulation of prefrontal neuronal ensembles in a subregion- and experience-specific manner, and learning appropriate responses to conditioned and initially generalized fear experiences is driven by gradually updating and rebalancing prefrontal memory representations.

Introduction

Survival relies on the ability to discriminate between danger and safety. Fear discrimination learning is of clinical importance, as there is growing evidence that the failure to subdue fear under safe conditions is a primary symptom found in people with posttraumatic stress disorder (PTSD) [247-249]. Human imaging studies of functional connectivity between the prefrontal cortex and amygdala have demonstrated impaired inhibition of the amygdala in PTSD [250]. Others found elevated amygdala activity associated with PTSD without any obvious changes in the prefrontal inhibition [251]. Thus, understanding prefrontal mechanisms underlying safety signal processing during fear discrimination learning is relevant to normal and abnormal brain function.

The Hull-Spence continuity theory of discrimination learning postulates that conditioned excitation (the result of reinforcement) and inhibition (the result of non-reinforcement) have generalization gradients and that discrimination learning is the summation of excitation and inhibition [48-50]. On the other hand, the widely recognized multiple memory systems theory postulates that different types of memory are consolidated via hardwired pathways [20]. Studies of the circuitry mediating fear modulation reveal that fear behavior is differentially regulated by the prelimbic (PL) and infralimbic (IL) regions of the medial prefrontal cortex (mPFC) [22, 53, 172, 173] via fear excitation and inhibition, respectively [22, 204], which may be due to differential connectivity with the amygdala [205, 206].

During contextual fear conditioning, associations between a contextual stimulus (conditioned stimulus, CS) and a foot shock (unconditioned stimulus, US) are directly

encoded via synaptic plasticity in the amygdala, which receives direct inputs from the hippocampus (Hip) [252]. The fact that expression of recent and remote long-term fear memories requires the dorsal Hip (dHip) and mPFC, respectively, suggests that the communication between these two brain regions controls the transition from a recent state to a remote state during system-level memory consolidation [16, 17, 20, 65, 253]. While the dHip and mPFC appear to track spatial information, the mPFC is likely to integrate contextual recognition of context-danger associations with distinctive roles in the infralimbic (IL) and prelimbic (PL) subregions of the mPFC [254, 255]. Thus, both dHip and mPFC appear to be engaged in context encoding related to defensive behaviors, and context-specific neuronal ensembles are found in both regions [256, 257].

The mPFC network has been strongly implicated in fear modulation, including extinction [27, 31, 166], fear renewal [60, 213] and fear discrimination [4, 5, 19]. The mPFC appears to play a critical role in the decoding differences between dangerous and generalized stimuli that drive the acquisition of the differential fear responses. Molecular mediators of long-term memory consolidation in the mPFC, such as the N-methyl-D-aspartate (NMDA) receptor, CREB and CREB-binding protein (CBP)'s intrinsic histone acetyltransferase (HAT) activity, are all required for successful discriminative fear learning [4, 5], consistent with the idea that new memory encoding within the prefrontal network drives fear inhibition.

While the circuit-, cellular- and molecular-level mechanisms of fear extinction have been studied extensively in the mPFC, how the neural circuitry of the mPFC contributes to fear discrimination learning remains unknown. In this study, we examined

prefrontal neuronal ensembles representing distinct experiences associated with learning to distinguish between dangerous and similar, but not identical, safe stimuli. These data revealed prefrontal subdivision-specific patterns of neuronal activation, distinct quantitative activation differences in response to dangerous and harmless experiences, and the formation of overlapping neuronal ensembles associated with successful fear discrimination learning. Evidence from a context-dependent fear discrimination learning task indicated that substantial changes in population activity patterns occurred within distinct subdivisions of the mPFC during differential conditioning. Unexpectedly, both IL and PL cortices mediate safety learning, supporting the idea that both these cortical regions cooperate in properly gating context-danger and context-safety contingencies during top-down control of appropriate fear responses.

Materials and Methods

Subjects

The UC Riverside Institutional Animal Care and Use Committee approved all procedures in accordance with the NIH guidelines for the care and use of laboratory animals. The bi-transgenic TetTag mice were generated by breeding knock-in Arc-tTA homozygotes (generated on the C57BL/J6 background) carrying a tTA knockin insertion downstream from the *Arc* gene promoter with transgenic Tg(tetO-HIST1H2BJ/GFP)47Efu mice [258]. Tg(tetO-HIST1H2BJ/GFP)47Efu mice were generated by introducing the transgenic construct to CD-1 donor eggs and the hemizygous line was maintained on the C57BL/J6 background. Mice were weaned at postnatal day 21 and were housed, 4 animals to a cage, with same-sex littermates. Mice had ad libitum access to food and water and were maintained on a 12 h light/dark cycle. Old bedding was exchanged for fresh autoclaved bedding every week. Mice were raised on a 40 mg/kg Dox diet (BioServ, Inc, Custom Made Cat No F-3958) since gestation to prevent GFP expression before experimental manipulations. To label active neurons during Event 1 (see Fig. 3.1A), the food diet was changed to regular food chow not containing Dox. To prevent GFP expression after Event 1, we have switched food died to food chow containing high levels of Dox (1g/kg) (BioServ, Inc, Custom Made Cat No F-7363) These levels of Dox were effective in turning off expression of GFP [69, 259]. Seizure was induced by pentylenetetrazole (PTZ, 50mg/kg, intraperitoneal injection).

Contextual fear conditioning assay (CFC)

Mice between 2 and 6 months of age were individually housed. Mice were then handled once a day for three days before starting the CFC assay shown on diagram (Fig. 3.1A). All fear conditioning was performed in a fear conditioning box (Lafayette Instrument Co.) placed in a sound-attenuating chamber, and performance was analyzed automatically using a video-based system controlled by FreezeFrame v. 4 software (Actimetrics). On day 1, animals were exposed to three US (foot shock, 2 sec, 0.75 mA) in context CS+ after a 180 sec baseline with a 90 sec inter-trial interval and a 60 sec post-shock period. On day 2, animals were exposed to 1xUS in context CS+ after a 180 sec baseline with a 60 sec post-shock period. During days 3-5, animals were taken off Dox diet. On day 5, animals were exposed to CS+ for 300 sec then placed back on high dose Dox (1mg/kg) diet for the remainder of the assay. On day 6, animals were exposed to either conditioned context stimuli CS+ (cfc/CS+ group) or novel stimuli CtxtC (cfc/CtxtC group) for 300 sec then immediately placed back in their home cage and sacrificed 1 hr later. The noUS mice underwent the same procedure as cfc/CS+ mice with the exception that this group was never exposed to US. Home Cage animals were given the same Dox treatment as other groups but remained in their home cage for the entirety of the assay. All freezing, expressed as "% freezing", is calculated as the percentage of time spent freezing during the first 180 sec of context exposure. The box was cleaned between trials with 70% ethanol then water.

Contextual fear discrimination assay (DC)

The contextual fear discrimination assay is divided into the following parts: habituation, fear conditioning and differential conditioning divided into two phases: early discrimination and late discrimination (see Fig 3.3A). In the habituation phase, animals were exposed to each tested context stimuli (CS+, CS-, CtxtC) without US for 10 min a day for three days before starting the assay. On the first day of fear conditioning training (day 1), animals were exposed to three US (foot shock, 2 sec, 0.75 mA) in CS+ after 180 sec baseline with 90 sec inter-trial interval and 60 sec post-shock period. During the second day of fear conditioning (day 2), animals were exposed to 1xUS in context CS+ after a 180 sec baseline with a 60 sec post-shock period. On the first day of early discrimination (day 3), animals were exposed to CS+ (paired with US) then CS- (not paired) for an equal amount of time (242 sec). During days 4-6, animals were taken off Dox diet. On day 6, animals were exposed to one of tested stimuli (CS+, CS- or CtxtC) without any reinforcement for 300 sec then placed back on high dose Dox (1mg/kg) diet for the remainder of the assay. During differential conditioning [43], animals were exposed to CS+, CS- and CtxtC in alternating order for equal amounts of time (242 sec). During days 7-11, animals never received US during exposure to CS- and CtxtC, while exposure to CS+ was paired with US delivered 180 sec after placing animals in the context. On day 12, animals were re-exposed to their test context for 300 sec without any reinforcement, immediately placed back in their home cage and sacrificed 1 hr later. Discrimination index was calculated using the freezing responses to CS+ and CS-

according to the formula DI=[(% freezing to CS+) – (% freezing to CS-)]/[(% freezing to CS+) + (% freezing to CS-)].

Context description

Context CS+ was a 12.0" L x 10.2" D x 12.0" H fear conditioning box (Lafayette Instrument Co.) housed in a sound-attenuating chamber. Modalities included a constant 400 ms frequency-modulated sweep, logarithmically modulated between 2 and 9 kHz and delivered at 0.5 Hz, lemon extract scent, uniform shock bars, a ventilation fan and a house light.

Context CS- was a 12.0" L x 10.2" D x 12.0" H fear conditioning box (Lafayette Instrument Co.) located within a sound-attenuated chamber. Modalities included black and white vertical striped walls, a constant 2.8 kHz tone, vanilla extract scent, uniform shock bars, a ventilation fan and a house light.

Context CtxtC was a 9" L x 6" D x 6.5" plastic box with Sani-Chips bedding located in a fear conditioning chamber (Lafayette Instrument Co.). Modalities included a ventilation fan and a house light. CS+ and CS- are designed to be similar yet distinct while CtxtC is substantially different and served as a neutral context. While CS+ predicted US; CS- and CtxtC did not predict US.

Histology

Mice were sacrificed using Nembutal (200 mg/kg, intraperitoneal injection) and transcardially perfused with 20 ml of PBS and then 20 ml of 4% PFA. Brains were extracted, soaked in 4% PFA overnight at 4°C then soaked in 20% sucrose at 4°C until the brains sank. The brains were then flash-frozen in embedding media (Tissue-Tek,

4583) using dry ice and ethanol before being stored at -80°C. Free-floating 40 μm coronal sections were sliced using a cryostat (Leica, CM1860) and stored in cryoprotectant (50% PBS, 30% ethylene glycol, 20% glycerol) at -20°C. Free-floating immunohistochemistry (IHC) was performed by washing sections 2 times for 10 min in 1x PBS followed by a 1 hr incubation in blocking buffer (4% normal goat serum in washing buffer) then washing 3 times for 10 min in washing buffer (1x PBS w/ 0.3% Triton X-100). The sections were then incubated overnight at 4°C in antibody diluent (2% normal goat serum in washing buffer) with primary antibodies (chicken anti-GFP polyclonal antibody, Thermo Fisher, A10262, 1:2000; mouse anti-NeuN monoclonal antibody, Millipore, MAB377, 1:2000; rabbit anti-Arc polyclonal antibody, Synaptic Systems, 156-003, 1:2500). After three washes with washing buffer, the sections were incubated with secondary antibodies (Alexa488 goat anti-chicken IgG, Thermo Fisher, A-11039, 1:1000;, Alexa568 goat anti-mouse IgG, Thermo Fisher, A-11031, 1:1000; Alexa647 donkey anti-rabbit IgG, Thermo Fisher, A-31573, 1:1000) for 3 hr at room temperature in antibody diluent. The sections were then washed once with washing buffer for 10 min and incubated with DAPI (Invitrogen, D1306, 1:1000) for 15 mins. Sections were then washed twice with 1x PBS for 10 min. Sections were mounted on glass slides (Superfrost Plus, 12-550-15) using mounting medium (ProLong Antifade, P36965) and sealed with nail polish before imaging.

Imaging

Coronal sections from 2.5 mm to 1.7 mm anterior to bregma were imaged at 20x (20x/0.95 *XLUMPlanFl* objective) magnification using a semi-automatic laser-scanning

confocal Olympus FV1000 microscope controlled by Olympus FV10-ASW software (v. 2.01). The gain and offset of each channel were balanced manually using Fluoview saturation tools for maximal contrast. All settings were tested on multiple slices before data collection and brain slices were imaged using identical microscope settings once established. Each channel was acquired in "Sequential Mode, Frame". All images were acquired using the "Integration Type: Line Kalman" and "Integration Count: 2" in order to increase the signal-to-noise ratio. Localization of the PL and IL regions within the mPFC was performed by overlaying images from the Allen Mouse Brain Atlas. For quantification, 10 optical sections were acquired from a 30 μm Z-stack encompassing both superficial and deep layers. GFP-positive (GFP+), Arc-positive (Arc+) and total number of cells (DAPI+ cells) per image were counted by an experimenter who was blind to the treatment status. For reactivation, GFP+ and Arc+ (GFP+ ∩ Arc+) overlap was counted only when the Arc signal and GFP signal came from the same cell over multiple optical sections. Images were quantified from both hemispheres of 5-9 anatomically matched sections per animal through the entire rostrocaudal axis of the mPFC. The number of GFP+ cells, number of Arc+ cells and percentage of overlap were calculated per image and then averaged to produce a single measurement per animal. Mean ± SEM of the total number of DAPI-positive nuclei per image from PL and IL were counted from 3–5 coronal sections per mouse (n=4). Mean ± SEM of Activation and Reactivation Rates were calculated per image as follows: Event 1 activation rate (GFP+ cells) was calculated as # of GFP+ cells per image. Event 2 activation rate (Arc+ neurons) was calculated as # of Arc+ neurons per image. Reactivation Rate (Overlapping Ensemble)

was calculated as [(GFP+ cells ∩ Arc+ cells)/Arc+ cells] x 100 per image. We have also compared measured reactivation index (calculated as [(GFP+ cells ∩ Arc+ cells)/DAPI+ cells] x 100 per image) to a predicted reactivation index calculated as a chance, where the chance was calculated as CHANCE = (GFP+ cells/DAPI+ cells) * (Arc+ cells/DAPI+ cells) * 100. All significant reactivation indexes that are reported in the manuscript were substantially higher than the calculated chance.

Data analysis

Experimenters were blind to group designations. The data represents the mean ± SEM. Statistical analysis was performed using GraphPad Prism and Excel (Microsoft, Inc.). Student's *t* test or ANOVA was used for statistical comparisons. Pearson's correlation (*r*) was used as an *effect size*. For one-way ANOVA, eta-squared (η^2) was used as an *effect size*. For learning assessment during fear conditioning and differential conditioning, repeated measures (RM) ANOVA and *post hoc* analysis with Tukey's's multiple comparisons test was used. Analysis of neuronal ensemble activation and reactivation was performed using ordinary one-way ANOVA followed by Dunnett's's many-to-one comparisons *post hoc* test. In order to compare neuronal activations between events during exposure and re-exposure to a specific stimulus, we performed RM ANOVA followed by multiple comparisons Sidak's *post hoc* test. In order to compare neuronal activation or reactivation between brain regions during exposure and re-exposure to a specific stimulus, we performed ordinary two-way ANOVA followed by multiple comparisons Sidak's *post hoc* test. Comparison with chance level was done using one sample t-test and an effect size. The relationship between the activation rate or

the reactivation index and behavioral performance was measured by simple linear correlations (Pearson correlation). Significance values were set at $p < 0.05$. Asterisks indicate statistical significance: *, $P < 0.05$; **, $P < 0.01$; ***, $P < 0.001$ and ns or absence of asterisk(s) indicates not significant.

Results

Fear memory retrieval triggers PL neural ensembles of context-danger association

Context-sensitive fear learning and modulation involves amygdala-hippocampus-mPFC circuitry [14]. The prefrontal cortex is strongly implicated in context-dependent fear modulation, such as fear extinction [44], fear renewal [60, 213], remote memories [65], reconsolidation [25], contextual learning after hippocampal loss [19] and fear discrimination learning [4, 5, 43]. The PL subdivision of the mPFC is engaged directly in context-dependent fear acquisition [255], while posttraining mPFC inactivation can trigger inhibition of fear expression during recent and remote contextual fear memory recall [17]. More recent studies show that direct optogenetic activation of mPFC neuronal populations triggered by US during fear conditioning leads to elevated fear in a novel environment when tested 2 or 12 days after conditioning [253]. Based on these data, we hypothesized that the PL network codes functional context-danger associations already during contextual fear conditioning and that these neuronal ensembles of contextual fear memory would be reactivated during consecutive memory retrievals.

To trace neuronal ensembles of contextual fear memories, we employed an activity-dependent genetic labeling system referred to as the TetTag system [69, 74, 259]. *cFos, Zif268* and *Arc* are immediate-early genes [58] frequently used as neuronal activity markers in various brain areas [260]. We employed an *Arc* promoter-driven genetic tagging system, which allowed us to label activated neuronal populations during two separate experiences, referred to as Event 1 and Event 2 (Fig. 3.1A-B). Exposure to a stimulus during Event 1 drove labeling of activated neurons with GFP, while the second

exposure to a stimulus (Event 2) drove Arc expression. Thus, single-labeled cells with GFP or Arc represented selectively distinctive populations induced during Event 1 or 2, and double-labeled cells were active during both events. The genetic GFP tagging of activated cells can occur only during a brief 3 day window, when animals were removed from the low dose Dox diet (40 mg/kg) and given regular food chow. To assure that unintentional labeling would not interfere with data interpretation, we designed number of procedures to control for any nonspecific labeling. All behavioral procedures were performed in dedicated behavioral rooms accessible only to experimenters. Week-long habituation prevented any accidental neuronal-activity gene induction. After genetic labeling was completed, animals received a high dose Dox diet (1 g/kg) to suppress expression of new GFP, as reported previously [259]. Figure 3.1C shows that expression of GFP in Dox-treated animals was negligible.

We evaluated the formation and stability of neuronal ensembles induced by the aversive contextual stimuli (CS+) within the IL and PL subdivisions of the mPFC (Fig. 3.1A). In a parallel control experiment, the performance of the animals was tested in exactly the same behavioral paradigm, including exposure to the same context, except that this group of animals was never exposed to any re-enforcer (Fig. 3.1A, noUS group). In addition, we have tested behavioral performance of cfc/CtxtC mice that were treated the same as the cfc/CS+ mice, but these animals were exposed to a novel, neutral context CtxtC (cfc/CtxtC group) during the second exposure (Event 2), while the cfc/CS+ mice were exposed to the same dangerous context CS+ during both Event 1 and 2. The cfc/CS+ and cfc/CtxtC groups showed good performance on fear conditioning training

task compared to the noUS group (Fig. 3.1E. Group x US: $F(8, 132) = 13.97$, $P<0.0001$; Group: $F(4, 132) = 65.47$, $P<0.0001$; US, $F(2, 33) = 18.4$, $P<0.0001$). As anticipated, the noUS group showed no fear during the first and second retrievals (Fig. 3.1F). The cfc/CS+ group showed marked levels of fear during exposure (Event 1) and re-exposure (Event 2) to the dangerous context, CS+ (Fig. 3.1F, Event 1 vs. Event 2: cfc/CS+, $P=0.3819$). The cfc/CtxtC group showed elevated fear responses during exposure to CS+ on day 5 (Event 1) and negligible freezing during exposure to the novel context, CtxtC, on day 6 (Fig. 3.1F, Event 1 vs. Event 2: cfc/CtxtC, $P<0.0001$). The control group of mice referred as to HC (Home Cage) underwent the same dietary Dox administration but was left in their home cages throughout the entirety of the assay.

To assess whether the TetTag system was reliable in marking context-danger experiences, we compared levels of reactivation in the mPFC of mice that were initially fear-conditioned in context CS+ followed by exposure (Event 1) and re-exposure (Event 2) to the dangerous context CS+ (group cfc/CS+) to levels of reactivation of the noUS group, which underwent the same treatment as the cfc/CS+ group but was never exposed to US (Fig. 3.1A). The activation rates during Event 1 and Event 2 observed in the noUS group were the same as in animals that spent their entire time in their home cages [95] (Fig. 3.2A: PL/E1: noUS vs HC, $P=0.8404$. Fig. 3.2B PL/E2: noUS vs HC, $P=0.2527$. Fig. 3.2D, IL/E1: noUS vs HC, $P= 0.4251$. Fig. 3.2E, IL/E2: noUS vs HC, $P=0.1245$). We observed increased activity in the PL during both consecutive retrievals of context-danger associations (Fig. 3.2A: PL/E1: noUS vs. cfc/CS+, $P=0.0469$; Fig. 3.2B: PL/E2: noUS vs. cfc/CS+, $P=0.0001$). In addition, the exposure and re-exposure to the aversive

context CS+ did not trigger increased activity in IL when those responses were compared to the noUS group (Fig. 3.2D-E). We observed substantial reactivation of PL neuronal ensembles induced by CS+ (predicting US) during re-exposure (Fig. 3.2C: Reactivation in PL, cfc/CS+ vs. noUS, $P<0.0001$), while the same but not-reinforced context failed to trigger reactivation of neuronal ensembles of non-reinforced contextual memory in PL (Fig. 3.2C: Reactivation in PL, HC vs. noUS, $P=0.8398$). None of the tested groups showed a reactivation of neuronal ensembles in IL during re-exposure (Fig. 3.2F: one-way ANOVA, $F(3, 17) = 0.3895$, $P=0.7621$). Clearly, the reactivation of ensembles associated with context-danger occurred specifically in PL. These data indicate that a majority of double-labeled cells (i.e., GFP+ and Arc+) in PL were specific to the contextual fear experience.

To investigate whether changes in the mPFC neuronal ensemble activation were experience-specific, we compared the performance of the cfc/CS+ groups with the cfc/CtxtC group. The cfc/CtxtC group underwent similar behavioral treatment as cfc/CS+, except that during Event 2, cfc/CS+ mice were exposed to a substantially different context stimulus, CtxtC, while cfc/CS+ animals were re-exposed to the context stimulus, CS+ (Fig. 3.1A). Training data showed that the cfc/CS+ and cfc/CtxtC groups learned the association between the conditioned stimulus CS+ and US compared to the noUS group (Fig. 3.1E: see above), and both experimental groups showed successful learning at the end of the training. Both cfc/CS+ and cfc/CtxtC groups showed elevated freezing during Event 1 (Fig. 3.1F: cfc/CS+ vs. noUS, $P<0.0001$; cfc/CtxtC vs. noUS, $P<0.0001$). While re-exposure to context CS+ induced elevated freezing (Fig. 3.1F: Event

2: cfc/CS+ vs. noUS, P=0.0042), exposure to the substantially different CtxtC stimulus during Event 2 did not trigger fear (Event 2: cfc/CtxtC vs. noUS, P=0.9976).

To evaluate how context specificity affected ensemble reactivation in the mPFC, we compared activity and reactivation in the mPFC of the cfc/CS+ group with the cfc/CtxtC group. Similar to cfc/CS+, the cfc/CtxtC group was also fear conditioned in context CS+ followed by exposure to CS+ (Event 1), but during Event 2 the cfc/CtxtC group was exposed to the novel context CtxtC. Thus, the cfc/CtxtC group allowed us to test whether two consecutive exposures to two different contextual stimuli would generate overlapping neuronal ensembles in the mPFC during the second exposure. Distinct experiences (i.e., CS+ vs. CtxtC) generated different and non-overlapping patterns of activity in the PL (Fig. 3.2C: Reactivation/PL: cfc/CtxtC vs. cfc/CS+, P =0.0001). Neither the cfc/CtxtC nor the cfc/CS+ group induced stable ensembles in IL (Fig. 3.2F: Reactivation in IL: one-way ANOVA F (3, 17) = 0.3895, P=0.7621). There was no difference between the cfc/CS+ and cfc/CtxtC groups in activation of PL or IL during exposure to CS+ during Event 1 (Fig. 3.2A: PL/E1: cfc/CS+ vs. CtxtC, P=0.9923; Fig. 3.2D: IL/E1: cfc/CS+ vs. CtxtC, P=0.9885). Induced neuronal activity patterns in the response to the novel context CtxtC during Event 2 were similar to those observed when the CS+ group was tested (Fig. 3.2B: PL/E2: cfc/CS+ vs. cfc/CtxtC, P=0.2720) suggesting that PL may be engaged during the generation of appropriate responses to both dangerous and novel, discriminated neutral-context stimuli after experience with US but if animals had no prior experience with US (noUS group). The neuronal response to neutral context CtxtC was also detected in IL (Fig. 3.2E: IL/E2 noUS vs. cfc/CtxtC,

P=0.047), but the activity in response to CtxtC was substantially lower in IL compared to PL (Fig. 3.2B, E: Event 2/PL vs IL: two-way ANOVA Group x Region: $F(3, 34) = 15.12$, $P<0.0001$; Region: $F(1, 34) = 89.6$, $P<0.0001$; Group: $F(3, 34) = 35.94$, $P<0.0001$; cfc/CtxtC PL vs IL, $P<0.0001$). These data provide evidence that the mPFC neuronal ensembles are highly engaged in processing information relevant to context-danger associations and that distinct context-danger related experiences generate different patterns of activity in the mPFC.

In summary, the TetTag system was reliable in marking contextual fear experiences in the mPFC. As we anticipated, distinct context-danger experiences generated distinctive non-overlapping patterns of activity in the mPFC. While both PL and IL circuits can be activated by aversive and neural context stimuli, the PL circuit is more likely to encode lasting memories of context-danger experiences.

Figure 3.1

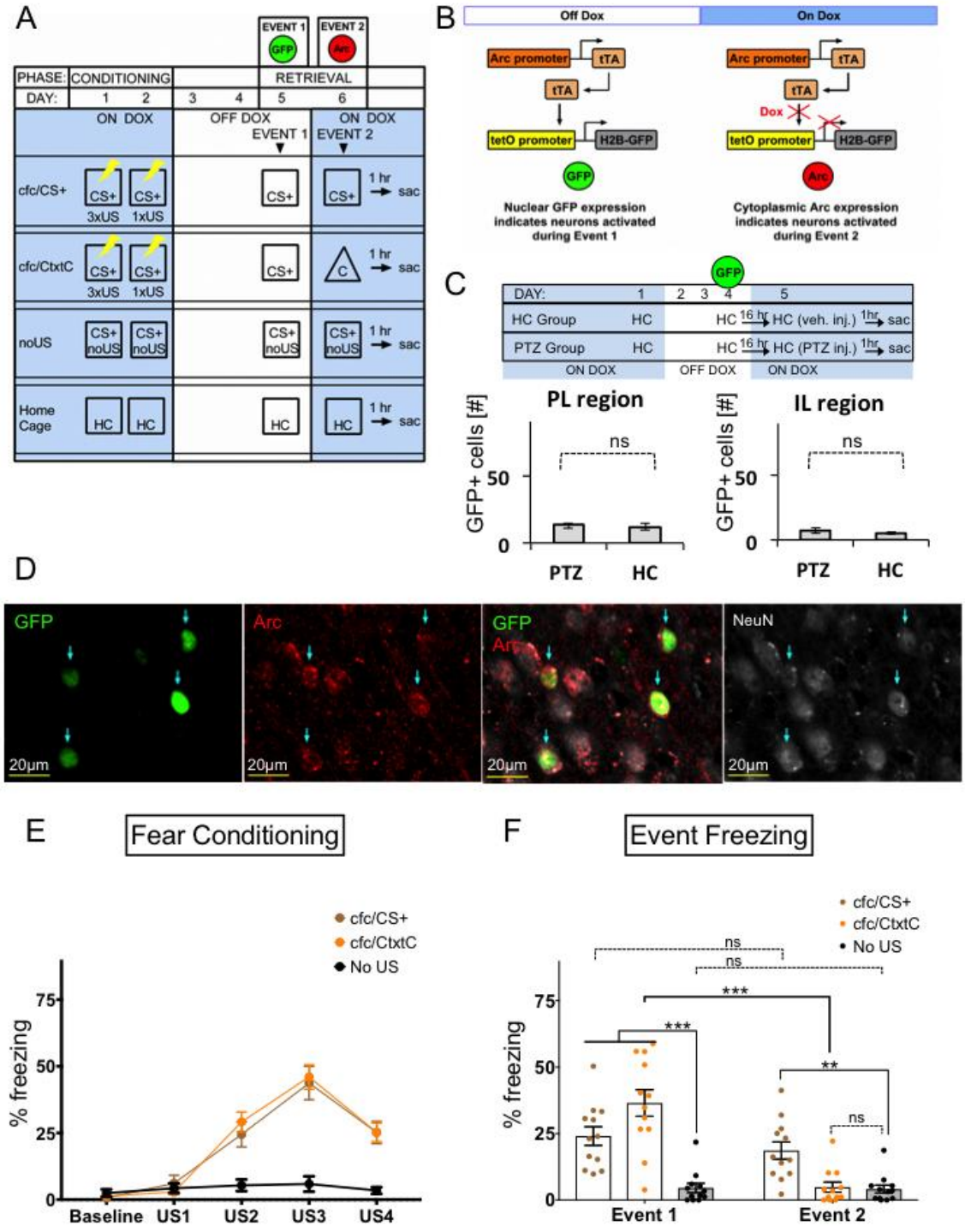
A
EVENT 1
EVENT 2
GFP
Arc
PHASE:
CONDITIONING
RETRIEVAL
DAY:
1
2
3
4
5
6
ON DOX
OFF DOX
EVENT 1
ON DOX
EVENT 2
cfc/CS+
CS+
3xUS
1xUS
1 hr
sac
cfc/CtxtC
C
noUS
CS+ noUS
Home Cage
HC
B
Off Dox
On Dox
Arc promoter
tTA
tetO promoter
H2B-GFP
Dox
Nuclear GFP expression indicates neurons activated during Event 1
Cytoplasmic Arc expression indicates neurons activated during Event 2
C
DAY:
HC Group
PTZ Group
16 hr
HC (veh. inj.)
HC (PTZ inj.)
ON DOX
OFF DOX
ON DOX
PL region
IL region
GFP+ cells [#]
ns
50
0
PTZ
HC
D
GFP
Arc
NeuN
20μm
E
Fear Conditioning
cfc/CS+
cfc/CtxtC
No US
% freezing
75
50
25
0
Baseline
US1
US2
US3
US4
F
Event Freezing
***
**
Event 1
Event 2

(Previous page) Figure 3.1: Genetic tagging of neuronal ensembles activated during two distinct events using the Arc-driven TetTag system and endogenous *Arc* gene expression. (**A**) Animals were fear conditioned to CS+, then exposed to conditioned stimuli, CS+, during first memory retrieval (Event 1), and then exposed either to CS+ again (cfc/CS+ group) or to a very different context, CtxtC (cfc/CtxtC). The noUS group was exposed to the same context as CS+ but without foot shocks (US) and then underwent the same testing as cfc/CS+ group. Home cage indicates animals were housed in their home cage during the duration of the assay. (**B**) This study used bi-transgenic mutants, in which the *Arc* promoter drove the expression of the tetracycline-controlled transactivator protein [72], which binds to the tetracycline-responsive promoter element (tetO), driving the expression of a fusion protein composed of histone 2B and green fluorescent protein (H2B-GFP) in activated neurons. Indelible labelling of transiently activated neurons during specific experiences was controlled by a doxycycline (Dox) diet. When animals were taken off Dox, neurons activated during Event 1 were labelled with GFP. Neurons activated during Event 2 were revealed by assessment of endogenous Arc expression. (**C**) Dox diet was effective in blocking GFP expression in the brain. In this experiment, mice were removed from regular Dox diet (40 mg/kg) similarly as shown in Fig. 3.1A and given regular food chow diet for 3 days. After switching to high dose Dox food diet (1 g/kg) for 16 hours, seizure was induced by pentylenetetrazole (PTZ) and mice were tested 1 hr later for GFP expression in the mPFC. Home cage [95] refers to mice that underwent the same Dox treatment as the PTZ mice but did not receive PTZ injection. Y-axis label "GFP+ cells [#]" refers to a number of GFP-positive cells found in PL (left) or IL (right). There was no difference in PL activity measured in HC ($M=12 \pm 2.352$, $n=6$) and PTZ ($M=13.22 \pm 1.701$, $n=3$) conditions; $t(7)=0.3387$, $p=0.7448$, $r=-0.133$. In addition, there was no difference in IL activity measured in HC ($M=5.607 \pm 1.073$, $n=6$) and PTZ ($M=7 \pm 2.211$, $n=3$) conditions; $t(7)=0.6522$, $p=0.5351$, $r=0.131$. (**D**) Representative images taken from the same region in the mPFC showing a comparison between permanently GFP-labelled neurons during Event 1 (GFP, green) and endogenous *Arc* gene expression during Event 2 (Arc, red). An overlap of GFP and Arc images reveal neurons activated during both Event 1 and Event 2. Cell identity is revealed via expression of a neuronal marker (NeuN). Representative images were acquired as a single optical section using 40x magnification with a digital zoom of 3.0 in the PL. Blue arrows indicate overlapping neurons activated during both Event 1 and Event 2. Scale bars indicate 20 μm. (**E**) The cfc/CS+ and cfc/CtxtC groups were successfully fear conditioned. RM two-way ANOVA of Group and US followed by Tukey's multiple comparison reveled robust fear acquisition compared to the noUS group (Group × US: $F(8, 132) = 13.97$, $P<0.0001$; Group: $F(4, 132) = 65.47$, $P<0.0001$; US, $F(2, 33) = 18.4$, $P<0.0001$ (Baseline: cfc/CS+ vs. cfc/CtxtC, P=0.9903, cfc/CS+ vs. noUS, P=0.9184, cfc/CtxtC vs. noUS, P=0.963; US1: cfc/CS+ vs. cfc/CtxtC, P=0.7502, cfc/CS+ vs. noUS, P=0.9101; cfc/CtxtC vs. noUS, P=0.9486; US2: cfc/CS+ vs. cfc/CtxtC, P=0.5577, cfc/CS+ vs. noUS, P=0.0001, cfc/CtxtC vs. noUS, <0.0001; US3: cfc/CS+ vs. cfc/CtxtC, P=0.868, cfc/CS+ vs. noUS, P=<0.0001, cfc/CtxtC vs. noUS, P=<0.0001; US4: cfc/CS+ vs. cfc/CtxtC, P=>0.9999, cfc/CS+ vs. noUS, P=<0.0001, cfc/CtxtC vs. noUS, P=<0.0001. (**F**) cfc/CtxtC mice show differential responses to two different stimuli: CS+ and CtxtC. After fear conditioning

(Fig. 3.1E), the cfc/CS+ and cfc/CtxtC groups were exposed to conditioned stimuli CS+ during first memory retrieval (Event 1), and then exposed either to CS+ again (cfc/CS+ group) or to a substantially different context, CtxtC (cfc/CtxtC), respectively. While the cfc/CtxtC group showed high fear in response to CS+ during Event 1 and low fear in response to CtxtC during Event 2, the cfc/CS+ group showed similar levels of fearful responses during both events. The noUS group was not fear conditioned and showed no fear throughout the conditioning phase. RM two-way ANOVA of Group and US followed by Sidak's multiple comparisons showed that the cfc/CtxtC group distinguished between two different contextual stimuli: CS+ and CtxtC. (Group × US: $F(2, 33) = 20.9$, $P<0.0001$; US: $F(1, 33) = 34.84$, $P<0.0001$; Group: $F(2, 33) = 15.24$, $P<0.0001$. Event 1 - Event 2: cfc/CS+, $P=0.3819$; cfc/CtxtC, $P<0.0001$; noUS, $P=0.9993$. Event 1: cfc/CS+ vs. noUS, $P<0.0001$, cfc/CtxtC vs. noUS, $P<0.0001$; Event 2: cfc/CS+ vs. noUS, $P=0.0042$; cfc/CtxtC vs. noUS, $P=0.9976$). Significance values were set at $p < 0.05$: *, $p < 0.05$; **, $p < 0.01$; ***, $p < 0.001$ and ns not significant.

Figure 3.2

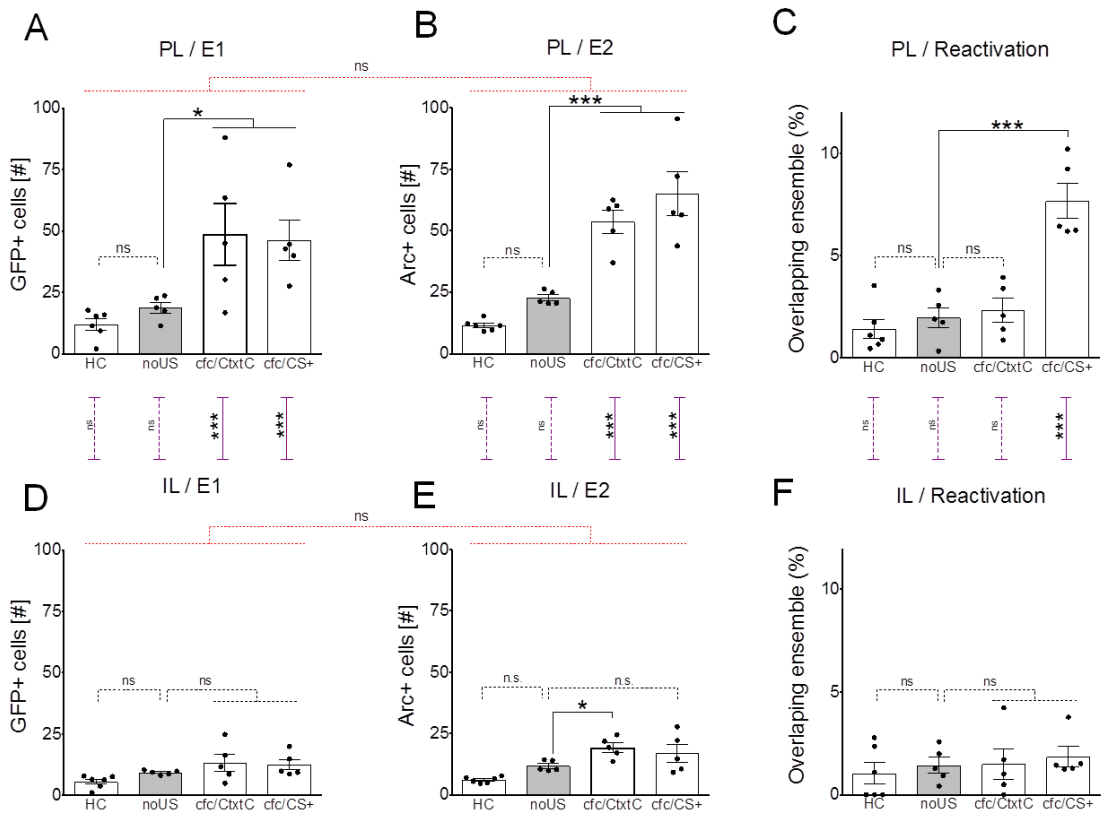
A
PL / E1
GFP+ cells [#]
B
PL / E2
Arc+ cells [#]
C
PL / Reactivation
Overlapping ensemble (%)
D
IL / E1
GFP+ cells [#]
E
IL / E2
Arc+ cells [#]
F
IL / Reactivation
Overlaping ensemble (%)
HC
noUS
cfc/CtxtC
cfc/CS+
ns
n.s.
*
***

(Previous page) Figure 3.2: Fear conditioning triggers specific neuronal ensembles of contextual stimuli encoding CS+ in the PL. (**A**) The cfc/CS+ and cfc/CtxtC groups had greater activation in the PL than the HC group during Event 1. Ordinary one-way ANOVA ($F(3, 17) = 6.757$, $P=0.0033$) followed by Dunnett's many-to-one comparisons with the noUS as a control: noUS vs. HC, $P=0.8404$; noUS vs. cfc/CtxtC, $P=0.0301$; noUS vs. cfc/CS+, $P=0.0469$. (**B**) The cfc/CS+ and cfc/CtxtC groups had greater activation of the PL than noUS group during Event 2. Ordinary one-way ANOVA (ANOVA, $F(3, 17) = 28.28$, $P<0.0001$) followed by Dunnett's many-to-one comparisons with the noUS as a control: $F(3, 17) = 28.28$, $P<0.0001$: noUS vs. HC $P=0.2527$, noUS vs. cfc/CtxtC, $P=0.001$; noUS vs. cfc/CS+, $P=0.0001$. (**C**) The cfc/CS+ group has greater reactivation of PL than cfc/CtxtC, noUS and HC groups. Ordinary one-way ANOVA ($F(3, 17) = 22.52$, $P<0.0001$) followed by Dunnett's many-to-one comparisons with the noUS as a control: noUS vs. HC, $P=0.8398$; noUS vs. cfc/CtxtC, $P=0.9524$; noUS vs. cfc/CS+, $P=0.0001$. (**D**) During Event 1, there was no difference in activation of IL between groups compared to the noUS group but the cfc/CtxtC group has higher activation than HC in the IL. Ordinary one-way ANOVA ($F(3, 17) = 3.194$, $P=0.0501$) followed by Dunnett's many-to-one comparisons with the noUS as a control: noUS vs. HC, $P=0.4251$; noUS vs. cfc/CtxtC, $P=0.4115$; noUS vs. cfc/CS+, $P=0.5672$. (**E**) During Event 2, only the cfc/CtxtC group showed increased activity in the IL compared to the noUS group but the cfc/CS+ and cfc/CtxtC groups had greater activation than HC. Ordinary one-way ANOVA ($F(3, 17) = 9.221$, $P=0.0008$) followed by Dunnett's many-to-one comparisons with the noUS as a control: noUS vs. HC, $P=0.1245$; noUS vs. cfc/CtxtC, $P=0.047$; noUS vs. cfc/CS+, $P=0.2212$. (**F**) There was no difference in reactivation of IL between groups. Ordinary one-way ANOVA: $F(3, 17) = 0.3895$, $P=0.7621$. Additional analysis involved comparing data sets across different panels. There was no difference in activation of PL between events (Fig. 3.2A, B). RM two-way ANOVA of Group × Event: Group x Event: $F(3, 17) = 1.567$, $P=0.2339$; Event: $F(1, 17) = 4.139$, $P=0.0578$; Group: $F(3, 17) = 18.03$, $P<0.0001$. There was no difference in activation of IL between events (Fig. 3.2D, E). Group × Event: $F(3, 17) = 1.073$, $P=0.3866$; Event: $F(1, 17) = 8.438$, $P=0.0099$; Group: $F(3, 17) = 8.642$, $P=0.0010$. The cfc/CtxtC, and cfc/CS+ groups show lower activation of IL compared to PL during Event 1 (Fig. 3.2A, D). Ordinary two-way ANOVA (Group × Region: $F(3, 34) = 4.204$ $P=0.0124$; Region: $F(1, 34) = 31.34$, $P<0.0001$; Group: $F(3, 34) = 8.797$, $P=0.0002$) followed by Sidak's multiple comparisons PL/E1 vs. IL/E1: HC, $P= 0.8455$; noUS, $P=0.6506$; cfc/CtxtC, $P=0.0003$; cfc/CS+, $P=0.0005$. The cfc/CtxtC, and cfc/CS+ groups show lower activation of IL compared to PL during Event 2 (Fig. 3.2B, E). Ordinary two-way ANOVA (Group × Region: $F(3, 34) = 15.12$, $P<0.0001$; Region $F(1, 34) = 89.6$, $P<0.0001$;Group: $F(3, 34) = 35.94$, $P<0.0001$. PL/E2 vs. IL/E2: HC, $P= 0.7334$; noUS, $P=0.1873$; cfc/CtxtC, $P<0.0001$; cfc/CS+, $P<0.0001$. The cfc/CS+ groups show lower reactivation of IL compared to PL during Event 2 (Fig. 3.2C, F). Ordinary two-way ANOVA Group × Region: $F(3, 34) = 10.04$, $P<0.0001$; Region : $F(1, 34) = 21.24$, $P<0.0001$; Group: $F(3, 34) = 15.13$, $P<0.0001$: PL vs. IL: HC, $P= 0.9827$; noUS, $P=0.9514$, cfc/CtxtC, $P=0.7861$; cfc/CS+, $P<0.0001$. Significance values were set at $p < 0.05$: *, $p < 0.05$; **, $p < 0.01$; ***, $p < 0.001$ and ns not significant. Black lines indicate

comparisons within a panel; the red lines indicate side-by-side comparisons and purple lines indicate top-bottom comparisons.

Differential fear conditioning (DC) coincides with generation of neuronal ensembles of context-safety associations across subdivisions of the mPFC

Previous research has shown that the mPFC is involved in fear discrimination learning but the role of its subdivisions remains unclear [4, 5, 43]. To test the involvement of PL and IL subdivisions of the mPFC in fear discrimination learning, we evaluated PL and IL responses during exposure to dangerous stimulus CS+ and initially non-discriminated, generalized CS- before DC and after (Fig. 3.3A).

To obtain more detailed insight into the prefrontal mechanisms driving fear discrimination learning, we used the TetTag genetic system to label neurons during the early and late phases of fear discrimination learning to evaluate changes in the neuronal ensembles in the PL and IL caused by exposure to three context stimuli during DC: the aversive context stimulus CS+; a similar yet distinct, safe stimulus, CS-; and a substantially different safe stimulus, CtxtC (Fig. 3.3A). The HC mice remained in their home cage during the entire behavioral treatment. The other three groups (dc/CS+, dc/CS-, and dc/CtxtC) were exposed to all three contextual stimuli before fear conditioning during habituation. The animals underwent contextual fear conditioning (days 1-2) followed by the memory retrieval test on day 3 (CS+ and CS- context testing). Then, the animals were taken off Dox food chow and exposed to one of three contexts (Event 1, day 6): CS+ (Group dc/CS+), CS- (Group dc/CS-), or CtxtC (Group dc/CtxtC), respectively, followed by a diet switch back to Dox food chow. Genetic tagging of neural ensembles induced by conditioned and generalized fear stimuli during Event 1 (day 6) was performed when the animals did not discriminate between CS+ and CS-. Following Event 1, these three groups of mice were subjected to 5 days of differential fear

conditioning (days 7-11). On the last day of the behavioral procedure (Event 2, day 12) each group (i.e., dc/CS+, dc/CS-, and dc/CtxtC) was exposed to a specific context stimulus, CS+, CS-, or CtxtC, respectively. Brains were collected 1 hour after the last exposure and were analyzed by histology for *Arc* gene promoter-dependent patterns of gene expression to evaluate genetically tagged neural ensembles of contextual memories. In the DC paradigm, the context stimulus CS+ was paired with the unconditioned stimulus (US), and the other stimuli, CS- and CtxtC, were not paired with the US. Therefore, CS+ predicted US, and the stimuli CS- and CtxtC did not predict US. While both stimuli CS- and CtxtC predicted safety, CS- initially triggered elevated levels of fear because CS- shared substantial similarities with CS+.

First, we assessed the behavioral performance of the tested animals. During the course of the test, the discrimination between CS+ and CS- steadily increased as animals learned to inhibit generalized fear to the safer stimulus CS-. The third context stimulus CtxtC served as a learning control. CtxtC was substantially different from CS+ and was a good predictor for safety during all phases of testing. All three groups dc/CS+, dc/CS and dc/CtxtC showed robust performance on differential fear conditioning (Fig. 3.3B. dc/CS+; RM ANOVA: Day $F(5, 115) = 16.82$ $P<0.0001$; Context $F(1, 23) = 84$ $P<0.0001$, Day x Context $F(5, 115) = 7.006$ $P<0.0001$) dc/CS-. Fig. 3.3C. dc/CS-; RM ANOVA: Day $F(5, 155) = 15.21$, $P<0.0001$, Context $F(1, 31) = 81.3{,}1$ $P<0.0001$, Day x Context $F(5, 155) = 14.47$, $P<0.0001$. Fig. 3.3D. dc/CtxtC; RM ANOVA: Day, $F(5, 55) = 4.539$ $P=0.0016$, Context, $F(1, 11) = 53.99$ $P<0.0001$, Day x Context, $F(5, 55) = 6.024$ $P=0.0002$) after acquisition of conditioned fear responses during day 1, and there were no

differences between groups during fear conditioning (Fig. 3.3E. RM two-way ANOVA Group x US: P= 0.671, US, P <0.0001, Group, P 0.7484). In addition, all three groups dc/CS+, dc/CS and dc/CtxtC showed similar patterns of freezing responses to CS+ and CS-, with elevated responses to CS+ across differential conditioning and descending responses to CS- (freezing to CS-: Fig. 3.3B, dc/CS+, Days 3 vs 11, $t(23)=6.97$, $p<0.0001$, $r=-0.541$; Fig. 3.3C, dc/CS-, $t(31)=7.35$, $p<0.0.0001$, $r=-0.584$; Fig. 3.3D, dc/CtxtC, Days 3 vs 11, $t(11)=3.654$, $p<0.0038$, $r=-0.450$). The dc/CS+, dc/CS- and dc/CtxtC groups showed no difference in performance monitored as a value of Discrimination Index across the differential fear conditioning task (Fig. 3.3F. RM ANOVA: Group x Day: P= 0.8098, Day, P <0.0001, Group, P= 0.3177). In addition, all three groups showed similar levels of generalization at the beginning of differential fear conditioning and similar levels of fear discrimination after differential fear conditioning (Fig. 3.3G. RM two-way ANOVA Group x Event: P= 0.0741, Event, P <0.0001, Group, P 0.0871 followed by Sidak's multiple comparisons: E1 vs. E2: dc/CtxtC, P= 0.0002, dc/CS-, P= <0.0001, dc/CS+, P <0.0001). These data indicate that dc/CS+, dc/CS-, and dc/CtxtC showed robust performance on the fear discrimination task and there were no noticeable differences in performance between these groups.

Second, we evaluated changes in the prefrontal circuitry associated with fear discrimination learning. We analyzed neuronal ensembles activated by CS+, CS-, or CtxtC during fear generalization (day 6), when the animals were unable to distinguish between conditioned and generalized fear stimuli, and we compared these with the neuronal ensembles activated after completion of the fear discrimination learning, when

the animals were able to discriminate between the dangerous and safe stimuli (day 12). To ensure that the activity-labeled neuronal ensembles represented the responses to CS+, CS-, and CtxtC stimuli relevant to fear differential conditioning, we analyzed animals in the dc/CS+, dc/CS- and dc/CtxtC groups that showed substantial generalization on day 3 (day 3, $-0.2 < DI < 0.2$) and appropriate freezing responses to CS+ (above 20% freezing on day 11). These criteria enabled us to determine the precise context-danger/safety functional relationships by monitoring the activated prefrontal neural ensembles of the context stimuli associated with a full range of fear responses to the tested context stimuli after completion of differential fear conditioning.

Exposure to the aversive CS+ and the initially generalized CS- context stimuli triggered neural activity in the PL cortex during Event 1 (Fig. 3.4A: Event 1 Activation in PL, ANOVA $F(3, 40) = 11.69$, $P<0.0001$; dc/CtxtC vs. HC: $P= 0.3445$, dc/CtxtC vs. dc/CS-: $P= 0.0029$; dc/CtxtC vs. dc/CS+: $P= 0.0023$). Activation of the PL was also high during re-exposure to both the aversive CS+ and the discriminated, safer context CS- (Fig. 3.4B: Event 2 Activation in PL, ANOVA $F(3, 40) = 11.86$, $P<0.0001$; dc/CtxtC vs. HC: $P=0.1974$, dc/CtxtC vs. dc/CS-: $P=0.0025$; dc/CtxtC vs. dc/CS+: $P= 0.0086$). The levels of response during exposure or re-exposure to CS+ and CS- were not different in PL (Fig. 3.4A-B: PL/E1: cfc/CS+ vs. cfc/CtxtC, $P=0.9999$, E2/PL: cfc/CS+ vs. cfc/CtxtC, $P=0.8981$). In addition, the activation level of PL during Event 2 was not different from Event 1 (Fig. 3.4A-B. PL/E1-E2 RM-ANOVA of Group x Event: Group x Event $F (3, 43) = 0.2482$ $P=0.8622$, Event $F (1, 43) = 1.216$ $P=0.2763$, Group $F (3, 43) = 21.25$ $P<0.0001$). The strong reactivation of the PL neural ensemble was observed during re-

exposure to CS+ after differential conditioning (Fig. 3.4C: PL/Reactivation, ANOVA, F (3, 40) = 16.38, P<0.0001. dc/CtxtC vs. dc/CS+, P= 0.0001), while re-exposure to CtxtC did not trigger reactivation of the CtxtC ensemble (Fig. 3.4C: dc/CtxtC vs. HC, P= 0.6994). There was also strong reactivation in PL in the dc/CS- group (Fig. 3.4C: PL/ Reactivation, dc/CtxtC vs. dc/CS-, P= 0.0002), indicating that inhibition of generalized fear may be mediated by the PL circuitry. Overall, these results suggest that the PL circuitry is involved in discriminatory fear learning; however, the PL tends to detect conditioned and generalized stimuli. Thus, generalized fear is detected in the PL subdivision of the mPFC, and the neuronal ensemble of generalized fear stimuli forms indelible memory representations in the PL during fear discrimination learning.

Using the genetic tagging system, we also tracked changes in the activation of neuronal ensembles in the IL during fear discrimination learning. We found that exposure to safer, discriminated context stimuli triggered elevated neural activity in the IL region during Event 2 (Fig. 3.4E: IL/E2, F (3, 40) = 19.27, P<0.0001; dc/CtxtC vs. dc/CS-, P= 0.0002, r=0.61; dc/CtxtC vs. HC, P= 0.0439, dc/CtxtC vs. dc/CS+, P= 0.8917), but only negligible IL activity in response to non-discriminated, generalized CS- stimulus was recorded during Event 1 compared to CtxtC (Fig. 3.4D: IL/E1, dc/CtxtC vs. dc/CS-, P= 0.7907, dc/CtxtC vs. HC, P= 0.0753; dc/CtxtC vs. dc/CS+, P= 0.9969). In addition, inhibition of generalized fear triggered neuronal ensembles of CS- in IL; the dc/CS- group was the only group that showed reactivation of the ensemble in the IL (Fig. 3.4F: IL/ Reactivation, one-way ANOVA: F (3, 40) = 8.979, P=0.0001; dc/CtxtC vs. dc/CS-, P= 0.0016, r=0.61, dc/CtxtC vs. HC, P= 0.5917, dc/CtxtC vs. dc/CS+, P= 0.9019, dc/CS+

vs. dc/CS-, P=0.0020, r=0.54). Thus, the learned inhibition of generalized fear coincided with an increase of IL activity in a stimuli-specific manner.

The IL responses during exposure and re-exposure to the dangerous context CS+ were markedly lower compared to those detected in the PL (Fig. 3.4A, D: E1/PL - IL, RM-ANOVA Group x Region: $F(3, 43) = 10.88$, $P<0.0001$; Region: $F(1, 43) = 67.78$, $P<0.0001$; Group: $F(3, 43) = 12.44$ $P<0.0001$; E1/PL – IL, dc/CS+, P=0.0001; Fig. 3.4B, E: E2/PL - IL, RM-ANOVA Group x Region: $F(3, 43) = 7.95$, P=0.0003; Region: $F(1, 43) = 14.89$, P=0.0004; Group: $F(3, 43) = 21.67$, $P<0.0001$; E2/PL – IL, dc/CS+, $P<0.0001$).

Remarkably, the activation of IL was dramatically increased as a result of successful differential fear conditioning, and this increase was detected in response to CS- only (Fig. 3.4D, E: IL/E1-E2 RM-ANOVA of Group x Event $F(3, 43) = 16.23$, $P<0.0001$; Event $F(1, 43) = 30.08$, $P<0.0001$; Group $F(3, 43) = 13.19$, $P<0.0001$; HC, $P>0.9999$; dc/CtxtC, P= 0.1045; dc/CS-, P= <0.0001; dc/CS+, P= 0.9139). In fact, the level of the IL response during re-exposure to CS- was similar to the PL response (Fig. 3.4E: E2/PL-IL RM-ANOVA Group x Region: $F(3, 43) = 7.95$, P=0.0003; Region: $F(1, 43) = 14.89$, P=0.0004; Group: $F(3, 43) = 21.67$, $P<0.0001$; HC, P= 0.9416; dc/CtxtC, P= 0.9998; dc/CS-, P= 0.5632; dc/CS+, $P<0.0001$), while the IL failed to respond to CS+ during Event 1, as mentioned above.

Representative images taken from the deep layers of the mPFC show differential activation and reactivation upon fear discrimination learning. The dc/CS+ and dc/CS- groups had greater activation and reactivation of PL region compared to dc/CtxtC

indicating that the PL detects conditioned and generalized stimuli (Fig. 3.5B-D). In IL, all groups showed similar activation during generalization on Event 1 however upon completion of fear discrimination, the dc/CS- group shows substantially increased IL activity (Fig. 3.5E-G).

Figure 3.3

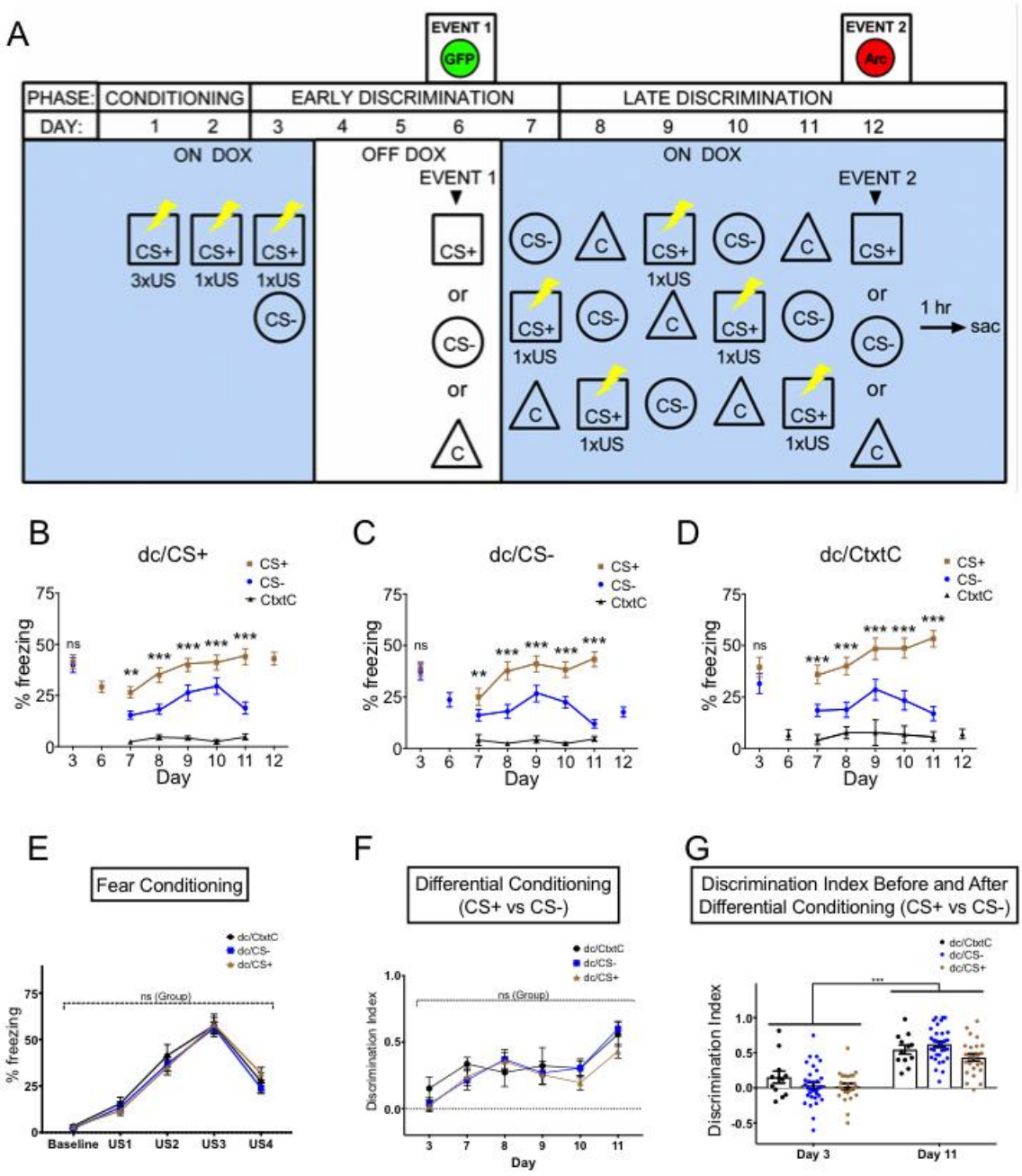
A
EVENT 1
GFP
EVENT 2
Arc
PHASE:
CONDITIONING
EARLY DISCRIMINATION
LATE DISCRIMINATION
DAY:
1 2 3 4 5 6 7 8 9 10 11 12
ON DOX
OFF DOX
ON DOX
EVENT 1
EVENT 2
CS+
3xUS
1xUS
1xUS
CS-
or
C
1 hr
sac
B
dc/CS+
C
dc/CS-
D
dc/CtxtC
CS+
CS-
CtxtC
% freezing
Day
ns
E
Fear Conditioning
dc/CtxtC
dc/CS-
dc/CS+
ns (Group)
Baseline US1 US2 US3 US4
F
Differential Conditioning
(CS+ vs CS-)
Discrimination Index
G
Discrimination Index Before and After
Differential Conditioning (CS+ vs CS-)
Day 3
Day 11

(Previous page) Figure 3.3: Tested groups show robust performance on a contextual fear discrimination learning task. (**A**) The context-dependent fear discrimination learning assay consists of three phases: fear conditioning, fear generalization (Early Discrimination) followed by additional differential conditioning (Late Discrimination). Details are described in the test. All three groups, (**B**) the dc/CS+, (**C**) dc/CS-, and (**D**) dc/CtxtC groups showed robust performance on differential fear conditioning. (**B**) dc/CS+, RM two-way ANOVA of Day (Days 3, 7-11) and Context (CS+, CS-) followed by Sidak's multiple comparisons: Day F (5, 115) = 16.82 P<0.0001; Context F (1, 23) = 84 P<0.0001; Day × Context F (5, 115) = 7.006 P<0.000. CS+ vs. CS-: Day 3, P= 0.9964; Day 7, P= 0.0015; Day 8, P= <0.0001; Day 9, P= <0.0001; Day 10, P= 0.0008; Day 11, P= <0.0001. There was a significant difference in freezing to CS- for Day 3 (M=39.93 +/-3.68) and Day 11 (M=18.88 +/-2.9) conditions; t(23)=6.97, p<0.0.0001, r=-0.541. There was no difference in freezing to CS+ for day 3 (M=41.43 +/-3.39) and day 11 (M=43.96 +/-3.9) conditions; t(23)=-0.73, p=0.472, r=0.070. (**C**) dc/CS-, RM two-way ANOVA of Day (Days 3, 7-11) and Context (CS+, CS-) followed by Sidak's multiple comparisons: Day , F (5, 155) = 15.21, P<0.0001; Context, F (1, 31) = 81.3,1, P<0.0001; Day × Context, F (5, 155) = 14.47, P<0.0001. CS+ vs. CS-: Day 3, P= 0.9938; Day 7, P= 0.0065; Day 8, P <0.0001; Day 9, P <0.0001; Day 10, P <0.0001; Day 11, P <0.0001. There was a significant difference in freezing to CS- for day 3 (M=37.16 +/-3.85) and day 11 (M=12.07 +/-2.05) conditions; t(31)=7.35, p<0.0.0001, r=-0.584. There was no difference in freezing to CS+ for day 3 (M=38.67 +/-3.34) and day 11 (M=43.27 +/-3.57) conditions; t(31)=7.35, p=0.151, r=0.117 (**D**) dc/CtxtC, RM two-way ANOVA of Day (Days 3, 7-11) and Context (CS+, CS-) followed by Sidak's multiple comparisons: Day, F (5, 55) = 4.539 P=0.0016; Context, F (1, 11) = 53.99 P<0.0001; Day × Context, F (5, 55) = 6.024 P=0.0002. CS+ vs. CS-: Day 3, P= 0.2214; Day 7, P= 0.0002; Day 8, P <0.0001; Day 9, P <0.0001; Day 10, P <0.0001; Day 11, P <0.0001. There was a significant difference in freezing to CS- for day 3 (M=31.51 +/-4.80) and day 11 (M=16.97 +/-3.41) conditions; t(11)=3.654, p<0.0038, r=-0.450. There was a significant difference in freezing to CS+ for Day 3 (M=39.48 +/-4.77) and Day 11 (M=53.27 +/-3.9) conditions; t(11)=4.138, p=0.0017, r=0.415 (**E**) The dc/CS+, dc/CS-, and dc/CtxtC groups showed robust performance on the fear conditioning. RM two-way ANOVA of Group and US followed by Tukey's multiple comparison revealed robust fear acquisition in all three groups. Group × US: P= 0.671, US, P <0.0001, Group, P 0.7484. Baseline: dc/CtxtC vs. dc/CS-, P= 0.9732; dc/CtxtC vs. dc/CS+, P= 0.9983; dc/CS- vs. dc/CS+, P= 0.9771. US1: dc/CtxtC vs. dc/CS-, P= 0.9241; dc/CtxtC vs. dc/CS+, P= 0.7635; dc/CS- vs. dc/CS+, P= 0.8977. US2: dc/CtxtC vs. dc/CS-, P= 0.6739; dc/CtxtC vs. dc/CS+, P= 0.5111; dc/CS- vs. dc/CS+, P= 0.9212. US3: dc/CtxtC vs. dc/CS-, P= 0.9635; dc/CtxtC vs. dc/CS+, P= 0.9976; dc/CS- vs. dc/CS+, P= 0.9105. US4: dc/CtxtC vs. dc/CS-, P= 0.7876; dc/CtxtC vs. dc/CS+, P= 0.7238; dc/CS- vs. dc/CS+, P= 0.1617. (**F**) The dc/CS+, dc/CS-, and dc/CtxtC groups showed similar level of performance on differential fear discrimination. RM two-way ANOVA of Group x Day (Days 3, 7-11) followed by Tukey's multiple comparison revealed the same performance in all three groups. Group × Day: P= 0.8098; Day, P <0.0001; Group, P= 0.3177. Day 3: dc/CtxtC vs. dc/CS-, P= 0.5661; dc/CtxtC vs. dc/CS+, P= 0.5099; dc/CS- vs. dc/CS+, P= 0.9834.

Day 7: dc/CtxtC vs. dc/CS-, P= 0.5434; dc/CtxtC vs. dc/CS+, P= 0.7056; dc/CS- vs. dc/CS+, P= 0.9581. Day 8: dc/CtxtC vs. dc/CS-, P= 0.665; dc/CtxtC vs. dc/CS+, P= 0.7621; dc/CS- vs. dc/CS+, P= 0.986. Day 9: dc/CtxtC vs. dc/CS-, P= 0.8891; dc/CtxtC vs. dc/CS+, P= 0.841; dc/CS- vs. dc/CS+, P= 0.9868. Day 10: dc/CtxtC vs. dc/CS-, P= >0.9999; dc/CtxtC vs. dc/CS+, P= 0.6363; dc/CS- vs. dc/CS+, P= 0.4526. Day 11: dc/CtxtC vs. dc/CS-, P= 0.9312; dc/CtxtC vs. dc/CS+, P= 0.5401; dc/CS- vs. dc/CS+, P= 0.1587. (**G**) The dc/CS+, dc/CS-, and dc/CtxtC groups showed generalized fear responses to CS- on day 3 (Event 1) and but successful fear discrimination by day 11 (Event 2). When comparing the first day of early discrimination with the last day of late discrimination, all three groups showed a robust discrimination index on day 11 but these groups were not able to discriminate between CS+ and CS- on day 3. RM two-way ANOVA of Group and Event followed by Sidak's multiple comparisons: Group × Event: P= 0.0741; Event, P <0.0001; Group, P 0.0871. Event 1 vs. Event 2: dc/CtxtC, P= 0.0002; dc/CS-, P= <0.0001; dc/CS+, P <0.0001. However, there were no differences in Discrimination Indexes between groups on Event 1 or Event 2 (P-values not shown). The discrimination index was calculated using the freezing responses to CS+ and CS- according to the formula DI=[[227] – [227]]/[[227] + [227]]. Significance values were set at $p < 0.05$: *, $p < 0.05$; **, $p < 0.01$; ***, $p < 0.001$ and ns not significant.

Figure 3.4

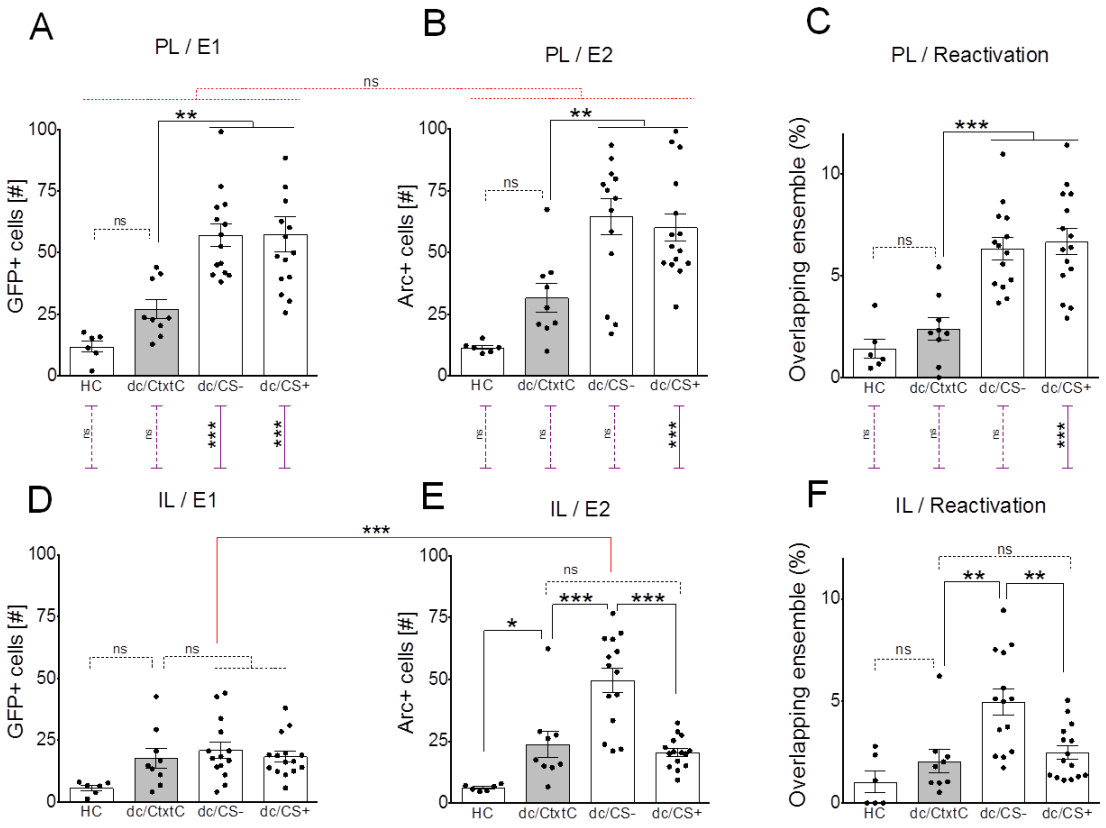
A
PL / E1
GFP+ cells [#]
B
PL / E2
Arc+ cells [#]
C
PL / Reactivation
Overlapping ensemble (%)
D
IL / E1
GFP+ cells [#]
E
IL / E2
Arc+ cells [#]
F
IL / Reactivation
Overlapping ensemble (%)
HC
dc/CtxtC
dc/CS-
dc/CS+
ns
*
**
***

(Previous page) Figure 3.4: Differential fear conditioning triggers elevated IL activity in response to the discriminated stimulus CS- and changes in neuronal ensembles of contextual stimuli in PL and IL. The activation analysis of dc/CS+, dc/CS-, and dc/CtxtC groups included subjects that generalized before differential conditioning on day 3 (DI ≤ 0.2) and showed appropriate fear responses to CS+ (day 11, % Freezing to CS+ > 20%) (Fig. 3.3B-D, F). (**A**) The dc/CS- and dc/CS+ groups showed similar levels of activity in PL during Event 1 and had greater activation of the PL than the dc/CtxtC group during Event 1, while re-exposure to the CtxtC was not different from the level of activation observed in HC. Ordinary one-way ANOVA (F (3, 40) = 11.69, P<0.0001) followed by Dunnett's many-to-one comparisons with the dc/CtxtC as a control: dc/CtxtC vs. HC, P= 0.3445; dc/CtxtC vs. dc/CS-, P= 0.0029; dc/CtxtC vs. dc/CS+, P= 0.0023. (**B**) The dc/CS- and dc/CS+ groups showed similar levels of activity in PL during Event 2 and had greater activation of the PL than the dc/CtxtC group during Event 2, while re-exposure to the CtxtC showed similar levels of activation observed in HC. Ordinary one-way ANOVA (F (3, 40) = 11.86, P<0.0001) followed by Dunnett's many-to-one comparisons with the dc/CtxtC as a control: dc/CtxtC vs. HC, P= 0.1974; dc/CtxtC vs. dc/CS-, P= 0.0025; dc/CtxtC vs. dc/CS+, P= 0.0086. (**C**) The dc/CS- and dc/CS+ groups showed similar levels of activity in PL and greater reactivation of PL than dc/CtxtC or HC groups. Ordinary one-way ANOVA (F (3, 40) = 16.38, P<0.0001) followed by Dunnett's many-to-one comparisons with the dc/CtxtC as a control: dc/CtxtC vs. HC, P= 0.6994; dc/CtxtC vs. dc/CS-, P= 0.0002; dc/CtxtC vs. dc/CS+, P= 0.0001. (**D**) The dc/CS- and dc/CS+ groups showed similar activation of the IL as the dc/CtxtC group but had greater activation in IL than HC during Event 1. Ordinary one-way ANOVA (F (3, 40) = 3.327, P=0.029) followed by Dunnett's many-to-one comparisons with the dc/CtxtC as a control: dc/CtxtC vs. HC, P= 0.0753; dc/CtxtC vs. dc/CS-, P= 0.7907; dc/CtxtC vs. dc/CS+, P= 0.9969. (**E**) The dc/CS- group showed elevated activation of the IL compared to all other tested groups during Event 2. This increased level of activity in IL of the dc/CS- was also higher compared to responses IL detected during Event 1 (IL/CS-/E1 vs IL/CS-/E2 = <0.0001, details are listed below). Ordinary one-way ANOVA (F (3, 40) = 19.27, P<0.0001) followed by Dunnett's many-to-one comparisons with the dc/CtxtC as a control: dc/CtxtC vs. HC, P= 0.0439; dc/CtxtC vs. dc/CS-, P= 0.0002; dc/CtxtC vs. dc/CS+, P= 0.8917. (**F**) The dc/CS- group showed elevated reactivation in the IL compared to all other tested groups. Ordinary one-way ANOVA (F (3, 40) = 8.979, P<0.0001) followed by Dunnett's many-to-one comparisons with the dc/CtxtC as a control: dc/CtxtC vs. HC, P= 0.5917; dc/CtxtC vs. dc/CS-, P= 0.0016; dc/CtxtC vs. dc/CS+, P= 0.9019. There was no difference in activation of PL between events (Fig 3.4A, B). RM two-way ANOVA of Group and Event: Group × Event F (3, 43) = 0.2482 P=0.8622; Event F (1, 43) = 1.216 P=0.2763; Group F (3, 43) = 21.25 P<0.0001. There was a marked difference in activation of IL in response to CS- between exposures before and after differential conditioning (Fig. 3.4D, E). Group × Event F (3, 43) = 16.23 P<0.0001; Event F (1, 43) = 30.08 P<0.0001; Group F (3, 43) = 13.19 P<0.0001. Event 1 - Event 2: HC, P>0.9999; dc/CtxtC, P= 0.1045; dc/CS-, P= <0.0001; dc/CS+, P= 0.9139. The dc/CS- and dc/CS+ groups showed lower activation of IL compared to PL during Event 1 (Fig. 3.4A, D). Ordinary two-way ANOVA of Group and Region (Group ×

Region: F (3, 43) = 10.88 P<0.0001; Region F (1, 43) = 67.78 P<0.0001; Group: F (3, 43) = 12.44 , P<0.0001. PL/E1 – IL/E1: HC, P= 0.8521; dc/CtxtC, P= 0.3577; dc/CS-, P<0.0001; dc/CS+, P<0.0001. The dc/CS+ group showed lower activation of IL compared to PL during Event 2 (Fig. 3.4B, E). Ordinary two-way ANOVA (Group x Region : F (3, 43) = 7.95 P=0.0003; Region F (1, 43) = 14.89 P=0.0004; Group: F (3, 43) = 21.67 P<0.0001. PL - IL / E2 HC, P= 0.9416; dc/CtxtC, P= 0.9998; dc/CS-, P= 0.5632; dc/CS+, P= <0.0001. The dc/CS+ group showed lower reactivation of IL compared to PL during Event 2 (Fig. 3.4C, F). Ordinary two-way ANOVA Group × Region: F (3, 43) = 6.627 P=0.0009; Region F (1, 43) = 17.41 P=0.0001; Group: F (3, 43) = 22.25 P<0.0001. Reactivation/PL vs. IL: HC, P= 0.9939, dc/CtxtC, P= 0.9415, dc/CS-, P= 0.1571, dc/CS+, P<0.0001. Significance values were set at $p < 0.05$: *, $p < 0.05$; **, $p < 0.01$; ***, $p < 0.001$ and ns not significant. Black lines indicate comparisons within a panel; the red lines indicate side-by-side comparisons and purple lines show top-bottom comparisons.

Figure 3.5

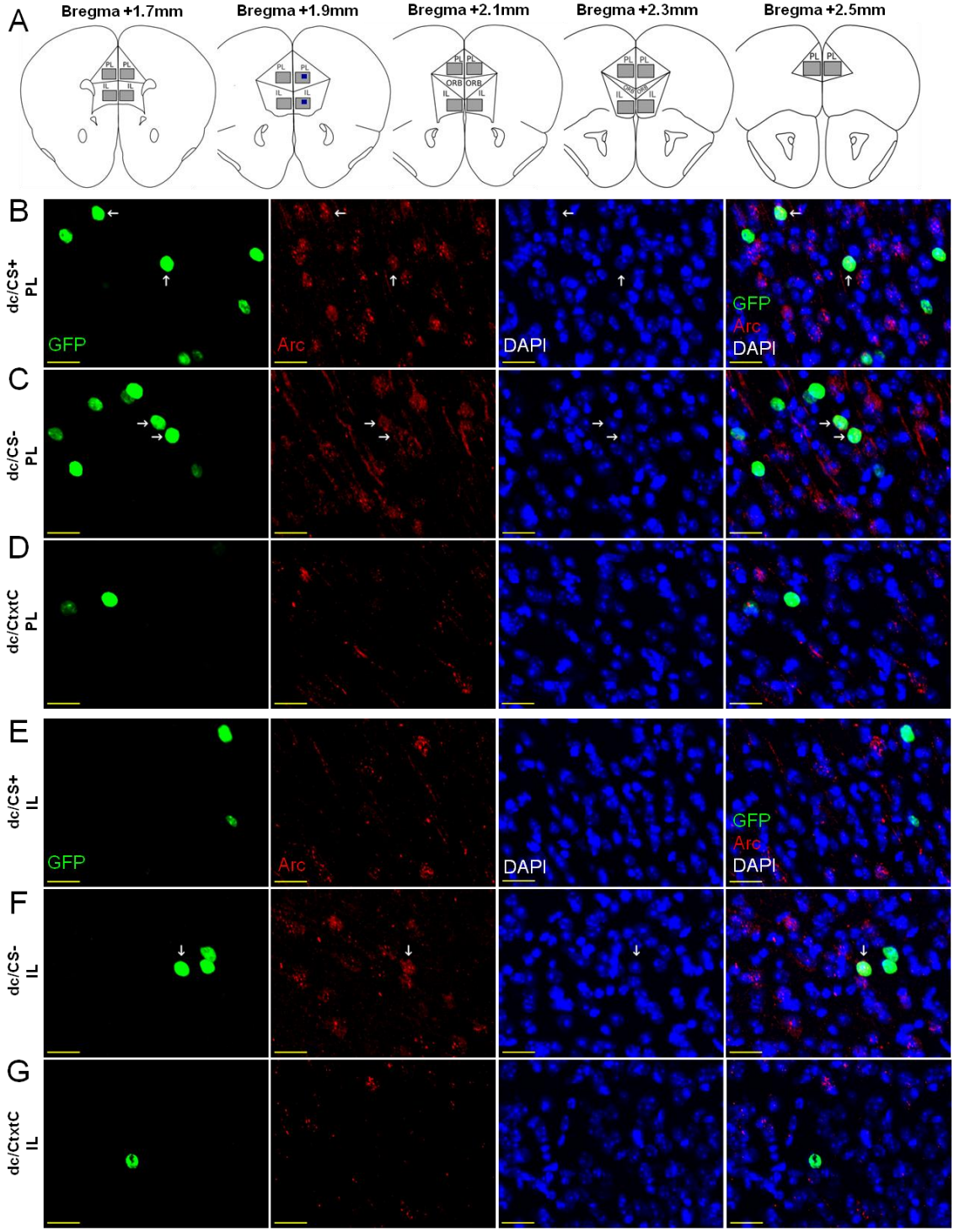
A
Bregma +1.7mm
Bregma +1.9mm
Bregma +2.1mm
Bregma +2.3mm
Bregma +2.5mm
PL
IL
ORB
B
dc/CS+ PL
GFP
Arc
DAPI
GFP
Arc
DAPI
C
dc/CS- PL
D
dc/CtxtC PL
E
dc/CS+ IL
GFP
Arc
DAPI
GFP
Arc
DAPI
F
dc/CS- IL
G
dc/CtxtC IL

(Previous page) Figure 3.5: Representative images showing differential activation and reactivation upon differential fear conditioning. (**A**) Diagram shows the range of Bregma points where sections were analyzed. Grey rectangles indicate the FOV acquired in each region. Blue rectangles indicate the location where representative images were taken. (**B-D**) PL region shows greater activation and reactivation in dc/CS+ and dc/CS- group compared to dc/CtxtC group. White arrows indicate overlap. (**E-G**) IL region shows greater activation and reactivation in dc/CS- group only. There are no differences between dc/CS+ and dc/CtxtC groups. White arrows indicate overlap. Scale bars indicate 20µm.

To obtain more insight into the relationship between ensemble activity patterns and differential fear conditioning learning outcome, we performed within-group analyses to evaluate the correlations between the value of a variable representing a measure of neuronal activity (i.e., activity rate or reactivation index in PL vs IL) and the value of behavioral performance (i.e., discrimination index or freezing level) (Fig. 3.6). Simple Pearson correlation analysis was used to evaluate if a stimulus-triggered ensemble reactivation in PL or IL correlated with behavioral performance (Fig. 3.6A-B). Specifically, we wanted to determine which of the ensemble reactivation variables (CS+ or CS-) and which region (PL or IL) correlated with the outcome of differential fear conditioning (i.e., discrimination rate on day 11). PL ensemble reactivation during re-exposure to CS+ significantly correlated with behavioral performance (CS+/PL, r=0.637, P=0.0106, R^2 =0.406). In addition, IL reactivation during re-exposure to CS- showed an inverse relationship with behavioral performance (CS-/IL, r=-0.7175, P=0.0039, R^2 =0.515).

One of the features of context-dependent fear discrimination learning is an inhibition of generalized fear to CS-, while preserving elevated responses to CS+ (Fig. 3.3B-D). To assess a potential relationship between region-specific ensemble activity and levels of fear, we plotted the activation rate of neuronal ensembles in the PL and IL during exposure or re-exposure to a contextual stimulus (i.e., CS+ or CS-) as a function of fear level (Fig. 3.6). This analysis did not directly consider the discrimination between CS+ and CS- but instead evaluated the relationship between activity and fear level. Pearson correlation analysis revealed that PL activation during re-exposure to CS- was

the only variable that was covariate with level of fear (Fig. 3.6D). Surprisingly, PL activation rate during re-exposure to the safer stimulus CS- showed a direct relationship with expressed level of fear during re-exposure to the safer stimulus CS- ($r=0.543$, $P=0.0451$), while PL activity in response to CS+ remained stable across levels of freezing ($r=-0.295$, $P=0.286$). In addition, detailed analysis of behavior during differential conditioning showed that level of fear to the safer stimulus, CS-, decreased with increasing discrimination index (Fig. 3.6C, $r=-0.710$, $P=0.0045$), indicating that animals showing a high level of fear to CS- did not perform well on the differential fear conditioning test. The direct relationship between PL activity rate and level of fear after differential conditioning was detected only during exposure to CS- and not during exposure to CS+. This indicates that PL engagement in mediating responses to safer contexts intensifies with the increase in the probability of failing the discrimination test, while lowered, likely more refined, PL activation occurs when there is a high probability of an appropriate fear response to a safer, discriminated contextual stimulus (CS-) is high.

The between-group analysis revealed that the PL was strongly engaged in responses to CS+ (dangerous) and CS- (initially generalized but later discriminated) before and after differential conditioning. Analysis of the correlation between reactivation indexes in PL during re-exposure to CS+ and CS- and behavioral performance of individual animals revealed additional details of activity patterns associated with performance during fear discrimination learning. The reactivation index for PL ensembles of CS+ and behavioral outcome tended to increase or decrease together, which suggests that improved performance correlates with increased overlapping

ensembles, presumably via strengthening functional connectivity within initially activated ensembles of dangerous stimuli in PL. Interestingly, exposure to CS- induced significant PL activity during the early and late phases of differential conditioning with significant levels of overlap between these ensembles.

Success of differential conditioning also correlated with emerging CS-induced neuronal activity in IL detected only during the late phase of differential conditioning. The initially generalized CS- stimulus triggered negligible activity in IL compared to the never generalized CtxtC stimulus. However, re-exposure to the discriminated, safer CS- stimulus evoked significant activity in IL when compared to CtxtC or the activity during the initial exposure to CS-. This newly emerged IL ensemble of CS- showed marked reactivation, which was specific, as both CS+ and CtxtC failed to show any reactivation. In addition, the IL ensemble of CS- showed lower rates of reactivation with increasing behavioral performance, indicating substantial levels of recruitment of newly activated cells as fear discrimination learning occurred.

These data suggest that balancing PL and IL networks while encoding more precise information about US-CS+ and noUS-CS- contingencies across subdivisions of the mPFC controls fear discrimination learning. Within-group correlation analysis of the relationships between activity patterns and behavioral performance showed three important correlates of fear discrimination learning outcome: 1) the direct relationship with PL reactivation index during re-exposure to CS+, 2) the inverse relationship with IL reactivation index during re-exposure to CS-, and 3) the inverse relationship between freezing and PL activity during re-exposure to CS-. In addition, freezing level to the

discriminated, safer CS- showed an inverse relationship with outcomes of fear discrimination learning. Furthermore, between-group analysis revealed robust activation and marked reactivation of the CS+ and CS- ensembles in PL and CS- ensembles in IL after differential fear conditioning.

Figure 3.6

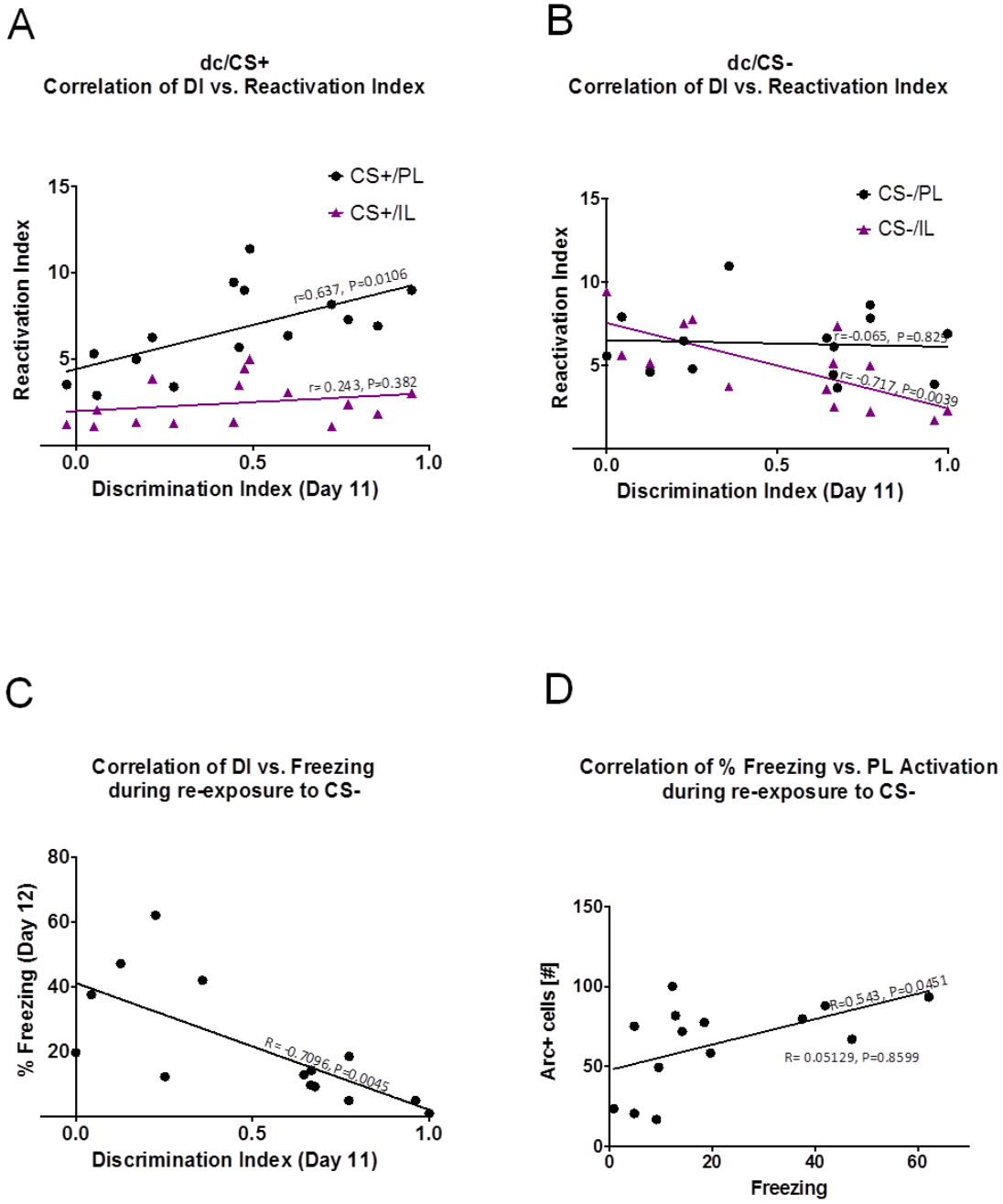
A
dc/CS+
Correlation of DI vs. Reactivation Index
CS+/PL
CS+/IL
r=0.637, P=0.0106
r= 0.243, P=0.382
Reactivation Index
Discrimination Index (Day 11)
B
dc/CS-
Correlation of DI vs. Reactivation Index
CS-/PL
CS-/IL
r=-0.065, P=0.825
r= -0.717, P=0.0039
Reactivation Index
Discrimination Index (Day 11)
C
Correlation of DI vs. Freezing
during re-exposure to CS-
R= -0.7096, P=0.0045
% Freezing (Day 12)
Discrimination Index (Day 11)
D
Correlation of % Freezing vs. PL Activation
during re-exposure to CS-
R=0.543, P=0.0451
R= 0.05129, P=0.8599
Arc+ cells [#]
Freezing

(Previous page) Figure 3.6: Simple Pearson correlation analysis revealed discrete codes associated with fear discrimination learning. (**A**) PL ensemble reactivation during re-exposure to CS+ significantly correlated with behavioral performance, (r=0.637, P=0.0106) while there was no correlation between IL ensemble reactivation during re-exposure to CS+ and fear discrimination learning (r= 0.243, P=0.382). (**B**) In addition, IL reactivation during re-exposure to CS- showed an inverse relationship with behavioral performance, r= -0.717, P=0.0039. PL ensemble reactivation during re-exposure to CS- did not correlate with behavioral performance, r=-0.065, P=0.825. (**C**) Freezing level variable showed an inverse relationship with fear discrimination learning outcome, r= -0.7096, P=0.0045. (**D**) PL activation rates showed a direct relationship with expressed levels of fear during re-exposure to safer stimulus, CS- (r=0.542, P=0.0451).

Discussion

While there is extensive research on the molecular and cellular mechanisms underlying fear acquisition and fear extinction, the neural mechanisms driving fear discrimination learning are not well understood. We examined prefrontal neuronal ensembles representing distinct experiences associated with learning to disambiguate between dangerous and similar, yet distinct, safe stimuli. These data revealed prefrontal subdivision-specific patterns of neuronal reactivation and distinct quantitative reactivation differences in response to neutral, conditioned, and generalized fear stimuli, all associated with successful fear discrimination learning. These data support the idea that gating responses to contextual stimuli within the fear modulation circuit appears to be critical for fear inhibition during learning safety cues in ambiguous circumstances.

The fact that the mPFC is a locus for gating fear discrimination and danger assessment is supported by animal studies in which mPFC lesions impair the ability to guide behavior, specifically when memory retrieval involves conflicting dangerous and safe contextual cues [236-239]. A decline in fear is associated with elevated activity in the mPFC, as determined by the activation of immediate-early genes [60, 64], blood oxygenation level [116], cell firing [208] and local field potentials [240]. The mPFC has dense reciprocal anatomical and functional connections with the sensory cortices such as the nucleus reuniens, memory systems, including the hippocampus, which is involved in space, time and multisensory processing, and the amygdala, a critical locus for fear processing. Neurons in the mPFC, basolateral amygdala (BLA) and hippocampus are

functionally coupled in the theta range (4-12 Hz oscillations) during fear conditioning [241, 242], conditioned extinction [240] and discriminative fear learning [243].

There is a large body of evidence demonstrating that the PL encodes and holds information about specific context-danger associations. Our data demonstrate that fear conditioning triggers neuronal ensembles of the context-danger association (Fig. 3.2-3.3). While blocking the PL cortex before fear conditioning has no effect on cued or contextual fear memory retrieval, post-training PL inactivation during the cued or contextual fear memory recall decreases the expression of learned fear [35]. In fact, learned fear expression and extinction failure are correlated with sustained conditioned responses in PL neurons [261]. Moreover, patterns of IEG gene expression confirm that the mPFC network monitors context-danger associations during fear conditioning [253] and neuronal ensembles of contextual fear memory were found in the PL cortex during fear retrieval [19, 255]. In addition, contextual fear memory retrieval after extinction, referred to as memory renewal, depends on the PL cortex [14, 210, 213, 262, 263]. Upregulation of the immediately early gene, *c-fos*, in the PL correlates with fear renewal [60], providing further evidence that the PL tracks context-danger associations.

Our data provide evidence for engagement of PL networks in mediating learning of fear discrimination. We demonstrated that fear discrimination learning involves lowering fear responses to CS- while maintaining a high level of response to CS+ (Fig. 3.3). The PL network is directly engaged during exposure to CS- before and after differential fear learning (Fig. 3.4). Moreover, we detected substantial reactivation of CS- neuronal ensembles in PL, suggesting that fear discrimination learning might coincide

with encoding memories of a discriminated, safer context into the PL network. Other findings are in line with this assessment, as general disengagement of PL networks due to treatment with muscimol blocked recall of discriminated fear [227]. This impairment was specific to responses to CS- only; emphasizing the importance of PL network integrity for the learning of appropriate responses to initially generalized stimuli during differential conditioning. Others reported that electrolytic lesions of PL administered after discrimination learning, presumably destroying already formed ensembles of contextual memory, were ineffective in disrupting context fear discrimination [264]. While PL neural ensembles of contextual memory may not always be critical for fear discrimination recall, these ensembles may be advantageous when the prefrontal-hippocampal memory system requires flexibility under more complex conditions, such as those observed during fear memory renewal [14, 60, 210, 213, 262, 263].

The observed PL reactivation coinciding with learning context-safety contingencies is surprising considering previous research on fear extinction. In fact, it is widely believed that the IL, but not PL, circuitry mediates learning underlying fear inhibition. Milad and Quirk demonstrated that the CS-evoked responses in the IL coincide with learned fear suppression [27]. This was later reproduced in several studies [22, 53, 172, 173, 204]. Research over the past two decades has revealed that the modulation of fear responses associated with fear extinction learning comprises the formation of a new memory trace that can actively suppress fear expression [51, 52]. The current model of fear extinction learning predicts that CS would induce IL activation during successful recall of fear extinction learning, followed by instructions to suppress

fear by tapping into the fear circuit via monosynaptic IL→GABAergic intercalated amygdala neurons (ITC) [34, 37] or, the more recently described, di-synaptic IL→BLA→ITC pathways [32, 33, 38]. In addition, direct optogenetic silencing of IL neurons during retrieval of auditory fear extinction is ineffective [265]. Moreover, both IL and PL have shown elevated firing rates during extinction recall [54], and both PL→BLA and IL→BLA connections show synaptic plasticity during extinction recall [36]. The PL, but not IL, cortex has been implicated in guiding context-appropriate behavior in responding to conflicting information in rats [266]. Furthermore, PL inactivation disrupts the encoding and expression of conditioned fear under the circumstance that animals must use contextual cues to disambiguate the significance of the stimuli [45]. Thus, encoding specific memories across larger PL and IL networks as reported in this study might be critical for proper gating of context-danger and context-safety contingencies during top-down control of appropriate fear responses.

While there is evidence that the PL is engaged in mediating responses to CS- and CS+, it is unclear if the PL component of ensembles representing inhibited fear is required for appropriate responses to discriminated stimuli after differential fear conditioning. Our data show that generalized, non-discriminated stimuli triggered CS- ensemble activity in the PL, but not in IL, network before differential conditioning (Fig. 3.4). Conversely, CS+ ensembles are localized in the PL through fear discrimination learning, and their reactivation rate within PL correlates with successful expression of discriminated fear. Notably, there was a direct relationship between the total number of cells activated in PL during Event 2 and expression of fear responses to the

discriminated, safer CS- stimulus. The ratio of the subset of cells activated by the safer stimulus CS- before and after differential conditioning to the total number of cells activated during re-exposure to context CS- appears to be stable across different levels of discrimination index, but the total number of activated cells in response to discriminated, safer stimuli decreases as animals lower their generalized fear. Taken together, these data suggest that PL might be involved in mediating inhibition of generalized fear via refinement of a subpopulation of CS- responsive cells.

Re-exposure to a discriminated and safer context after differential conditioning induced a modified CS- ensemble present in both PL and IL (Fig 3.4). Conditioned and generalized stimuli triggered only negligible responses in IL, while discriminated, safer stimuli elicited stimulus specific activity in IL. Interestingly, IL reactivation rates during re-exposure to CS- showed an inverse relationship with performance in fear discrimination learning, suggesting recruitment of new neurons to IL ensembles of CS- as a result of fear discrimination learning. CS- ensembles in the lateral amygdala respond similarly during fear discrimination learning [267]. One feasible interpretation is that PL and IL are both involved in balancing an enlarged CS- ensemble spreading across the entire mPFC while learning appropriate responses to discriminated, safer stimuli. This interpretation of our data is consistent with recently published work demonstrating that PL projections to IL are directly involved in initial but not late learning of fear extinction [30]. Thus, it is conceivable that PL projections to IL provide pathways for information transfer and/or circuit expansion between PL and IL during learning of fear inhibition to conditioned or generalized stimuli. If these predictions are correct, the enlarged IL-PL

ensemble of discriminated, safer CS- stimuli would emerge as an expansion of the CS- ensemble detected initially only in PL during generalization. Our findings are consistent with a potential role of PL→IL communications in the generation of new IL ensembles of CS- during differential conditioning. Thus, increased reactivation of the CS+ ensemble in the PL and PL-initiated reorganization of CS- ensemble across IL subdivisions of the mPFC are both hallmarks of fear discrimination learning.

In summary, both IL and PL are engaged during differential fear conditioning, yielding inhibition of generalized fear, while fear conditioning triggers stable memory representations of the conditioned stimulus in the PL subdivision of the mPFC. Initial experiences with conditioned (CS+) and generalized (CS-) stimuli during early differential fear conditioning elicit neuronal activity distributed across the PL network only. Surprisingly, the PL activity rate of CS- ensembles increased with the triggered level of fear, suggesting that inhibition of generalized fear may involve lowering the number of CS- specific cells in PL. In addition, CS+ ensemble reactivation index showed a direct correlation with fear discrimination performance. It appears that IL cortices were recruited during the late phase of differential fear conditioning, which coincided with successful fear discrimination. Compression of CS- ensembles in PL coincided with enlargement of CS- ensembles in IL during fear discrimination learning. In fact, the CS- reactivation rate in IL during re-exposure to the discriminated, safer stimulus CS- was one of the best predictors of fear discrimination learning outcome. These data demonstrate that learning safety signals involves large network changes across both PL and IL subdivisions of the mPFC.

Chapter 4: Conclusion

4.1 Prefrontal consolidation supports fear memory accuracy

In Chapter 2.1, we investigated the role of prefrontal consolidation on the attainment of fear memory accuracy by manipulating cAMP response element binding protein (CREB)- and CREB binding protein (CBP)-dependent transcription specifically in the medial prefrontal cortex (mPFC). Despite uncertainty on how CBP controls neuronal function via acetyltransferase activity and interaction with multiple regulatory proteins, considerable evidence indicates that CBP is a critical component of the neural signaling underlying cognitive functioning [141-149]. Previous studies have shown that CREB-dependent transcription subsequent to learning plays an important role in the conversion of short-term to long-term memory across species [124-129]. In a fruit fly model, it was discovered that formation of long-term aversive associations requires trancriptional cycling between cFos and CREB in a subset of cells where olfactory associations are stored [268]. Investigaters reported that pre-existing CREB is required for intial cFos induction while cFos is then required to further increase CREB expression [268]. Moreover, inhibiting or activating cFos-positive neuronal ensembles inhibits memory recall or induces memory-associated behaviors, respectively [268]. Rodent studies also reveal the necessity of CREB-dependent signaling in memory formation and consolidation. Experiments show that increasing the level of CREB in a neuronal population increased the probability that those cells are incorporated into the memory trace whereas decreasing levels of CREB had the opposite effect [269, 270]. Subsequent studies showed that inhibition of these CREB-positive cells impairs memory recall thus

demonstrating the necessity of CREB signaling in memory retrieval [200, 269]. Together these data suggest that relative CREB levels can affect which neurons are incorporated in a memory trace, a phenomenon known as memory allocation.

By generating mutant mice expressing either he dominant negative CREB mutant (mCREB) or the dominant negative CBP without acetyltransferase activity (CBPΔHAT), we tested the impact of CREB- and CBP-dependent transcription in the mPFC on fear memory specificity. Previous studies indicate that mCREB decreased CREB function and block neuronal CREB-dependent gene expression [130, 131, 155, 156] while CBPΔHAT lacks histone acetyltransferase activity [142], blocks c-fos expression in neurons [142] but retains all protein-protein interaction domains. Evidence from contextual and auditory fear discrimation tasks indicated that mPFC consolidation is crucial for acquiring the fear memory accuracy necessary to recognize subtle differences between aversive and non-aversive stimuli. Analysis of response patterns to aversive (CS+) and non-aversive (CS-) stimuli in control animals revealed that the improvement of contextual fear memory accuracy was due to increased freezing behavior to the CS+ and a decrease in freezing to CS-. However, CREB and CBP hypofunction in the mPFC altered the ability to learn discriminatory responses to CS+ versus CS- by disrupting the learning pattern curve for CS- only. These data indicate that CREB- and CBP-dependent signaling in the mPFC is critical for the suppression of fear to similar, yet distinct, non-aversive stimuli; a necessary process towards improvement of fear memory accuracy.

4.2 Prefrontal NMDA receptors control fear discrimination and fear extinction

In Chapter 2.2, we investigated the involvement of prefrontal N-methyl-D-aspartate receptors (NMDARs) expressed specifically in CamKIIα positive excitatory neurons in adaptive behaviors such as fear discrimination and fear extinction. NMDAR-dependent long-term potentiation is an experimental model of synaptic plasticity and is widely hypothesized to be the neural mechanism by which memory traces are encoded and stored in the brain [230]. There is also strong evidence for prefrontal NMDARs in mechanism underlying extinction of conditioned fear [208, 209]. Studies show that lesions in the mPFC produce deficits in the extinction of conditioned fear [21, 166, 212-214] and consolidation of fear extinction memory recruits mechanisms controlled by NMDARs, mitogen-activated protein kinase and protein synthesis [173, 215]. Involvement of NMDARs in mPFC-dependent learning mechanism is supported by studies showing that NMDAR receptors are effective mediators of synaptic plasticity in prefrontal excitatory neurons [216]. Pharmacological blockers of NMDARs trigger profound cortical activation in behaving rodents [218] and human volunteers [219-222] suggesting that the effect of NMDAR antagonists in pharmacological studies is predominately targeted to inhibitory neurons producing disinhibition of excitatory network. Moreover, it has been shown that activation of synaptic NMDARs supports phosphorylation of CREB on its critical transcriptional residue promotes CREB-dependent gene expression and neuronal survival while upon extrasynaptic NMDAR activation, CREB is only transiently phosphorylated thus CRE-dependent gene expression is not activated, and hippocampal neurons die [271]. These results indicate

that NMDAR- and CREB-dependent signaling are crucial for normal neuronal function and survival. The objective of the present study was to determine involvement of NMDARs expressed specifically in CamKIIα positive excitatory neurons in mPFC-dependent adaptive behaviors such as fear discrimination and fear extinction.

We tested mice with locally deleted *Grin1* gene encoding the obligatory NR1 subunit of the NMDAR from prefrontal excitatory neurons for their ability to distinguish frequency modulated (FM) tones in a fear discrimination test. We demonstrated that NMDAR-dependent signaling in the mPFC is critical for effective fear discrimination following initial generalization of conditioned fear. While mice with deficient NMDARs in prefrontal excitatory neurons maintained normal responses to a dangerous fear-conditioned stimulus, they exhibit abnormal decrement of fear generalization. We also found that selective deletion of NMDAR in the mPFC leads to a deficits in fear extinction. Previous studies have shown that infusion of the NMDAR blocker 2-amino-5-phosphonovalerate (APV) into the amygdala during extinction substantially interferes with extinction of conditioned fear to tone, light, and contextual stimuli [231, 232] while overexpression of NMDAR subunit NR2B in mice improves extinction learning [233]. Moreover, consolidation of fear extinction requires NMDAR-dependent bursting in the mPFC suggesting that fear extinction learning involves NMDAR-mediated plasticity in prefrontal–amygdala circuits [208]. These studies provide evidence that NMDAR-dependent neuronal signaling in the mPFC is a component of neural mechanisms disambiguating the meaning of fear signals and supporting discriminative fear learning and fear extinction by properly gating information.

4.3 Fear discrimination generates prefrontal neuronal ensembles of safety

In Chapter 3, we investigated the role of the prelimbic (PL) and infralimbic (IL) subdivisions of the mPFC in contextual fear conditioning and fear discrimination. The PL and IL subregions exert excitatory and inhibitory effects on the fear circuit, respectively, but the mechanisms driving fear discrimination are unknown. To trace neuronal ensembles of contextual fear memories, we employed an activity-dependent genetic tagging system referred to as the TetTag system [69, 74, 259]. This tetTAG system is driven by Arc expression, an immediate early gene (IEG) that has garnered much attention in the learning and memory field. Studies show that Arc expression increases after context-specific spatial learning and Arc regulates α-amino-3-hydroxy-5-methyl-4-isoxazolepropionic acid (AMPA) receptor trafficking, a key component of synaptic plasticity required for learning and memory [55, 56]. Moreover, Arc is required for hippocampal LTP and consolidation of contextual and fear memories in both the hippocampus and amygdala [58, 59]. Therefore, Arc is not only an effective marker for contextual learning but also regulates the mechanism by which learning and memory occurs.

Recent studies using IEG-driven genetic tagging systems have shown that optogenetically stimulating a fear conditioning-induced population of neurons in a novel context was able to produce a fear response [74]. In a separate study, they label a population of neurons activated by exploring a specific context (ctxA) then they stimulated these cells paired with a foot shock in a different context (ctxB) and when animals were placed back into ctxA, they showed a fear response. Taken together these

studies reveal that activation of a sparsely distributed sensory-induced neuronal population in the hippocampus is sufficient to reproduce a complex sensory experience. However, similar results have been reported in the neocortical region called the retrosplenial cortex (RSC), an output area of the hippocampus with projections to a wide variety of other cortical areas [76]. Investigators found that stimulation of naturally activating neurons in the RSC at the time of contextual fear conditioning was sufficient to produce a fear response [77]. These data suggest that at the time of learning, a neuronal ensemble representing the context forms in both the hippocampus and the neocortex.

To obtain insight into the mechanisms underlying contextual fear discrimination, we investigated prefrontal neuronal ensembles representing distinct experiences associated with learning to disambiguate between dangerous and similar, yet distinct, harmless stimuli. We showed distinct quantitative activation differences in response to conditioned and generalized fearful experiences, as well as modulation of the neuronal ensembles associated with successful acquisition of context-safety contingencies. These findings suggest that prefrontal neuronal ensemble patterns code functional context-danger and context-safety relationships. The PL subdivision monitors contextual danger associations to conditioned fear, whereas differential conditioning generates additional ensembles associated with the inhibition of generalized fear in both the PL and IL subdivisions of the mPFC. These data suggest that both IL and PL cortices mediate safety learning, supporting the idea that both these cortical regions cooperate in properly gating context-danger and context-safety contingencies during top-down control of appropriate fear responses.

4.4 Clinical significance

Functional neuroimaging studies in humans revealed that the amygdala, hippocampus, and PFC are dysfunctional in the common fear disorder, posttraumatic stress disorder (PTSD). PTSD patients typically display fear over-generalization and deficiency in extinction of fear memory which leads to irrational fear and anxiety [2]. Neuroimaging studies within the PFC have found that two regions, the anterior cingulate cortex (ACC) and ventromedial prefrontal cortex (vmPFC), are implicated in PTSD. In two separate studies, PTSD patients failed to activate the ACC during exposure to traumatic scripts or pictures compared to healthy controls [83, 111]. Within the vmPFC, studies found less activation in medial frontal gyrus in response to traumatic stimuli in PTSD patients relative to those without [82, 112]. In agreement with this data, others found decreased ACC and medial frontal gyrus activation during exposure to traumatic imagery among those with PTSD compared to traumatized individuals without PTSD [113]. Several MRI studies have also reported decreased frontal cortex volume in PTSD [93, 114, 115]. Taken together these research studies suggest that decreased prefrontal activity and volume is associated with PTSD. Moreover, functional neuroimaging studies have found that the vmPFC is also involved during the recall of fear extinction in humans. During the recall of the extinction, activation of the vmPFC predicted extinction success and correlated with amygdala activity [116] which is consistent with animal studies showing that the infralimbic cortex inhibits the amygdala during extinction recall [27]. Then they extended these results to investigate extinction recall the day following extinction training using fMRI. PTSD patients had reduced activity in the vmPFC and

hippocampus, yet increased ACC activity during extinction recall [2]. A subsequent study showed that during extinction recall, participants with PTSD had both reduced vmPFC activity and increased ACC activity during exposure to the extinction context [118]. These findings indicate that hyperactivity in the ACC and hypoactivity in the vmPFC may lead to impairment in fear extinction and an inability to use contextual cues to predict safety ultimately leading to overgeneralized fear, a clinical hallmark of PTSD and phobias.

Ultimately, the etiology of fear related disorders such as PTSD involves structural and functional dysfunction of the following regions: amygdala, hippocampus and PFC. Neuroimaging research have revealed that increased activation of the amygdala accompanied by diminished activity of the PFC is associated with the etiology of PTSD. Additionally, evidence suggests that hippocampal volume, integrity and functionality may be also impaired in PTSD. The current model suggests that decreased PFC and hippocampal functionality leads to reduced inhibitory control of the amygdala that then drives increased amydalar activity leading to irrational fear and anxiety [2]. Human and animals studies alike provide abundant evidence suggesting that the amygdala, hippocampus, PFC neuronal circuit is evolutionarily preserved and underlies the ability to acquire, modulate and extinguish fear.

4.5 The role of the mPFC in fear conditioning and fear discrimination learning

In Chapter 2, we investigated the role of prefrontal consolidation and neuronal signaling in fear discrimination learning. By manipulating CREB-, CBP- and NMDAR-dependent signaling in the mPFC, we showed that these animals have deficits in contextual and auditory fear discrimination learning. Interestingly, these animals have elevated fear to similar, yet distinct, non-aversive stimuli while maintaining normal fear responses to fear-conditioned stimuli. These data suggest that the proper mPFC function is critical for fear memory specificity. However, these studies were not able to probe for the differential role of the subregions within the mPFC in fear discrimination learning. In Chapter 3, we investigated the role of PL and IL subdivisions of the mPFC in contextual fear conditioning and fear discrimination using an activity-driven genetic tagging system. Upon exposure and re-exposure to the aversive fear-conditioned stimuli, we see elevated activation and reactivation of the PL region, respectively. There was no difference in IL activation or reactivation during contextual fear conditioning. Only the PL subdivision monitors contextual danger associations to conditioned fear. Next, we used the TetTag genetic system to label neurons during the early and late phases of fear discrimination learning to evaluate changes in the neuronal ensembles in the PL and IL caused by exposure to three contextal stimuli during fear discrimination: the aversive context stimulus, CS+; a similar yet distinct, safe stimulus, CS-; and a substantially different safe stimulus, CtxtC. In the PL region, we see elevated activation and reactivation upon exposure and re-exposure to conditioned and generalized stimuli throughout the discrimination phase. We detected substantial reactivation of CS- neuronal ensembles in

PL, suggesting that fear discrimination learning coincides with encoding memories of a discriminated, safer context into the PL network. Other findings are in line with this assessment, as general disengagement of PL networks due to treatment with muscimol blocked recall of discriminated fear [227]. This impairment was specific to responses to CS- only; emphasizing the importance of PL network integrity for the learning of appropriate responses to initially generalized stimuli. During the intial phase of fear discrimination when the animals generalize, there was neglible IL activation in all groups however upon successful fear discrimination learning, IL activation is greatly elevated during exposure to the generalized stimuli only. IL reactivation rates during re-exposure to CS- showed an inverse relationship with performance in fear discrimination learning, suggesting recruitment of new neurons to IL ensembles of CS- as a result of fear discrimination learning. These data suggest that both IL and PL cortices mediate safety learning, supporting the idea that both these cortical regions cooperate in properly gating context-danger and context-safety contingencies during top-down control of appropriate fear responses as presented in Figure 4.1.

To investigate the relationship between ensemble activity patterns and differential fear conditioning learning outcome, we performed within-group analyses to evaluate correlations between a variable representing a measure of neuronal activity (i.e., activity rate or reactivation index in PL vs IL) and the value of behavioral performance (i.e., discrimination index or freezing). PL ensemble reactivation during re-exposure to CS+ positively correlated with behavioral performance (CS+/PL, r=0.637, P=0.0106, R^2 =0.406). In addition, IL reactivation during re-exposure to CS- showed an inverse

relationship with behavioral performance (CS-/IL, r=-0.7175, P=0.0039, R^2 =0.515). Detailed analysis of behavior during differential conditioning showed that level of fear to the safer stimulus, CS-, decreased with increasing discrimination index (r=-0.710, P=0.0045) indicating that animals showing a high level of fear to CS- did not perform well on the differential fear conditioning test. The direct relationship between PL activity rate and level of fear after differential conditioning was detected only during exposure to CS-. This indicates that PL engagement in mediating responses to safer contexts intensifies with the increase in fear generalization, while lowered, likely more refined, PL activation occurs when there is a high probability of fear memory specificity.

Success of differential conditioning also correlated with emerging CS-induced neuronal activity in IL detected only during the late phase of differential conditioning. The initially generalized CS- stimulus triggered negligible activity in IL compared to the never generalized CtxtC stimulus. However, re-exposure to the discriminated, safer CS- stimulus evoked significant activity in IL when compared to CtxtC or the activity during the initial exposure to CS-. This newly emerged IL ensemble of CS- showed marked reactivation compared to both CS+ and CtxtC groups that failed to show any reactivation. In addition, the IL ensemble of CS- showed lower rates of reactivation with increasing behavioral performance, indicating substantial levels of recruitment of newly activated cells as fear discrimination learning occurred.

These data suggest that balancing PL and IL networks while encoding more precise information about US-CS+ and noUS-CS- contingencies across subdivisions of the mPFC controls fear discrimination learning. Within-group correlation analysis of the

relationships between activity patterns and behavioral performance showed three important correlates of fear discrimination learning outcome: 1) the direct relationship with PL reactivation index during re-exposure to CS+, 2) the inverse relationship with IL reactivation index during re-exposure to CS-, and 3) the inverse relationship between freezing and PL activity during re-exposure to CS-. In addition, freezing level to the discriminated, safer CS- showed an inverse relationship with outcomes of fear discrimination learning.

One feasible interpretation is that PL and IL are both involved in balancing an enlarged CS- ensemble spreading across the entire mPFC while learning appropriate responses to discriminated, safer stimuli. This interpretation of our data is consistent with recently published work demonstrating that PL projections to IL are directly involved in initial but not late learning of fear extinction [30]. Thus, it is possible that PL projections to IL provide pathways for information transfer and/or circuit expansion between PL and IL during learning of fear inhibition to conditioned or generalized stimuli. If these predictions are correct, the enlarged IL-PL ensemble of discriminated, safer CS- stimuli would emerge as an expansion of the CS- ensemble detected initially only in PL during generalization. Our findings are consistent with a potential role of PL→IL communications in the generation of new IL ensembles of CS- during differential conditioning. In conclusion, increased reactivation of the CS+ ensemble in the PL and PL-initiated reorganization of CS- ensemble across IL subdivisions of the mPFC are both hallmarks of fear discrimination learning.

Figure 4.1

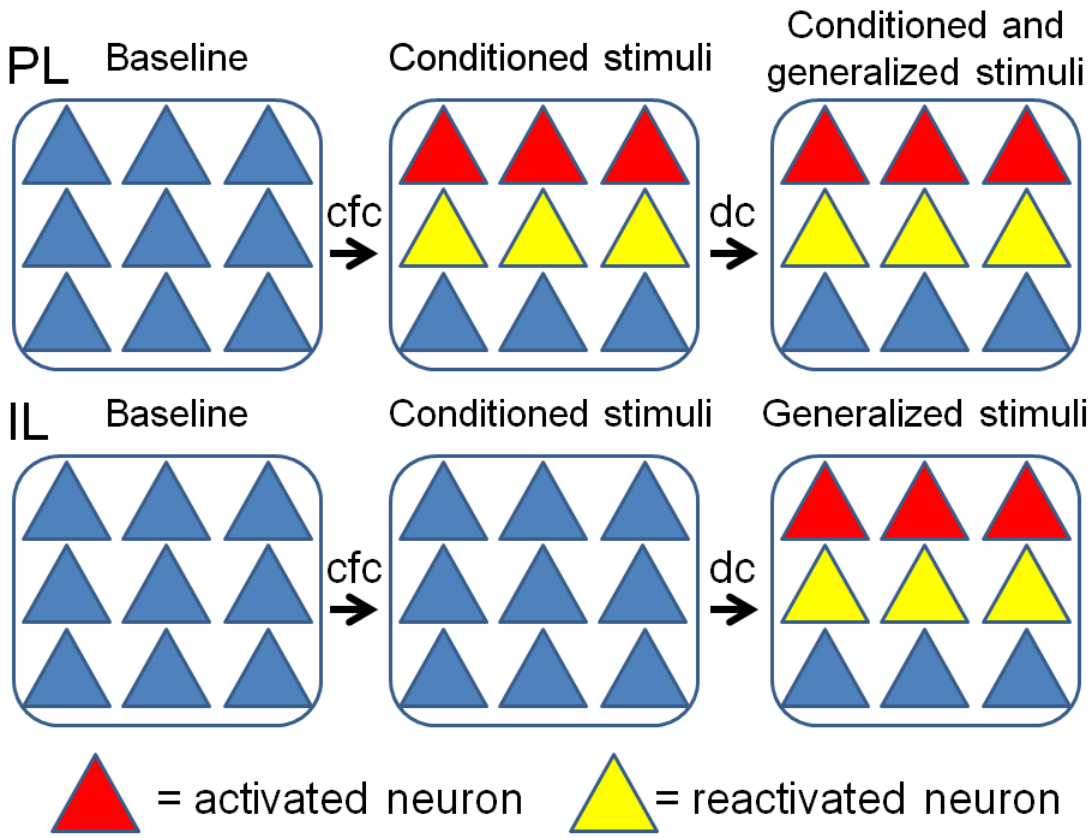

Figure 4.1: Model for the role of the mPFC circuitry in contextual fear conditioning and fear discrimination learning. Upon acquisiton of contextual fear conditioning (cfc), there is elevated PL activation and reactivation when animals are exposed or re-exposed to conditioned stimuli (i.e. CS+) while the IL region shows no differences in activation or reactivation relative to non fear-conditioned animals. Once animals successfully acqire differential fear conditioning (dc), there is an increase in IL activation and reactivation specifically to the similar, yet distinct, generalized stimuli (i.e. CS-). In the PL region, exposure and re-exposure to either the conditioned or generalized stimuli increase PL activation and reactivation, respectively. These data suggest that during contextual fear conditioning, the PL region monitors contextual danger associations while both the PL and IL regions mediate safety learning during fear discrimination learning.

References

1. Mahan AL, Ressler KJ: Fear conditioning, synaptic plasticity and the amygdala: implications for posttraumatic stress disorder. *Trends Neurosci* 2012, 35(1):24-35.

2. Milad MR, Pitman RK, Ellis CB, Gold AL, Shin LM, Lasko NB, Zeidan MA, Handwerger K, Orr SP, Rauch SL: Neurobiological basis of failure to recall extinction memory in posttraumatic stress disorder. *Biol Psychiatry* 2009, 66(12):1075-1082.

3. Xu W, Südhof TC: A neural circuit for memory specificity and generalization. *Science* 2013, 339(6125):1290-1295.

4. Vieira PA, Lovelace JW, Corches A, Rashid AJ, Josselyn SA, Korzus E: Prefrontal consolidation supports the attainment of fear memory accuracy. *Learn Mem* 2014, 21(8):394-405.

5. Vieira PA, Corches A, Lovelace JW, Westbrook KB, Mendoza M, Korzus E: Prefrontal NMDA receptors expressed in excitatory neurons control fear discrimination and fear extinction. *Neurobiol Learn Mem* 2015, 119:52-62.

6. Pavlov IP: Conditioned reflexes: an investigation of the physiological activity of the cerebral cortex. England: Oxford Univ. Press; 1927.

7. Rescorla RA, Wagner AR: A theory of Pavlovian conditioning: Variations in the effectiveness of reinforcement and nonreinforcement. In., vol. 21: Appleton-Century-Crofts; 1972.

8. Pearce JM, Hall G: A model for Pavlovian learning: variations in the effectiveness of conditioned but not of unconditioned stimuli. *Psychol Rev* 1980, 87(6):532-552.

9. Maren S, Fanselow MS: Synaptic plasticity in the basolateral amygdala induced by hippocampal formation stimulation in vivo. *J Neurosci* 1995, 15(11):7548-7564.

10. Pitkänen A, Pikkarainen M, Nurminen N, Ylinen A: Reciprocal connections between the amygdala and the hippocampal formation, perirhinal cortex, and postrhinal cortex in rat. A review. *Ann N Y Acad Sci* 2000, 911:369-391.

11. LeDoux JE, Sakaguchi A, Reis DJ: Subcortical efferent projections of the medial geniculate nucleus mediate emotional responses conditioned to acoustic stimuli. *J Neurosci* 1984, 4(3):683-698.

12. LeDoux JE, Ruggiero DA, Reis DJ: Projections to the subcortical forebrain from anatomically defined regions of the medial geniculate body in the rat. *J Comp Neurol* 1985, 242(2):182-213.

13. Nabavi S, Fox R, Proulx CD, Lin JY, Tsien RY, Malinow R: Engineering a memory with LTD and LTP. *Nature* 2014, 511(7509):348-352.

14. Jin J, Maren S: Prefrontal-Hippocampal Interactions in Memory and Emotion. *Front Syst Neurosci* 2015, 9:170.

15. Kim WB, Cho JH: Synaptic Targeting of Double-Projecting Ventral CA1 Hippocampal Neurons to the Medial Prefrontal Cortex and Basal Amygdala. *J Neurosci* 2017, 37(19):4868-4882.

16. Kim JJ, Fanselow MS: Modality-specific retrograde amnesia of fear. *Science* 1992, 256(5057):675-677.

17. Quinn JJ, Ma QD, Tinsley MR, Koch C, Fanselow MS: Inverse temporal contributions of the dorsal hippocampus and medial prefrontal cortex to the expression of long-term fear memories. *Learn Mem* 2008, 15(5):368-372.

18. Tse D, Takeuchi T, Kakeyama M, Kajii Y, Okuno H, Tohyama C, Bito H, Morris RG: Schema-dependent gene activation and memory encoding in neocortex. *Science* 2011, 333(6044):891-895.

19. Zelikowsky M, Bissiere S, Hast TA, Bennett RZ, Abdipranoto A, Vissel B, Fanselow MS: Prefrontal microcircuit underlies contextual learning after hippocampal loss. *Proc Natl Acad Sci U S A* 2013, 110(24):9938-9943.

20. Squire LR: Mechanisms of memory. *Science* 1986, 232(4758):1612-1619.

21. Morgan MA, Romanski LM, LeDoux JE: Extinction of emotional learning: contribution of medial prefrontal cortex. *Neurosci Lett* 1993, 163(1):109-113.

22. Sierra-Mercado D, Padilla-Coreano N, Quirk GJ: Dissociable roles of prelimbic and infralimbic cortices, ventral hippocampus, and basolateral amygdala in the expression and extinction of conditioned fear. *Neuropsychopharmacology* 2011, 36(2):529-538.

23. Vidal-Gonzalez I, Vidal-Gonzalez B, Rauch SL, Quirk GJ: Microstimulation reveals opposing influences of prelimbic and infralimbic cortex on the expression of conditioned fear. *Learn Mem* 2006, 13(6):728-733.

24. Sharpe MJ, Killcross S: The prelimbic cortex directs attention toward predictive cues during fear learning. *Learn Mem* 2015, 22(6):289-293.

25. Stern CA, Gazarini L, Vanvossen AC, Hames MS, Bertoglio LJ: Activity in prelimbic cortex subserves fear memory reconsolidation over time. *Learn Mem* 2013, 21(1):14-20.

26. Chang CH, Maren S: Medial prefrontal cortex activation facilitates re-extinction of fear in rats. *Learn Mem* 2011, 18(4):221-225.

27. Milad MR, Quirk GJ: Neurons in medial prefrontal cortex signal memory for fear extinction. *Nature* 2002, 420(6911):70-74.

28. Milad MR, Vidal-Gonzalez I, Quirk GJ: Electrical stimulation of medial prefrontal cortex reduces conditioned fear in a temporally specific manner. *Behav Neurosci* 2004, 118(2):389-394.

29. Fitzgerald PJ, Whittle N, Flynn SM, Graybeal C, Pinard CR, Gunduz-Cinar O, Kravitz AV, Singewald N, Holmes A: Prefrontal single-unit firing associated with deficient extinction in mice. *Neurobiol Learn Mem* 2014, 113:69-81.

30. Marek R, Xu L, Sullivan RKP, Sah P: Excitatory connections between the prelimbic and infralimbic medial prefrontal cortex show a role for the prelimbic cortex in fear extinction. *Nat Neurosci* 2018, 21(5):654-658.

31. Quirk GJ, Likhtik E, Pelletier JG, Paré D: Stimulation of medial prefrontal cortex decreases the responsiveness of central amygdala output neurons. *J Neurosci* 2003, 23(25):8800-8807.

32. Royer S, Martina M, Paré D: An inhibitory interface gates impulse traffic between the input and output stations of the amygdala. *J Neurosci* 1999, 19(23):10575-10583.

33. Royer S, Paré D: Bidirectional synaptic plasticity in intercalated amygdala neurons and the extinction of conditioned fear responses. *Neuroscience* 2002, 115(2):455-462.

34. Likhtik E, Popa D, Apergis-Schoute J, Fidacaro GA, Paré D: Amygdala intercalated neurons are required for expression of fear extinction. *Nature* 2008, 454(7204):642-645.

35. Corcoran KA, Quirk GJ: Activity in prelimbic cortex is necessary for the expression of learned, but not innate, fears. *J Neurosci* 2007, 27(4):840-844.

36. Cho JH, Deisseroth K, Bolshakov VY: Synaptic encoding of fear extinction in mPFC-amygdala circuits. *Neuron* 2013, 80(6):1491-1507.

37. Pinard CR, Mascagni F, McDonald AJ: Medial prefrontal cortical innervation of the intercalated nuclear region of the amygdala. *Neuroscience* 2012, 205:112-124.

38. Strobel C, Marek R, Gooch HM, Sullivan RK, Sah P: Prefrontal and Auditory Input to Intercalated Neurons of the Amygdala. *Cell Rep* 2015.

39. Gutman DA, Keifer OP, Magnuson ME, Choi DC, Majeed W, Keilholz S, Ressler KJ: A DTI tractography analysis of infralimbic and prelimbic connectivity in the mouse using high-throughput MRI. *Neuroimage* 2012, 63(2):800-811.

40. Hardy SG, Leichnetz GR: Frontal cortical projections to the periaqueductal gray in the rat: a retrograde and orthograde horseradish peroxidase study. *Neurosci Lett* 1981, 23(1):13-17.

41. Vianna DM, Brandão ML: Anatomical connections of the periaqueductal gray: specific neural substrates for different kinds of fear. *Braz J Med Biol Res* 2003, 36(5):557-566.

42. Hoover WB, Vertes RP: Anatomical analysis of afferent projections to the medial prefrontal cortex in the rat. *Brain Struct Funct* 2007, 212(2):149-179.

43. Lovelace JW, Vieira PA, Corches A, Mackie K, Korzus E: Impaired fear memory specificity associated with deficient endocannabinoid-dependent long-term plasticity. *Neuropsychopharmacology* 2014, 39(7):1685-1693.

44. Morgan MA, LeDoux JE: Contribution of ventrolateral prefrontal cortex to the acquisition and extinction of conditioned fear in rats. *Neurobiol Learn Mem* 1999, 72(3):244-251.

45. Sharpe MJ, Killcross S: The prelimbic cortex uses higher-order cues to modulate both the acquisition and expression of conditioned fear. *Front Syst Neurosci* 2014, 8:235.

46. Burgos-Robles A, Kimchi EY, Izadmehr EM, Porzenheim MJ, Ramos-Guasp WA, Nieh EH, Felix-Ortiz AC, Namburi P, Leppla CA, Presbrey KN *et al*: Amygdala inputs to prefrontal cortex guide behavior amid conflicting cues of reward and punishment. *Nat Neurosci* 2017, 20(6):824-835.

47. Sangha S, Robinson PD, Greba Q, Davies DA, Howland JG: Alterations in reward, fear and safety cue discrimination after inactivation of the rat prelimbic and infralimbic cortices. *Neuropsychopharmacology* 2014, 39(10):2405-2413.

48. Spence KW: The differential response in animals to stimuli varying within a single dimension. *Psychological Review* 1937, 44(5):430-444.

49. Hull CL: A Behavior System: Yale University Press; 1952.

50. Klein SB: Learning: Principles and Applications, 7 edn: SAGE Publications Ltd, Thousand Oaks, CA; 2014.

51. Bouton ME: Context, ambiguity, and unlearning: sources of relapse after behavioral extinction. *Biol Psychiatry* 2002, 52(10):976-986.

52. Myers KM, Ressler KJ, Davis M: Different mechanisms of fear extinction dependent on length of time since fear acquisition. *Learn Mem* 2006, 13(2):216-223.

53. Courtin J, Bienvenu TC, Einarsson E, Herry C: Medial prefrontal cortex neuronal circuits in fear behavior. *Neuroscience* 2013, 240:219-242.

54. Holmes A, Fitzgerald PJ, MacPherson KP, DeBrouse L, Colacicco G, Flynn SM, Masneuf S, Pleil KE, Li C, Marcinkiewcz CA *et al*: Chronic alcohol remodels prefrontal neurons and disrupts NMDAR-mediated fear extinction encoding. *Nat Neurosci* 2012, 15(10):1359-1361.

55. Guzowski JF, McNaughton BL, Barnes CA, Worley PF: Environment-specific expression of the immediate-early gene Arc in hippocampal neuronal ensembles. *Nat Neurosci* 1999, 2(12):1120-1124.

56. Chowdhury S, Shepherd JD, Okuno H, Lyford G, Petralia RS, Plath N, Kuhl D, Huganir RL, Worley PF: Arc/Arg3.1 interacts with the endocytic machinery to regulate AMPA receptor trafficking. *Neuron* 2006, 52(3):445-459.

57. Czerniawski J, Ree F, Chia C, Ramamoorthi K, Kumata Y, Otto TA: The importance of having Arc: expression of the immediate-early gene Arc is required for hippocampus-dependent fear conditioning and blocked by NMDA receptor antagonism. *J Neurosci* 2011, 31(31):11200-11207.

58. Guzowski JF, Lyford GL, Stevenson GD, Houston FP, McGaugh JL, Worley PF, Barnes CA: Inhibition of activity-dependent arc protein expression in the rat hippocampus impairs the maintenance of long-term potentiation and the consolidation of long-term memory. *J Neurosci* 2000, 20(11):3993-4001.

59. Ploski JE, Pierre VJ, Smucny J, Park K, Monsey MS, Overeem KA, Schafe GE: The activity-regulated cytoskeletal-associated protein (Arc/Arg3.1) is required for

memory consolidation of pavlovian fear conditioning in the lateral amygdala. *J Neurosci* 2008, 28(47):12383-12395.

60. Knapska E, Maren S: Reciprocal patterns of c-Fos expression in the medial prefrontal cortex and amygdala after extinction and renewal of conditioned fear. *Learn Mem* 2009, 16(8):486-493.

61. Orsini CA, Yan C, Maren S: Ensemble coding of context-dependent fear memory in the amygdala. *Front Behav Neurosci* 2013, 7:199.

62. Hefner K, Whittle N, Juhasz J, Norcross M, Karlsson RM, Saksida LM, Bussey TJ, Singewald N, Holmes A: Impaired fear extinction learning and cortico-amygdala circuit abnormalities in a common genetic mouse strain. *J Neurosci* 2008, 28(32):8074-8085.

63. Morrow BA, Elsworth JD, Inglis FM, Roth RH: An antisense oligonucleotide reverses the footshock-induced expression of fos in the rat medial prefrontal cortex and the subsequent expression of conditioned fear-induced immobility. *J Neurosci* 1999, 19(13):5666-5673.

64. Herry C, Mons N: Resistance to extinction is associated with impaired immediate early gene induction in medial prefrontal cortex and amygdala. *Eur J Neurosci* 2004, 20(3):781-790.

65. Frankland PW, Bontempi B, Talton LE, Kaczmarek L, Silva AJ: The involvement of the anterior cingulate cortex in remote contextual fear memory. *Science* 2004, 304(5672):881-883.

66. Bremner JD, Vermetten E, Schmahl C, Vaccarino V, Vythilingam M, Afzal N, Grillon C, Charney DS: Positron emission tomographic imaging of neural correlates of a fear acquisition and extinction paradigm in women with childhood sexual-abuse-related post-traumatic stress disorder. *Psychol Med* 2005, 35(6):791-806.

67. Smeyne RJ, Schilling K, Robertson L, Luk D, Oberdick J, Curran T, Morgan JI: fos-lacZ transgenic mice: mapping sites of gene induction in the central nervous system. *Neuron* 1992, 8(1):13-23.

68. Wang KH, Majewska A, Schummers J, Farley B, Hu C, Sur M, Tonegawa S: In vivo two-photon imaging reveals a role of arc in enhancing orientation specificity in visual cortex. *Cell* 2006, 126(2):389-402.

69. Reijmers LG, Perkins BL, Matsuo N, Mayford M: Localization of a stable neural correlate of associative memory. *Science* 2007, 317(5842):1230-1233.

70. Xie H, Liu Y, Zhu Y, Ding X, Yang Y, Guan JS: In vivo imaging of immediate early gene expression reveals layer-specific memory traces in the mammalian brain. *Proc Natl Acad Sci U S A* 2014, 111(7):2788-2793.

71. Czajkowski R, Jayaprakash B, Wiltgen B, Rogerson T, Guzman-Karlsson MC, Barth AL, Trachtenberg JT, Silva AJ: Encoding and storage of spatial information in the retrosplenial cortex. *Proc Natl Acad Sci U S A* 2014, 111(23):8661-8666.

72. Gossen M, Bujard H: Tight control of gene expression in mammalian cells by tetracycline-responsive promoters. *Proc Natl Acad Sci U S A* 1992, 89(12):5547-5551.

73. Boyden ES, Zhang F, Bamberg E, Nagel G, Deisseroth K: Millisecond-timescale, genetically targeted optical control of neural activity. *Nat Neurosci* 2005, 8(9):1263-1268.

74. Liu X, Ramirez S, Pang PT, Puryear CB, Govindarajan A, Deisseroth K, Tonegawa S: Optogenetic stimulation of a hippocampal engram activates fear memory recall. *Nature* 2012, 484(7394):381-385.

75. Ramirez S, Liu X, Lin PA, Suh J, Pignatelli M, Redondo RL, Ryan TJ, Tonegawa S: Creating a false memory in the hippocampus. *Science* 2013, 341(6144):387-391.

76. Corcoran KA, Yamawaki N, Leaderbrand K, Radulovic J: Role of retrosplenial cortex in processing stress-related context memories. *Behav Neurosci* 2018, 132(5):388-395.

77. Cowansage KK, Shuman T, Dillingham BC, Chang A, Golshani P, Mayford M: Direct reactivation of a coherent neocortical memory of context. *Neuron* 2014, 84(2):432-441.

78. Kessler RC, Berglund P, Demler O, Jin R, Merikangas KR, Walters EE: Lifetime prevalence and age-of-onset distributions of DSM-IV disorders in the National Comorbidity Survey Replication. *Arch Gen Psychiatry* 2005, 62(6):593-602.

79. McCloskey LA, Walker M: Posttraumatic stress in children exposed to family violence and single-event trauma. *J Am Acad Child Adolesc Psychiatry* 2000, 39(1):108-115.

80. Heron-Delaney M, Kenardy J, Charlton E, Matsuoka Y: A systematic review of predictors of posttraumatic stress disorder (PTSD) for adult road traffic crash survivors. *Injury* 2013, 44(11):1413-1422.

81. Schnurr PP, Lunney CA, Sengupta A: Risk factors for the development versus maintenance of posttraumatic stress disorder. *J Trauma Stress* 2004, 17(2):85-95.

82. Shin LM, Orr SP, Carson MA, Rauch SL, Macklin ML, Lasko NB, Peters PM, Metzger LJ, Dougherty DD, Cannistraro PA *et al*: Regional cerebral blood flow in the amygdala and medial prefrontal cortex during traumatic imagery in male and female Vietnam veterans with PTSD. *Arch Gen Psychiatry* 2004, 61(2):168-176.

83. Bremner JD, Staib LH, Kaloupek D, Southwick SM, Soufer R, Charney DS: Neural correlates of exposure to traumatic pictures and sound in Vietnam combat veterans with and without posttraumatic stress disorder: a positron emission tomography study. *Biol Psychiatry* 1999, 45(7):806-816.

84. Pissiota A, Frans O, Fernandez M, von Knorring L, Fischer H, Fredrikson M: Neurofunctional correlates of posttraumatic stress disorder: a PET symptom provocation study. *Eur Arch Psychiatry Clin Neurosci* 2002, 252(2):68-75.

85. Rauch SL, van der Kolk BA, Fisler RE, Alpert NM, Orr SP, Savage CR, Fischman AJ, Jenike MA, Pitman RK: A symptom provocation study of posttraumatic stress disorder using positron emission tomography and script-driven imagery. *Arch Gen Psychiatry* 1996, 53(5):380-387.

86. Britton JC, Phan KL, Taylor SF, Fig LM, Liberzon I: Corticolimbic blood flow in posttraumatic stress disorder during script-driven imagery. *Biol Psychiatry* 2005, 57(8):832-840.

87. Etkin A, Wager TD: Functional neuroimaging of anxiety: a meta-analysis of emotional processing in PTSD, social anxiety disorder, and specific phobia. *Am J Psychiatry* 2007, 164(10):1476-1488.

88. Yang RJ, Mozhui K, Karlsson RM, Cameron HA, Williams RW, Holmes A: Variation in mouse basolateral amygdala volume is associated with differences in stress reactivity and fear learning. *Neuropsychopharmacology* 2008, 33(11):2595-2604.

89. Gianaros PJ, Sheu LK, Matthews KA, Jennings JR, Manuck SB, Hariri AR: Individual differences in stressor-evoked blood pressure reactivity vary with activation, volume, and functional connectivity of the amygdala. *J Neurosci* 2008, 28(4):990-999.

90. Morey RA, Gold AL, LaBar KS, Beall SK, Brown VM, Haswell CC, Nasser JD, Wagner HR, McCarthy G, Workgroup M-AM: Amygdala volume changes in posttraumatic stress disorder in a large case-controlled veterans group. *Arch Gen Psychiatry* 2012, 69(11):1169-1178.

91. Karl A, Schaefer M, Malta LS, Dörfel D, Rohleder N, Werner A: A meta-analysis of structural brain abnormalities in PTSD. *Neurosci Biobehav Rev* 2006, 30(7):1004-1031.

92. Akiki TJ, Averill CL, Wrocklage KM, Schweinsburg B, Scott JC, Martini B, Averill LA, Southwick SM, Krystal JH, Abdallah CG: The Association of PTSD Symptom Severity with Localized Hippocampus and Amygdala Abnormalities. *Chronic Stress (Thousand Oaks)* 2017, 1.

93. Fennema-Notestine C, Stein MB, Kennedy CM, Archibald SL, Jernigan TL: Brain morphometry in female victims of intimate partner violence with and without posttraumatic stress disorder. *Biol Psychiatry* 2002, 52(11):1089-1101.

94. Woon FL, Hedges DW: Amygdala volume in adults with posttraumatic stress disorder: a meta-analysis. *J Neuropsychiatry Clin Neurosci* 2009, 21(1):5-12.

95. Sui SG, Wu MX, King ME, Zhang Y, Ling L, Xu JM, Weng XC, Duan L, Shan BC, Li LJ: Abnormal grey matter in victims of rape with PTSD in Mainland China: a voxel-based morphometry study. *Acta Neuropsychiatr* 2010, 22(3):118-126.

96. Herringa R, Phillips M, Almeida J, Insana S, Germain A: Post-traumatic stress symptoms correlate with smaller subgenual cingulate, caudate, and insula volumes in unmedicated combat veterans. *Psychiatry Res* 2012, 203(2-3):139-145.

97. Fuchs E, Gould E: Mini-review: in vivo neurogenesis in the adult brain: regulation and functional implications. *Eur J Neurosci* 2000, 12(7):2211-2214.

98. Conrad CD: Chronic stress-induced hippocampal vulnerability: the glucocorticoid vulnerability hypothesis. *Rev Neurosci* 2008, 19(6):395-411.

99. Popoli M, Yan Z, McEwen BS, Sanacora G: The stressed synapse: the impact of stress and glucocorticoids on glutamate transmission. *Nat Rev Neurosci* 2011, 13(1):22-37.

100. Pavić L, Gregurek R, Rados M, Brkljacić B, Brajković L, Simetin-Pavić I, Ivanac G, Pavlisa G, Kalousek V: Smaller right hippocampus in war veterans with posttraumatic stress disorder. *Psychiatry Res* 2007, 154(2):191-198.

101. Kühn S, Gallinat J: Gray matter correlates of posttraumatic stress disorder: a quantitative meta-analysis. *Biol Psychiatry* 2013, 73(1):70-74.

102. Sussman D, Pang EW, Jetly R, Dunkley BT, Taylor MJ: Neuroanatomical features in soldiers with post-traumatic stress disorder. *BMC Neurosci* 2016, 17:13.

103. Logue MW, van Rooij SJH, Dennis EL, Davis SL, Hayes JP, Stevens JS, Densmore M, Haswell CC, Ipser J, Koch SBJ *et al*: Smaller Hippocampal Volume in Posttraumatic Stress Disorder: A Multisite ENIGMA-PGC Study: Subcortical Volumetry Results From Posttraumatic Stress Disorder Consortia. *Biol Psychiatry* 2018, 83(3):244-253.

104. Pederson CL, Maurer SH, Kaminski PL, Zander KA, Peters CM, Stokes-Crowe LA, Osborn RE: Hippocampal volume and memory performance in a community-based sample of women with posttraumatic stress disorder secondary to child abuse. *J Trauma Stress* 2004, 17(1):37-40.

105. Golier JA, Yehuda R, De Santi S, Segal S, Dolan S, de Leon MJ: Absence of hippocampal volume differences in survivors of the Nazi Holocaust with and without posttraumatic stress disorder. *Psychiatry Res* 2005, 139(1):53-64.

106. Jatzko A, Rothenhöfer S, Schmitt A, Gaser C, Demirakca T, Weber-Fahr W, Wessa M, Magnotta V, Braus DF: Hippocampal volume in chronic posttraumatic stress disorder (PTSD): MRI study using two different evaluation methods. *J Affect Disord* 2006, 94(1-3):121-126.

107. Bremner JD, Vythilingam M, Vermetten E, Southwick SM, McGlashan T, Staib LH, Soufer R, Charney DS: Neural correlates of declarative memory for emotionally valenced words in women with posttraumatic stress disorder related to early childhood sexual abuse. *Biol Psychiatry* 2003, 53(10):879-889.

108. Sherin JE, Nemeroff CB: Post-traumatic stress disorder: the neurobiological impact of psychological trauma. *Dialogues Clin Neurosci* 2011, 13(3):263-278.

109. Shin LM, Shin PS, Heckers S, Krangel TS, Macklin ML, Orr SP, Lasko N, Segal E, Makris N, Richert K *et al*: Hippocampal function in posttraumatic stress disorder. *Hippocampus* 2004, 14(3):292-300.

110. Gilbertson MW, Shenton ME, Ciszewski A, Kasai K, Lasko NB, Orr SP, Pitman RK: Smaller hippocampal volume predicts pathologic vulnerability to psychological trauma. *Nat Neurosci* 2002, 5(11):1242-1247.

111. Hou C, Liu J, Wang K, Li L, Liang M, He Z, Liu Y, Zhang Y, Li W, Jiang T: Brain responses to symptom provocation and trauma-related short-term memory recall in coal mining accident survivors with acute severe PTSD. *Brain Res* 2007, 1144:165-174.

112. Lindauer RJ, Booij J, Habraken JB, Uylings HB, Olff M, Carlier IV, den Heeten GJ, van Eck-Smit BL, Gersons BP: Cerebral blood flow changes during script-driven imagery in police officers with posttraumatic stress disorder. *Biol Psychiatry* 2004, 56(11):853-861.

113. Lanius RA, Williamson PC, Densmore M, Boksman K, Gupta MA, Neufeld RW, Gati JS, Menon RS: Neural correlates of traumatic memories in posttraumatic stress disorder: a functional MRI investigation. *Am J Psychiatry* 2001, 158(11):1920-1922.

114. Carrion VG, Weems CF, Eliez S, Patwardhan A, Brown W, Ray RD, Reiss AL: Attenuation of frontal asymmetry in pediatric posttraumatic stress disorder. *Biol Psychiatry* 2001, 50(12):943-951.

115. Woodward SH, Kaloupek DG, Streeter CC, Martinez C, Schaer M, Eliez S: Decreased anterior cingulate volume in combat-related PTSD. *Biol Psychiatry* 2006, 59(7):582-587.

116. Phelps EA, Delgado MR, Nearing KI, LeDoux JE: Extinction learning in humans: role of the amygdala and vmPFC. *Neuron* 2004, 43(6):897-905.

117. Milad MR, Quinn BT, Pitman RK, Orr SP, Fischl B, Rauch SL: Thickness of ventromedial prefrontal cortex in humans is correlated with extinction memory. *Proc Natl Acad Sci U S A* 2005, 102(30):10706-10711.

118. Rougemont-Bücking A, Linnman C, Zeffiro TA, Zeidan MA, Lebron-Milad K, Rodriguez-Romaguera J, Rauch SL, Pitman RK, Milad MR: Altered processing of contextual information during fear extinction in PTSD: an fMRI study. *CNS Neurosci Ther* 2011, 17(4):227-236.

119. O'Reilly RC, McClelland JL: Hippocampal conjunctive encoding, storage, and recall: avoiding a trade-off. *Hippocampus* 1994, 4(6):661-682.

120. Leutgeb JK, Leutgeb S, Moser MB, Moser EI: Pattern separation in the dentate gyrus and CA3 of the hippocampus. *Science* 2007, 315(5814):961-966.

121. Sahay A, Wilson DA, Hen R: Pattern separation: a common function for new neurons in hippocampus and olfactory bulb. *Neuron* 2011, 70(4):582-588.

122. Xu W, Morishita W, Buckmaster PS, Pang ZP, Malenka RC, Südhof TC: Distinct neuronal coding schemes in memory revealed by selective erasure of fast synchronous synaptic transmission. *Neuron* 2012, 73(5):990-1001.

123. DeVito LM, Lykken C, Kanter BR, Eichenbaum H: Prefrontal cortex: role in acquisition of overlapping associations and transitive inference. *Learn Mem* 2010, 17(3):161-167.

124. Dash PK, Hochner B, Kandel ER: Injection of the cAMP-responsive element into the nucleus of Aplysia sensory neurons blocks long-term facilitation. *Nature* 1990, 345(6277):718-721.

125. Bourtchuladze R, Frenguelli B, Blendy J, Cioffi D, Schutz G, Silva AJ: Deficient long-term memory in mice with a targeted mutation of the cAMP-responsive element-binding protein. *Cell* 1994, 79(1):59-68.

126. Yin JC, Wallach JS, Del Vecchio M, Wilder EL, Zhou H, Quinn WG, Tully T: Induction of a dominant negative CREB transgene specifically blocks long-term memory in Drosophila. *Cell* 1994, 79(1):49-58.

127. Josselyn SA, Shi C, Carlezon WA, Neve RL, Nestler EJ, Davis M: Long-term memory is facilitated by cAMP response element-binding protein overexpression in the amygdala. *J Neurosci* 2001, 21(7):2404-2412.

128. Kida S, Josselyn SA, Peña de Ortiz S, Kogan JH, Chevere I, Masushige S, Silva AJ: CREB required for the stability of new and reactivated fear memories. *Nat Neurosci* 2002, 5(4):348-355.

129. Pittenger C, Huang YY, Paletzki RF, Bourtchouladze R, Scanlin H, Vronskaya S, Kandel ER: Reversible inhibition of CREB/ATF transcription factors in region CA1 of the dorsal hippocampus disrupts hippocampus-dependent spatial memory. *Neuron* 2002, 34(3):447-462.

130. Gonzalez GA, Yamamoto KK, Fischer WH, Karr D, Menzel P, Biggs W, Vale WW, Montminy MR: A cluster of phosphorylation sites on the cyclic AMP-regulated nuclear factor CREB predicted by its sequence. *Nature* 1989, 337(6209):749-752.

131. Chrivia JC, Kwok RP, Lamb N, Hagiwara M, Montminy MR, Goodman RH: Phosphorylated CREB binds specifically to the nuclear protein CBP. *Nature* 1993, 365(6449):855-859.

132. Bannister AJ, Kouzarides T: The CBP co-activator is a histone acetyltransferase. *Nature* 1996, 384(6610):641-643.

133. Korzus E, Torchia J, Rose DW, Xu L, Kurokawa R, McInerney EM, Mullen TM, Glass CK, Rosenfeld MG: Transcription factor-specific requirements for

coactivators and their acetyltransferase functions. *Science* 1998, 279(5351):703-707.

134. Gu W, Roeder RG: Activation of p53 sequence-specific DNA binding by acetylation of the p53 C-terminal domain. *Cell* 1997, 90(4):595-606.

135. Lu Q, Hutchins AE, Doyle CM, Lundblad JR, Kwok RP: Acetylation of cAMP-responsive element-binding protein (CREB) by CREB-binding protein enhances CREB-dependent transcription. *J Biol Chem* 2003, 278(18):15727-15734.

136. Kouzarides T: Acetylation: a regulatory modification to rival phosphorylation? *EMBO J* 2000, 19(6):1176-1179.

137. Sterner DE, Berger SL: Acetylation of histones and transcription-related factors. *Microbiol Mol Biol Rev* 2000, 64(2):435-459.

138. Yang XJ: Lysine acetylation and the bromodomain: a new partnership for signaling. *Bioessays* 2004, 26(10):1076-1087.

139. Glozak MA, Sengupta N, Zhang X, Seto E: Acetylation and deacetylation of non-histone proteins. *Gene* 2005, 363:15-23.

140. Kimura A, Matsubara K, Horikoshi M: A decade of histone acetylation: marking eukaryotic chromosomes with specific codes. *J Biochem* 2005, 138(6):647-662.

141. Alarcón JM, Malleret G, Touzani K, Vronskaya S, Ishii S, Kandel ER, Barco A: Chromatin acetylation, memory, and LTP are impaired in CBP+/- mice: a model for the cognitive deficit in Rubinstein-Taybi syndrome and its amelioration. *Neuron* 2004, 42(6):947-959.

142. Korzus E, Rosenfeld MG, Mayford M: CBP histone acetyltransferase activity is a critical component of memory consolidation. *Neuron* 2004, 42(6):961-972.

143. Wood MA, Kaplan MP, Park A, Blanchard EJ, Oliveira AM, Lombardi TL, Abel T: Transgenic mice expressing a truncated form of CREB-binding protein (CBP) exhibit deficits in hippocampal synaptic plasticity and memory storage. *Learn Mem* 2005, 12(2):111-119.

144. Chen G, Zou X, Watanabe H, van Deursen JM, Shen J: CREB binding protein is required for both short-term and long-term memory formation. *J Neurosci* 2010, 30(39):13066-13077.

145. Barrett RM, Malvaez M, Kramar E, Matheos DP, Arrizon A, Cabrera SM, Lynch G, Greene RW, Wood MA: Hippocampal focal knockout of CBP affects specific

histone modifications, long-term potentiation, and long-term memory. *Neuropsychopharmacology* 2011, 36(8):1545-1556.

146. Valor LM, Pulopulos MM, Jimenez-Minchan M, Olivares R, Lutz B, Barco A: Ablation of CBP in forebrain principal neurons causes modest memory and transcriptional defects and a dramatic reduction of histone acetylation but does not affect cell viability. *J Neurosci* 2011, 31(5):1652-1663.

147. Peixoto L, Abel T: The role of histone acetylation in memory formation and cognitive impairments. *Neuropsychopharmacology* 2013, 38(1):62-76.

148. Maddox SA, Watts CS, Schafe GE: p300/CBP histone acetyltransferase activity is required for newly acquired and reactivated fear memories in the lateral amygdala. *Learn Mem* 2013, 20(2):109-119.

149. Valor LM, Viosca J, Lopez-Atalaya JP, Barco A: Lysine acetyltransferases CBP and p300 as therapeutic targets in cognitive and neurodegenerative disorders. *Curr Pharm Des* 2013, 19(28):5051-5064.

150. Lopez-Atalaya JP, Ciccarelli A, Viosca J, Valor LM, Jimenez-Minchan M, Canals S, Giustetto M, Barco A: CBP is required for environmental enrichment-induced neurogenesis and cognitive enhancement. *EMBO J* 2011, 30(20):4287-4298.

151. Aimone JB, Deng W, Gage FH: Resolving new memories: a critical look at the dentate gyrus, adult neurogenesis, and pattern separation. *Neuron* 2011, 70(4):589-596.

152. Cetin A, Komai S, Eliava M, Seeburg PH, Osten P: Stereotaxic gene delivery in the rodent brain. *Nat Protoc* 2006, 1(6):3166-3173.

153. Lim F, Neve RL: Generation of high-titer defective HSV-1 vectors. *Curr Protoc Neurosci* 2001, Chapter 4:Unit 4.13.

154. Neve RL, Lim F: Overview of gene delivery into cells using HSV-1-based vectors. *Curr Protoc Neurosci* 2001, Chapter 4:Unit 4.12.

155. Barrot M, Olivier JD, Perrotti LI, DiLeone RJ, Berton O, Eisch AJ, Impey S, Storm DR, Neve RL, Yin JC *et al*: CREB activity in the nucleus accumbens shell controls gating of behavioral responses to emotional stimuli. *Proc Natl Acad Sci U S A* 2002, 99(17):11435-11440.

156. Olson VG, Zabetian CP, Bolanos CA, Edwards S, Barrot M, Eisch AJ, Hughes T, Self DW, Neve RL, Nestler EJ: Regulation of drug reward by cAMP response

element-binding protein: evidence for two functionally distinct subregions of the ventral tegmental area. *J Neurosci* 2005, 25(23):5553-5562.

157. Fanselow MS: Conditioned and unconditional components of post-shock freezing. *Pavlov J Biol Sci* 1980, 15(4):177-182.

158. Goosens KA, Hobin JA, Maren S: Auditory-evoked spike firing in the lateral amygdala and Pavlovian fear conditioning: mnemonic code or fear bias? *Neuron* 2003, 40(5):1013-1022.

159. Paxinos G, Franklin KBJ: The mouse brain in stereotaxic coordinates. San Diego: Academic Press; 2001.

160. Guan Z, Giustetto M, Lomvardas S, Kim JH, Miniaci MC, Schwartz JH, Thanos D, Kandel ER: Integration of long-term-memory-related synaptic plasticity involves bidirectional regulation of gene expression and chromatin structure. *Cell* 2002, 111(4):483-493.

161. Kesner RP, Rogers J: An analysis of independence and interactions of brain substrates that subserve multiple attributes, memory systems, and underlying processes. *Neurobiol Learn Mem* 2004, 82(3):199-215.

162. Blumenfeld RS, Ranganath C: Prefrontal cortex and long-term memory encoding: an integrative review of findings from neuropsychology and neuroimaging. *Neuroscientist* 2007, 13(3):280-291.

163. Hirsch JC, Crepel F: Postsynaptic calcium is necessary for the induction of LTP and LTD of monosynaptic EPSPs in prefrontal neurons: an in vitro study in the rat. *Synapse* 1992, 10(2):173-175.

164. Morris SH, Knevett S, Lerner EG, Bindman LJ: Group I mGluR agonist DHPG facilitates the induction of LTP in rat prelimbic cortex in vitro. *J Neurophysiol* 1999, 82(4):1927-1933.

165. Takita M, Izaki Y, Jay TM, Kaneko H, Suzuki SS: Induction of stable long-term depression in vivo in the hippocampal-prefrontal cortex pathway. *Eur J Neurosci* 1999, 11(11):4145-4148.

166. Quirk GJ, Russo GK, Barron JL, Lebron K: The role of ventromedial prefrontal cortex in the recovery of extinguished fear. *J Neurosci* 2000, 20(16):6225-6231.

167. Izaki Y, Takita M, Nomura M: Local properties of CA1 region in hippocampo-prefrontal synaptic plasticity in rats. *Neuroreport* 2002, 13(4):469-472.

168. Maroun M, Richter-Levin G: Exposure to acute stress blocks the induction of long-term potentiation of the amygdala-prefrontal cortex pathway in vivo. *J Neurosci* 2003, 23(11):4406-4409.

169. Santini E, Ge H, Ren K, Peña de Ortiz S, Quirk GJ: Consolidation of fear extinction requires protein synthesis in the medial prefrontal cortex. *J Neurosci* 2004, 24(25):5704-5710.

170. Kawashima H, Izaki Y, Grace AA, Takita M: Cooperativity between hippocampal-prefrontal short-term plasticity through associative long-term potentiation. *Brain Res* 2006, 1109(1):37-44.

171. Richter-Levin G, Maroun M: Stress and amygdala suppression of metaplasticity in the medial prefrontal cortex. *Cereb Cortex* 2010, 20(10):2433-2441.

172. Sotres-Bayon F, Cain CK, LeDoux JE: Brain mechanisms of fear extinction: historical perspectives on the contribution of prefrontal cortex. *Biol Psychiatry* 2006, 60(4):329-336.

173. Quirk GJ, Mueller D: Neural mechanisms of extinction learning and retrieval. *Neuropsychopharmacology* 2008, 33(1):56-72.

174. Akirav I, Khatsrinov V, Vouimba RM, Merhav M, Ferreira G, Rosenblum K, Maroun M: Extinction of conditioned taste aversion depends on functional protein synthesis but not on NMDA receptor activation in the ventromedial prefrontal cortex. *Learn Mem* 2006, 13(3):254-258.

175. Marr D: Simple memory: a theory for archicortex. *Philos Trans R Soc Lond B Biol Sci* 1971, 262(841):23-81.

176. McHugh TJ, Jones MW, Quinn JJ, Balthasar N, Coppari R, Elmquist JK, Lowell BB, Fanselow MS, Wilson MA, Tonegawa S: Dentate gyrus NMDA receptors mediate rapid pattern separation in the hippocampal network. *Science* 2007, 317(5834):94-99.

177. Kumaran D, McClelland JL: Generalization through the recurrent interaction of episodic memories: a model of the hippocampal system. *Psychol Rev* 2012, 119(3):573-616.

178. Nakashiba T, Cushman JD, Pelkey KA, Renaudineau S, Buhl DL, McHugh TJ, Rodriguez Barrera V, Chittajallu R, Iwamoto KS, McBain CJ *et al*: Young dentate granule cells mediate pattern separation, whereas old granule cells facilitate pattern completion. *Cell* 2012, 149(1):188-201.

179. Navawongse R, Eichenbaum H: Distinct pathways for rule-based retrieval and spatial mapping of memory representations in hippocampal neurons. *J Neurosci* 2013, 33(3):1002-1013.

180. Zeng FG, Nie K, Stickney GS, Kong YY, Vongphoe M, Bhargave A, Wei C, Cao K: Speech recognition with amplitude and frequency modulations. *Proc Natl Acad Sci U S A* 2005, 102(7):2293-2298.

181. Fanselow MS, LeDoux JE: Why we think plasticity underlying Pavlovian fear conditioning occurs in the basolateral amygdala. *Neuron* 1999, 23(2):229-232.

182. LeDoux JE: Emotion circuits in the brain. *Annu Rev Neurosci* 2000, 23:155-184.

183. Letzkus JJ, Wolff SB, Meyer EM, Tovote P, Courtin J, Herry C, Lüthi A: A disinhibitory microcircuit for associative fear learning in the auditory cortex. *Nature* 2011, 480(7377):331-335.

184. Eckner R, Ewen ME, Newsome D, Gerdes M, DeCaprio JA, Lawrence JB, Livingston DM: Molecular cloning and functional analysis of the adenovirus E1A-associated 300-kD protein (p300) reveals a protein with properties of a transcriptional adaptor. *Genes Dev* 1994, 8(8):869-884.

185. RUBINSTEIN JH, TAYBI H: Broad thumbs and toes and facial abnormalities. A possible mental retardation syndrome. *Am J Dis Child* 1963, 105:588-608.

186. Petrij F, Giles RH, Dauwerse HG, Saris JJ, Hennekam RC, Masuno M, Tommerup N, van Ommen GJ, Goodman RH, Peters DJ: Rubinstein-Taybi syndrome caused by mutations in the transcriptional co-activator CBP. *Nature* 1995, 376(6538):348-351.

187. Arany Z, Sellers WR, Livingston DM, Eckner R: E1A-associated p300 and CREB-associated CBP belong to a conserved family of coactivators. *Cell* 1994, 77(6):799-800.

188. Ogryzko VV, Schiltz RL, Russanova V, Howard BH, Nakatani Y: The transcriptional coactivators p300 and CBP are histone acetyltransferases. *Cell* 1996, 87(5):953-959.

189. Yao TP, Oh SP, Fuchs M, Zhou ND, Ch'ng LE, Newsome D, Bronson RT, Li E, Livingston DM, Eckner R: Gene dosage-dependent embryonic development and proliferation defects in mice lacking the transcriptional integrator p300. *Cell* 1998, 93(3):361-372.

190. Sugiura H, Yamauchi T: Developmental changes in the levels of Ca2+/calmodulin-dependent protein kinase II alpha and beta proteins in soluble and particulate fractions of the rat brain. *Brain Res* 1992, 593(1):97-104.
191. Kojima N, Wang J, Mansuy IM, Grant SG, Mayford M, Kandel ER: Rescuing impairment of long-term potentiation in fyn-deficient mice by introducing Fyn transgene. *Proc Natl Acad Sci U S A* 1997, 94(9):4761-4765.
192. Rosenfeld MG, Glass CK: Coregulator codes of transcriptional regulation by nuclear receptors. *J Biol Chem* 2001, 276(40):36865-36868.
193. Vogel-Ciernia A, Matheos DP, Barrett RM, Kramár EA, Azzawi S, Chen Y, Magnan CN, Zeller M, Sylvain A, Haettig J *et al*: The neuron-specific chromatin regulatory subunit BAF53b is necessary for synaptic plasticity and memory. *Nat Neurosci* 2013, 16(5):552-561.
194. Puri PL, Sartorelli V, Yang XJ, Hamamori Y, Ogryzko VV, Howard BH, Kedes L, Wang JY, Graessmann A, Nakatani Y *et al*: Differential roles of p300 and PCAF acetyltransferases in muscle differentiation. *Mol Cell* 1997, 1(1):35-45.
195. ALLFREY VG, FAULKNER R, MIRSKY AE: ACETYLATION AND METHYLATION OF HISTONES AND THEIR POSSIBLE ROLE IN THE REGULATION OF RNA SYNTHESIS. *Proc Natl Acad Sci U S A* 1964, 51:786-794.
196. Pogo BG, Allfrey VG, Mirsky AE: RNA synthesis and histone acetylation during the course of gene activation in lymphocytes. *Proc Natl Acad Sci U S A* 1966, 55(4):805-812.
197. Kurdistani SK, Grunstein M: Histone acetylation and deacetylation in yeast. *Nat Rev Mol Cell Biol* 2003, 4(4):276-284.
198. Karlić R, Chung HR, Lasserre J, Vlahovicek K, Vingron M: Histone modification levels are predictive for gene expression. *Proc Natl Acad Sci U S A* 2010, 107(7):2926-2931.
199. Markowetz F, Mulder KW, Airoldi EM, Lemischka IR, Troyanskaya OG: Mapping dynamic histone acetylation patterns to gene expression in nanog-depleted murine embryonic stem cells. *PLoS Comput Biol* 2010, 6(12):e1001034.
200. Rogerson T, Cai DJ, Frank A, Sano Y, Shobe J, Lopez-Aranda MF, Silva AJ: Synaptic tagging during memory allocation. *Nat Rev Neurosci* 2014, 15(3):157-169.
201. Squire LR: Memory and the hippocampus: a synthesis from findings with rats, monkeys, and humans. *Psychol Rev* 1992, 99(2):195-231.
202. Medina JF, Repa JC, Mauk MD, LeDoux JE: Parallels between cerebellum- and amygdala-dependent conditioning. *Nat Rev Neurosci* 2002, 3(2):122-131.

203. Frankland PW, Bontempi B: The organization of recent and remote memories. *Nat Rev Neurosci* 2005, 6(2):119-130.

204. Sotres-Bayon F, Quirk GJ: Prefrontal control of fear: more than just extinction. *Curr Opin Neurobiol* 2010, 20(2):231-235.

205. Gabbott PL, Warner TA, Jays PR, Salway P, Busby SJ: Prefrontal cortex in the rat: projections to subcortical autonomic, motor, and limbic centers. *J Comp Neurol* 2005, 492(2):145-177.

206. Vertes RP: Differential projections of the infralimbic and prelimbic cortex in the rat. *Synapse* 2004, 51(1):32-58.

207. Collins DR, Paré D: Differential fear conditioning induces reciprocal changes in the sensory responses of lateral amygdala neurons to the CS(+) and CS(-). *Learn Mem* 2000, 7(2):97-103.

208. Burgos-Robles A, Vidal-Gonzalez I, Santini E, Quirk GJ: Consolidation of fear extinction requires NMDA receptor-dependent bursting in the ventromedial prefrontal cortex. *Neuron* 2007, 53(6):871-880.

209. Santini E, Muller RU, Quirk GJ: Consolidation of extinction learning involves transfer from NMDA-independent to NMDA-dependent memory. *J Neurosci* 2001, 21(22):9009-9017.

210. Maren S, Quirk GJ: Neuronal signalling of fear memory. *Nat Rev Neurosci* 2004, 5(11):844-852.

211. Bouton ME, Nelson JB: Context-specificity of target versus feature inhibition in a feature-negative discrimination. *J Exp Psychol Anim Behav Process* 1994, 20(1):51-65.

212. Gewirtz JC, Falls WA, Davis M: Normal conditioned inhibition and extinction of freezing and fear-potentiated startle following electrolytic lesions of medical prefrontal cortex in rats. *Behav Neurosci* 1997, 111(4):712-726.

213. Orsini CA, Kim JH, Knapska E, Maren S: Hippocampal and prefrontal projections to the basal amygdala mediate contextual regulation of fear after extinction. *J Neurosci* 2011, 31(47):17269-17277.

214. Orsini CA, Maren S: Neural and cellular mechanisms of fear and extinction memory formation. *Neurosci Biobehav Rev* 2012, 36(7):1773-1802.

215. Sotres-Bayon F, Diaz-Mataix L, Bush DE, LeDoux JE: Dissociable roles for the ventromedial prefrontal cortex and amygdala in fear extinction: NR2B contribution. *Cereb Cortex* 2009, 19(2):474-482.

216. Hirsch JC, Crepel F: Blockade of NMDA receptors unmasks a long-term depression in synaptic efficacy in rat prefrontal neurons in vitro. *Exp Brain Res* 1991, 85(3):621-624.

217. Homayoun H, Moghaddam B: NMDA receptor hypofunction produces opposite effects on prefrontal cortex interneurons and pyramidal neurons. *J Neurosci* 2007, 27(43):11496-11500.

218. Jackson ME, Homayoun H, Moghaddam B: NMDA receptor hypofunction produces concomitant firing rate potentiation and burst activity reduction in the prefrontal cortex. *Proc Natl Acad Sci U S A* 2004, 101(22):8467-8472.

219. Breier A, Su TP, Saunders R, Carson RE, Kolachana BS, de Bartolomeis A, Weinberger DR, Weisenfeld N, Malhotra AK, Eckelman WC *et al*: Schizophrenia is associated with elevated amphetamine-induced synaptic dopamine concentrations: evidence from a novel positron emission tomography method. *Proc Natl Acad Sci U S A* 1997, 94(6):2569-2574.

220. Lahti AC, Holcomb HH, Medoff DR, Tamminga CA: Ketamine activates psychosis and alters limbic blood flow in schizophrenia. *Neuroreport* 1995, 6(6):869-872.

221. Suzuki Y, Jodo E, Takeuchi S, Niwa S, Kayama Y: Acute administration of phencyclidine induces tonic activation of medial prefrontal cortex neurons in freely moving rats. *Neuroscience* 2002, 114(3):769-779.

222. Vollenweider FX, Leenders KL, Oye I, Hell D, Angst J: Differential psychopathology and patterns of cerebral glucose utilisation produced by (S)- and (R)-ketamine in healthy volunteers using positron emission tomography (PET). *Eur Neuropsychopharmacol* 1997, 7(1):25-38.

223. Jacobs NS, Cushman JD, Fanselow MS: The accurate measurement of fear memory in Pavlovian conditioning: Resolving the baseline issue. *J Neurosci Methods* 2010, 190(2):235-239.

224. Bliss TV, Collingridge GL: A synaptic model of memory: long-term potentiation in the hippocampus. *Nature* 1993, 361(6407):31-39.

225. Tsien JZ, Huerta PT, Tonegawa S: The essential role of hippocampal CA1 NMDA receptor-dependent synaptic plasticity in spatial memory. *Cell* 1996, 87(7):1327-1338.

226. Holt W, Maren S: Muscimol inactivation of the dorsal hippocampus impairs contextual retrieval of fear memory. *J Neurosci* 1999, 19(20):9054-9062.

227. Lee YK, Choi JS: Inactivation of the medial prefrontal cortex interferes with the expression but not the acquisition of differential fear conditioning in rats. *Exp Neurobiol* 2012, 21(1):23-29.

228. Gilmartin MR, McEchron MD: Single neurons in the medial prefrontal cortex of the rat exhibit tonic and phasic coding during trace fear conditioning. *Behav Neurosci* 2005, 119(6):1496-1510.

229. Pape HC, Pare D: Plastic synaptic networks of the amygdala for the acquisition, expression, and extinction of conditioned fear. *Physiol Rev* 2010, 90(2):419-463.

230. Martin SJ, Grimwood PD, Morris RG: Synaptic plasticity and memory: an evaluation of the hypothesis. *Annu Rev Neurosci* 2000, 23:649-711.

231. Falls WA, Miserendino MJ, Davis M: Extinction of fear-potentiated startle: blockade by infusion of an NMDA antagonist into the amygdala. *J Neurosci* 1992, 12(3):854-863.

232. Lee H, Kim JJ: Amygdalar NMDA receptors are critical for new fear learning in previously fear-conditioned rats. *J Neurosci* 1998, 18(20):8444-8454.

233. Tang YP, Shimizu E, Dube GR, Rampon C, Kerchner GA, Zhuo M, Liu G, Tsien JZ: Genetic enhancement of learning and memory in mice. *Nature* 1999, 401(6748):63-69.

234. Barria A, Malinow R: NMDA receptor subunit composition controls synaptic plasticity by regulating binding to CaMKII. *Neuron* 2005, 48(2):289-301.

235. Sobczyk A, Scheuss V, Svoboda K: NMDA receptor subunit-dependent [Ca2+] signaling in individual hippocampal dendritic spines. *J Neurosci* 2005, 25(26):6037-6046.

236. Birrell JM, Brown VJ: Medial frontal cortex mediates perceptual attentional set shifting in the rat. *J Neurosci* 2000, 20(11):4320-4324.

237. Dias R, Robbins TW, Roberts AC: Dissociation in prefrontal cortex of affective and attentional shifts. *Nature* 1996, 380(6569):69-72.

238. Ragozzino ME, Kim J, Hassert D, Minniti N, Kiang C: The contribution of the rat prelimbic-infralimbic areas to different forms of task switching. *Behav Neurosci* 2003, 117(5):1054-1065.

239. Rich EL, Shapiro ML: Prelimbic/infralimbic inactivation impairs memory for multiple task switches, but not flexible selection of familiar tasks. *J Neurosci* 2007, 27(17):4747-4755.

240. Lesting J, Narayanan RT, Kluge C, Sangha S, Seidenbecher T, Pape HC: Patterns of coupled theta activity in amygdala-hippocampal-prefrontal cortical circuits during fear extinction. *PLoS One* 2011, 6(6):e21714.

241. Popa D, Duvarci S, Popescu AT, Léna C, Paré D: Coherent amygdalocortical theta promotes fear memory consolidation during paradoxical sleep. *Proc Natl Acad Sci U S A* 2010, 107(14):6516-6519.

242. Seidenbecher T, Laxmi TR, Stork O, Pape HC: Amygdalar and hippocampal theta rhythm synchronization during fear memory retrieval. *Science* 2003, 301(5634):846-850.

243. Likhtik E, Stujenske JM, Topiwala MA, Harris AZ, Gordon JA: Prefrontal entrainment of amygdala activity signals safety in learned fear and innate anxiety. *Nat Neurosci* 2014, 17(1):106-113.

244. Gazendam FJ, Kamphuis JH, Kindt M: Deficient safety learning characterizes high trait anxious individuals. *Biol Psychol* 2013, 92(2):342-352.

245. Reinecke A, Becker ES, Hoyer J, Rinck M: Generalized implicit fear associations in generalized anxiety disorder. *Depress Anxiety* 2010, 27(3):252-259.

246. Jovanovic T, Kazama A, Bachevalier J, Davis M: Impaired safety signal learning may be a biomarker of PTSD. *Neuropharmacology* 2012, 62(2):695-704.

247. Jovanovic T, Ressler KJ: How the neurocircuitry and genetics of fear inhibition may inform our understanding of PTSD. *Am J Psychiatry* 2010, 167(6):648-662.

248. Jovanovic T, Norrholm SD, Blanding NQ, Davis M, Duncan E, Bradley B, Ressler KJ: Impaired fear inhibition is a biomarker of PTSD but not depression. *Depress Anxiety* 2010, 27(3):244-251.

249. Jovanovic T, Ely T, Fani N, Glover EM, Gutman D, Tone EB, Norrholm SD, Bradley B, Ressler KJ: Reduced neural activation during an inhibition task is associated with impaired fear inhibition in a traumatized civilian sample. *Cortex* 2013, 49(7):1884-1891.

250. Lanius RA, Williamson PC, Densmore M, Boksman K, Neufeld RW, Gati JS, Menon RS: The nature of traumatic memories: a 4-T FMRI functional connectivity analysis. *Am J Psychiatry* 2004, 161(1):36-44.

251. Gilboa A, Shalev AY, Laor L, Lester H, Louzoun Y, Chisin R, Bonne O: Functional connectivity of the prefrontal cortex and the amygdala in posttraumatic stress disorder. *Biol Psychiatry* 2004, 55(3):263-272.

252. Fanselow MS, Wassum KM: The Origins and Organization of Vertebrate Pavlovian Conditioning. *Cold Spring Harb Perspect Biol* 2015, 8(1):a021717.

253. Kitamura T, Ogawa SK, Roy DS, Okuyama T, Morrissey MD, Smith LM, Redondo RL, Tonegawa S: Engrams and circuits crucial for systems consolidation of a memory. *Science* 2017, 356(6333):73-78.

254. Frankland PW, Cestari V, Filipkowski RK, McDonald RJ, Silva AJ: The dorsal hippocampus is essential for context discrimination but not for contextual conditioning. *Behav Neurosci* 1998, 112(4):863-874.

255. Zelikowsky M, Hersman S, Chawla MK, Barnes CA, Fanselow MS: Neuronal ensembles in amygdala, hippocampus, and prefrontal cortex track differential components of contextual fear. *J Neurosci* 2014, 34(25):8462-8466.

256. Euston DR, Gruber AJ, McNaughton BL: The role of medial prefrontal cortex in memory and decision making. *Neuron* 2012, 76(6):1057-1070.

257. Hyman JM, Ma L, Balaguer-Ballester E, Durstewitz D, Seamans JK: Contextual encoding by ensembles of medial prefrontal cortex neurons. *Proc Natl Acad Sci U S A* 2012, 109(13):5086-5091.

258. Tumbar T, Guasch G, Greco V, Blanpain C, Lowry WE, Rendl M, Fuchs E: Defining the epithelial stem cell niche in skin. *Science* 2004, 303(5656):359-363.

259. Cai DJ, Aharoni D, Shuman T, Shobe J, Biane J, Song W, Wei B, Veshkini M, La-Vu M, Lou J *et al*: A shared neural ensemble links distinct contextual memories encoded close in time. *Nature* 2016, 534(7605):115-118.

260. Renier N, Adams EL, Kirst C, Wu Z, Azevedo R, Kohl J, Autry AE, Kadiri L, Umadevi Venkataraju K, Zhou Y *et al*: Mapping of Brain Activity by Automated Volume Analysis of Immediate Early Genes. *Cell* 2016, 165(7):1789-1802.

261. Burgos-Robles A, Vidal-Gonzalez I, Quirk GJ: Sustained conditioned responses in prelimbic prefrontal neurons are correlated with fear expression and extinction failure. *J Neurosci* 2009, 29(26):8474-8482.

262. Maren S, Phan KL, Liberzon I: The contextual brain: implications for fear conditioning, extinction and psychopathology. *Nat Rev Neurosci* 2013, 14(6):417-428.

263. Jin J, Maren S: Fear renewal preferentially activates ventral hippocampal neurons projecting to both amygdala and prefrontal cortex in rats. *Sci Rep* 2015, 5:8388.

264. Kim EJ, Kim N, Kim HT, Choi JS: The prelimbic cortex is critical for context-dependent fear expression. *Front Behav Neurosci* 2013, 7:73.

265. Do-Monte FH, Manzano-Nieves G, Quiñones-Laracuente K, Ramos-Medina L, Quirk GJ: Revisiting the role of infralimbic cortex in fear extinction with optogenetics. *J Neurosci* 2015, 35(8):3607-3615.

266. Marquis JP, Killcross S, Haddon JE: Inactivation of the prelimbic, but not infralimbic, prefrontal cortex impairs the contextual control of response conflict in rats. *Eur J Neurosci* 2007, 25(2):559-566.

267. Grosso A, Santoni G, Manassero E, Renna A, Sacchetti B: A neuronal basis for fear discrimination in the lateral amygdala. *Nat Commun* 2018, 9(1):1214.

268. Miyashita T, Kikuchi E, Horiuchi J, Saitoe M: Long-Term Memory Engram Cells Are Established by c-Fos/CREB Transcriptional Cycling. *Cell Reports* 2018, 25(10):2716-28.

269. Han JH, Kushner SA, Yiu AP, Cole CJ, Matynia A, Brown RA, Neve RL, Guzowski JF, Silva AJ, Josselyn SA: Neuronal competition and selection during memory formation. *Science* 2007, 316(5823):457-60.

270. Yiu AP, Mercaldo V, Yan C, Richards B, Rashid AJ, Hsiang HL, Pressey J, Mahadevan V, Tran MM, Kushner SA, Woodin MA: Neurons are recruited to a memory trace based on relative neuronal excitability immediately before training. *Neuron* 2014, 83(3):722-35.

271. Hardingham GE, Fukunaga Y, Bading H: Extrasynaptic NMDARs oppose synaptic NMDARs by triggering CREB shut-off and cell death pathways. *Nature Neuroscience* 2002, 5(5):405.